

GENETIC ANALYSIS OF MOTOR AXON PATHFINDING IN ZEBRAFISH

DISSERTATION

Presented in Partial Fulfillment of the Requirements for
the Degree Doctor of Philosophy in the
Graduate School of The Ohio State University

By

Louise Rose Rodino-Klapac, B.S.

The Ohio State University
2005

Dissertation Committee:

Dr. Christine E. Beattie, Advisor

Dr. Paul Henion

Dr. Mark Seeger

Dr. Anthony Brown

Approved by

Advisor
Graduate Program in
Molecular Genetics

ABSTRACT

In the developing nervous system, motoneurons extend their axons in a highly stereotyped manner in order to reach their appropriate targets in muscle. Studying how motor axons navigate and make proper connections will contribute to our understanding of neuromuscular development and motoneuron diseases. Utilizing forward genetics in zebrafish, we have isolated a recessive mutation in the *topped* gene that specifically affects the ventral primary motoneuron, CaP (Caudal Primary). All other neuronal projections analyzed, including the dorsal primary motor neuron, MiP (Middle Primary), were shown to be unaffected. From mosaic studies, we showed that Topped was functioning specifically in ventromedial fast muscle cells to promote ventral motor axon outgrowth.

In order to understand how Topped is functioning on a molecular and biochemical level, it is necessary to identify the gene that is disrupted. Using a positional cloning strategy, we mapped the mutation to a critical region near the centromere of chromosome 24. Predicted sequence homology then revealed a candidate gene in this region homologous to *semaphorin5a* in mouse and human, which we found to be expressed in the ventral myotome in zebrafish. To determine if the *sema5a* gene is disrupted in *topped* mutants, we undertook a multifaceted approach. We showed that *topped* mutants could be rescued with

either injection of BAC clones containing portions of the *sema5a* gene or by injecting rat *sema5a* RNA. In addition, knock-down of *Sema5a* phenocopies the *topped* mutant phenotype. Taken together, these data strongly suggest that the *topped* mutant phenotype results from a mutation in the *sema5a* gene. To verify this conclusion, we are sequencing the zebrafish *sema5a* gene in wild-type and *topped* mutant embryos to identify a mutation.

To uncover the genetic pathway that guides ventral motor axons, we looked for genetic interactions between known zebrafish axon guidance mutants, *stumpy* and *topped*, and also screened for additional mutations. We isolated three mutations, *OS4*, *OS11*, and *OS12* that revealed a genetic interaction with *stumpy*, but not *topped* mutants. Identifying the genes that are disrupted in each of the mutants will greatly contribute to our understanding of the genetic and biochemical pathway that guides ventral motor axons.

Dedicated to my husband, Anthony Klapac, who has given me his unconditional love and support throughout my graduate career, and my parents, Thomas and Janet Rodino, who have always been there to encourage me to pursue all of my dreams and goals.

ACKNOWLEDGMENTS

I wish to thank my advisor, Christine Beattie, for all her guidance in molding me as a scientist, her enthusiasm and fortitude during difficult times, and her contagious love of developmental biology and science as a whole. I thank my committee members, Paul Henion, Mark Seeger, and Anthony Brown for helpful suggestions and guidance throughout my graduate career.

I am grateful to my lab members, Chunping Wang, Michelle McWhorter, Emily Tansey, Tessa Carrel, Sean Lewis and former members Michelle Gray, and Anil Challa for all their support and helpful discussions throughout the years. I would also like to thank the members of the Henion Lab, Brigitte Arduini, Min An, Myron Ignatius, Roopa Nambiar, and Marsha Lucas for making it a great experience in the zebrafish group.

I thank Frank Stockdale, Michael Granato, David Kantor, and Alex Koldkin for reagents and zebrafish lines. I am grateful to Cynthia Herpolsheimer for her early work on the *topped* mutant line. This work has been supported by the National Science Foundation.

VITA

April 3, 1978. Born – Hazleton, PA

May 17, 2000. B.S. Biology
King's College, PA

2001 - 2002. Graduate Teaching Associate
The Ohio State University.

2001 – 2005. Graduate Research Associate
The Ohio State University.

PUBLICATIONS

Research Publications

1. Rodino-Klapac, LR, and Beattie, CE. (2004) Zebrafish topped is required for ventral motor axon guidance. *Developmental Biology* **273**: 308–320.

FIELDS OF STUDY

Major Field: Molecular Genetics

TABLE OF CONTENTS

	<u>Page</u>
Abstract	ii
Dedication	iv
Acknowledgments	v
Vita	vi
List of Tables.xii
List of Figuresxiii
List of Abbreviations.xvi
Chapter 1: Introduction.	1
Overview.	1
Early studies on motor axon pathfinding.	3
Motor axons respond to chemotropic gradients.	4
Cellular Cues.	5
Molecular Cues.	7
Mechanisms of motor axon pathfinding.	12
Genetic Screens.	16
Zebrafish as a model for axial innervation.	18
Zebrafish mutants provide insight into ventral pathfinding.	22

Chapter 2: Zebrafish <i>topped</i> is required in ventral motor axon guidance.	28
Introduction.	28
Materials and Methods.	31
Fish Care and Maintenance	31
Generation of Mutants.	31
Genetic Mapping.	32
Whole-mount antibody labeling.	32
Whole-mount RNA in situ hybridization.	33
Single cell labeling.	33
Blastula Transplants.	34
Genotyping from blastulae.	35
Results.	36
<i>topped</i> is a recessive, semi-lethal mutation.	36
CaP axons in <i>topped</i> mutants are delayed entering the ventral myotome.	36
Topped is required for the proper outgrowth of ventral motor nerves.	38
Dorsally projecting axons are unaffected in <i>topped</i> mutants.	39
Other neuronal cell types and myotome are unaffected in <i>topped</i> mutants.	40
Genetic mosaics reveal that Topped function is non-cell autonomous for CaP axons	42
Topped is required in ventromedial fast muscle.	43

Discussion.	46
Ventral motor axon outgrowth is specifically affected in <i>topped</i> mutants.	46
Fast muscle and ventral axon outgrowth.	48

Chapter 3: Zebrafish *semaphorin5a* and positional cloning of *topped*

Introduction.	64
Materials and Methods.	67
Fish Strains and Maintenance.	67
Generation of Mutants.	67
Genetic Mapping.	68
Genomic Cloning and Sequencing.	68
BAC and Heterologous RNA Rescue.	69
Morpholino Analysis.	69
Whole-Mount Antibody Labeling.	70
Whole-Mount In Situ Hybridization.	70
Results.	70
Positional cloning of zebrafish <i>topped</i>	70
Cloning of zebrafish <i>sema5a</i>	72
Analysis of <i>sema5a</i> as a candidate for <i>topped</i>	74
Zebrafish <i>sema5a</i> is expressed in the ventral myotome.	75
BAC rescue analysis	76
Heterologous RNA rescue with rat <i>sema5a</i>	77

Knockdown of zebrafish <i>sema5a</i> phenocopies the <i>topped</i> mutant phenotype.	78
Overexpression of <i>sema5a</i> results in abberant motor axons	80
Sema5a function in ventral motor axon pathfinding	80
Discussion.	81
The <i>topped</i> critical region contains other predicted genes	82
Isolation of a mutation in the <i>sema5a</i> gene in <i>topped</i> mutants.	83
<i>Sema5a</i> is expressed in the ventral myotome.	84
Zebrafish <i>sema5a</i> and <i>sema5b</i> have non-overlapping expression patterns.	85
<i>Topped</i> may be a hypomorphic allele of <i>sema5a</i>	85
Sema5a may be modulated by proteoglycans in the myotome or CaP axon growth cones.	86
Sema5a is functioning in ventral motor axon pathfinding	87
 Chapter 4: Genetic Dissection of Ventral Axial Motor Axon Pathfinding in Zebrafish.	 116
Introduction.	116
Materials and Methods.	118
Fish Strains and Maintenance.	118
Generation of Mutants.	118
Whole-Mount Antibody Labeling.	119
Results.	119
<i>Topped</i> and <i>stumpy</i> function in the same genetic pathway.	119

OS4, OS11, and OS12 genetically interact with <i>stumpy</i>	122
OS4, OS11, and OS12 exhibit homozygous lethality.	123
Discussion.	123
Genetic pathways as revealed by mutant analysis.	123
Identifying the deletion responsible for the OS4, OS11, and OS12 CaP axon phenotype.	125
CaP motor axon outgrowth is defined by a complex genetic pathway.	126
Chapter 5: Discussion.	130
List of References.	133

LIST OF TABLES

Table	Page
2.1 Topped is non-cell-autonomous for CaP motoneurons.	59
2.2 Topped is required in ventromedial fast muscle.	62
3.1 Predicted transcripts in <i>topped</i> critical region	89
3.2 Primers used to clone the zebrafish <i>sema5a</i> gene.	93
3.3 Exon sequences for zebrafish <i>sema5a</i>	95
3.4 Zebrafish BAC clones containing portions of the <i>sema5a</i> gene rescue the <i>topped</i> phenotype.	108

LIST OF FIGURES

Figure	Page
1.1 The Semaphorin family of axon guidance ligands is comprised of eight classes	25
1.2 Motor axon organization in amniotes.	26
1.3 Motor axon organization in zebrafish.	27
2.1 Schematic diagram of the primary motor axon pathways at 26 h.	51
2.2 CaP axons in <i>topped</i> mutants exhibit a stall phenotype at the first intermediate target.	52
2.3 CaP axons are delayed entering the ventral myotome in <i>topped</i> mutants.	53
2.4 Formation of ventral nerves is delayed in <i>topped</i> mutants.	54
2.5 MiP and RoP axons are unaffected in <i>topped</i> mutants.	55
2.6 Other neuronal cell types are unaffected in <i>topped</i> mutants.	56
2.7 Myotome is unaffected in <i>topped</i> mutants.	57

2.8	Topped acts non-cell-autonomously with respect to CaP.	58
2.9	Wild-type muscle rescues the CaP axon defect in <i>topped</i> mutants.	60
2.10	Topped is functioning in ventromedial fast muscle to promote CaP axon outgrowth into the ventral myotome.	61
2.11	Schematic depiction of wild-type muscle cells that rescue CaP axons in <i>topped</i> mutants.	63
3.1	Genetic Linkage Map of <i>topped</i>	88
3.2	Zebrafish <i>sema5a</i> cDNA sequence	90
3.3	Genomic organization of zebrafish <i>sema5a</i>	94
3.4	Cross species homology of <i>sema5a</i> cDNA	98
3.5	Sema5a protein cross species alignment	99
3.6	cDNA alignment of zebrafish <i>sema5a</i> and predicted <i>sema5b</i>	102
3.7	Zebrafish <i>sema5a</i> is expressed in the ventral myotome.	106
3.8	Zebrafish <i>sema5b</i> is expressed in the brain and notochord	107
3.9	Heterologous rescue of CaP axons in <i>topped</i> mutants with rat full-length <i>sema5a</i> RNA.	109
3.10	Knockdown of <i>sema5a</i> with SI antisense oligos	110

3.11	Knockdown of zebrafish <i>Sema5a</i> with antisense oligonucleotide morpholinos phenocopies the <i>topped</i> mutant phenotype.	111
3.12	Knock-down of <i>Sema5a</i> in <i>topped</i> mutants exacerbates the <i>topped</i> phenotype.	114
3.13	Overexpression of <i>sema5a</i> transcript induces CaP axon defects	115
4.1	<i>topped</i> and <i>stumpy</i> genetically interact.	127
4.2	<i>Stumpy</i> ^{+/-} ; <i>topped</i> ^{+/-} transheterozygotes remain affected at 36 hpf . . .	128
4.2	<i>OS4</i> , <i>OS11</i> , and <i>OS12</i> exhibit a transheterozygous interaction with <i>stumpy</i>	129

LIST OF ABBREVIATIONS

BAC	bacterial artificial chromosome
CAM	Cell adhesion molecule
CaP	Caudal Primary
°C	degrees Celsius
<i>comm</i>	<i>Commissureless</i>
DAB	diaminobenzidine
dpf	days post fertilization
ENU	ethylnitrosourea
EST	expressed sequence tag
hpf	hours post fertilization
ISN	Intersegmental Nerve
MiP	Middle Primary
MO	morpholino
RoP	Rostral Primary
<i>robo</i>	<i>roundabout</i>
<i>sema5a</i>	<i>semaphorin5a</i>
SSLP	simple sequence length polymorphism
TSR	thrombospondin domain

CHAPTER 1

INTRODUCTION

Overview

Neuromuscular specification is a complex, developmentally timed process in which motor axons exiting the spinal cord must reach their proper muscle targets to establish the appropriate neuromuscular connections necessary for normal motor function. Vertebrate motor axons must navigate along specific and often long pathways to reach those final destinations. This journey is precisely navigated by the presentation of the appropriate cues by environmental substrates along the motor axon pathway, and the subsequent interpretation of these cues by the motor axon growth cone. The elucidation of the genetic and biochemical pathways that guide these processes has important implications for understanding neuromuscular development and motoneuron diseases caused by defects in this process.

As early as the 16th century, Leonardo da Vinci recognized that nerves projected throughout the body in a stereotyped fashion, while some time later Ramon y Cajal discovered the uniquely shaped tips of growing axons which he named growth cones (reviewed in Goodman and Tessier-Lavigne, 1997; Schneider and Granato, 2005). The advent of cell culture techniques by Harrison

in 1910 allowed researchers to visualize individual growth cones and manipulate the substrate through which they extended. The use of culture studies persisted and led to the conclusions that growth cones respond to chemotrophic gradients of guidance cues (Sperry, 1963; Tessier-Lavigne, 1995; Nakamoto et al., 1996). Subsequent cellular studies identified the cell types these cues are functioning in, and soon after researchers began to identify the molecules acting as guidance cues (Lance-Jones and Landmesser, 1980; Ferguson, 1983)

Molecular advances included the use of large and small directed mutagenesis screens in *Drosophila* and *C. elegans* which revealed genes critical for cell and/or axon migration (Seeger et al., 1993; Zallen et al., 1999; Wightman et al., 1997; Kraut et al., 2001, and Van Vactor et al., 1993). Zebrafish subsequently emerged as a vertebrate model in which large scale genetic screens were performed that revealed mutations that affected axon pathfinding (Granato et al., 1996). Smaller, more directed antibody and reporter screens specifically designed to isolate genes important for motor axon pathfinding were more recently conducted (Beattie et al., 1999; Birely et al., 2005). These screens revealed mutants that affect the outgrowth of the primary motoneurons in zebrafish.

Here, a chronological summary of the field of motor axon pathfinding will be reviewed including early work in which the hypothesis arose that cellular cues guide axons to distinct targets. The field advanced from cell culture techniques, to more advanced anatomical manipulations which defined the cell types guidance cues were functioning in. Finally, advancement of molecular genetics

allowed researchers to identify the molecular identity of the guidance cues guiding motor axons to their targets. The mechanisms of motor axon pathfinding will also be described in detail, followed by a discussion of the genetic screens which revealed that molecular cues that guide axons. Lastly, zebrafish will be described as an excellent model system to study motor axon pathfinding based on researchers ability to perform genetic, cellular, and molecular techniques in one model.

Early studies on motor axon pathfinding

At the turn of the 20th century, Ramon y Cajal first proposed that sensory structures on the tips of axons, termed growth cones, may be guided by gradients of attractive diffusible factors emanating from distant targets (reviewed in Goodman and Tessier-Lavigne, 1997). In 1910, with the advent of cell culture, Harrison was able to confirm Cajal's hypothesis that growth cones extend from cell bodies and consequently form axons. Some time later, in the 1950s, work from Sperry reignited the idea of axon target specificity. Sperry studied retinal pathfinding in amphibians, and found after being severed, the optic nerve showed a high degree of specificity in reforming its proper connections (Sperry, 1963). From this work, Sperry formed the "chemoaffinity hypothesis" which suggested that neuronal growth cones use specific surface markers to recognize both pathways and targets (Sperry, 1963; Goodman and Tessier-Lavigne, 1997). This idea of external cues guiding axon migration was confirmed in the peripheral nervous system (PNS) in chick, and both the PNS and CNS in zebrafish in the

1980s (Landmesser, 1978, 1980; Jones and Landmesser, 1981; Eisen et al., 1986; Kuwada, 1986).

Motor axons respond to chemotrophic gradients

Using the retinotectal system as a model, Sperry postulated that positional information may be conveyed to axons by gradients of signaling molecules. He proposed these cues would “stamp each cell with its appropriate latitude and longitude” (Sperry, 1963). It was later hypothesized that the gradient a retinal axon responds to is the result of two opposing gradients of ligands, one attractive, another repulsive (Gierer, 1987). Bonhoeffer and colleagues later showed in vitro evidence for spatially derived cues in tectal cells. They found when temporal retinal axons were presented with the choice of cells from different anterior-posterior regions of the tectum, they could respond to both, but preferred the anterior cells, their normal targets (Bonhoeffer and Huf, 1980, 1982, 1985). These findings were confirmed with the advent of the classic “stripe assay”, in which axons were presented with stripes of tectal membranes as opposed to live tectal cells (Walter et al, 1987). With this technique, researchers were able to decipher the mechanism responsible for the preference, and found it was based on avoidance of the posterior tectum, rather than attraction to the anterior tectum (Walter et al., 1990). Baier and Bonhoeffer (1992) added to this data, by developing an assay that demonstrates that temporal retinal axons could respond to a smooth gradient of posterior tectal membranes by being deflected from their pathway. These data provided evidence that retinal axons respond to

a gradient of cues that guides them to their tectal targets. The advent of the stripe assay was revolutionary for the field of axon guidance, and is commonly used today to test the preference of axons for various axon guidance molecules (Kantor et al., 2004).

Cellular Cues

Prior to the 1990s, studies regarding axon pathfinding were largely based on descriptive work. For example, topographical studies in chick showed organized patterns of neuronal connections in the visual system. These were defined by retinal ganglion cell axons stereotypically projecting onto the tectum (Sperry, 1963; Grier, 1987; Thanos and Bonhoeffer, 1986; Goodman and Tessier-Lavigne, 1997). Grafting experiments in which retinal explants were removed from different dorsoventral locations of the retina and grafted onto an uninnervated tectum revealed the axons projected to the region of the tectum appropriate for the location from which they were derived (Thanos and Dutton, 1987). This data suggested the presence of cues within the tectum responsible for the proper pathfinding of retinal axons.

Culture studies in chick also revealed that axons followed stereotyped pathways. However, they further revealed that axons reached their appropriate targets even after the environment through which the axons grew was manipulated by reversal of the spinal cord, suggesting the presence of local cues (Lance-Jones and Landmesser, 1980). Additional studies using the chick limb as

a model then revealed that when the limb bud was rotated about the dorsoventral axis, motor axons were able to respond to the axis as well (Ferguson, 1983). These data suggested cellular cues existed to guide axons to their targets; however, the data did not discern whether there was a critical point in development when these axons could no longer respond to cellular changes and consequently, cues.

Studies in zebrafish added to our understanding of cellular cues. In zebrafish, there is one primary motoneuron that extends dorsally, MIP (Middle Pimary), while another, CaP (Caudal Pimary) extends ventrally. A series of myotome transplant experiments revealed that when the myotome was reversed about the dorsoventral axis prior to axogenesis (16 hpf), CaP axons could extend normally (Beattie and Eisen, 1997). In contrast, when the transplants were performed subsequent to the onset of axogenesis (19 hpf), CaP axons failed to extend. These data indicated that prior to axogenesis the polarity of the myotome was not fixed, and axons could still extend normally. Additional experiments demonstrated that there is a notochord-dependent change that alters the dorsal myotome non-permissive coincidental with axogenesis. From these studies it was concluded that there is some degree of plasticity between axon outgrowth and environmentally derived cues, however the identity of these cues remained unclear.

Studies in invertebrates where either the axon or its target was manipulated revealed potential cellular sources of cues important for axon outgrowth. For example, when specific muscle targets were ablated in both

grasshopper and *Drosophila* embryos, axons abnormally innervated neighboring muscle segments (Ball et al., 1985; Sink and Whitington, 1991). These studies and others suggested the presence of molecular cues along axon pathways that guide axons to their appropriate targets. However, it was difficult to infer the molecular basis from the cellular studies; therefore mutational analysis was used to identify genes that affect axon outgrowth.

Molecular Cues

Initially, the cues that guide motor axons were thought to be divided into three categories: long-range diffusible cues, non-diffusible extracellular matrix (ECM) molecules that function in cell-ECM adhesion, and cell surface molecules that function as local cues in cell-cell interactions. It was later shown that the molecules identified did not fit neatly into these categories, and were often found to have multiple functions. Two major families of cell-adhesion molecules (CAMs) were identified and shown to function in axon guidance: the immunoglobulin (Ig) superfamily, and cadherins, characterized by tandem arrays of Ig and fibronectin type III domains, and cadherin domains respectively (Edelman, 1993; Takeichi, 1995). NCAM (neural cell adhesion molecule) and N-cadherin were the first family members to be identified. In one example, NCAM, along with PSA (polysialic acid) was found to mediate axon-axon adhesion in the chick cranial and sciatic plexuses. When PSA levels were enzymatically reduced,

axons exiting the plexus exhibited pathfinding errors due to increases in fasciculation (Tang et al., 1994; Landmesser, 1990).

In addition to functioning in cell adhesion, certain CAMs have been shown to function as signaling receptors with or without the presence of an obvious signal sequence. For example, the receptor protein tyrosine kinase (RPTK), ARK is expressed in the mouse brain, and can bind in a homophilic fashion (Bellosta et al., 1995). Examples of nonreceptor protein tyrosine kinases (PTKs) include Abl, Src, Fyn, and Yes, which are highly expressed in growth cones and have been shown to function in motor axon guidance (Comer et al., 1998; Finn et al., 2003; Wills et al., 1999; Bixby and Jhabvala, 1993). Genetic studies revealed that different tyrosine kinases are functioning downstream of CAMs such as NCAM and L1. NCAM and L1 neurite outgrowth was inhibited, when PTKs, Fyn and Src were mutated (Beggs et al., 1994; Ignelzi et al., 1994). Taken together, these data suggested that PTKs function downstream of specific CAMs to promote axon outgrowth.

Extracellular matrix (ECM) molecules, including laminin, tenascin, collagen, thrombospondins, and proteoglycans, have been shown to have both attractive and inhibitory effects on motor axon outgrowth (Lander, 1987; Schachner, 1994). Receptors for these molecules include the integrins and certain proteoglycans (Goodman and Tessier-Lavigne, 1997).

Netrins are a family of axon guidance molecules related to laminins that can function as bifunctional cues (Culotti and Kolodkin, 1996). The netrins are an interesting class of molecules in that they were discovered in parallel by two

unique approaches. The first netrin family member, UNC-6 was discovered in *C. elegans* based on its mutant phenotype which included defects in cell migration and axon guidance (Hedgecock et al., 1990; Ishii et al., 1992). In another approach, an in vitro assay was developed based on the ability of chick floor plate cells to secrete a molecule that promoted outgrowth of axons of the dorsal spinal cord (Tessier-Lavigne et al., 1988). The molecules purified from the assay were netrin-1 and netrin-2. In addition to their outgrowth promoting activity in chick floor plate, netrins also inhibit dorsally projecting hindbrain motoneurons, including trochlear motor axons (Colamarino and Tessier-Lavigne, 1995; Varela-Echavarria et al., 1997). However, *netrin-1* deficient mice, exhibited no trochlear motor axon defects, implying different mechanisms among chick and mice, or redundant guidance cues working in concert with netrin-1 (Serafini et al., 1997).

Semaphorins

Semaphorins (Semas) are large family of membrane-bound and secreted axon guidance ligands conserved from insects to humans (Kolodkin et al., 1993). Semaphorins were first identified in a monoclonal antibody screen for surface antigens on fasciculating axons in grasshopper, which led to the identification of fasciclin IV, later renamed Semaphorin I (Kolodkin et al., 1992). A PCR based approach was subsequently used to identify family members in *Drosophila* and human (Kolodkin et al., 1993). The Sema family is subdivided into eight classes based on structure and sequence similarity (Semaphorin Nomenclature Committee, 1999). Classes one and two are invertebrate classes, while classes

three through seven are vertebrate classes. The last class, class V is found in a few neurotrophic DNA viruses (Figure 1.1). The receptors for these molecules have been shown to be members of the Plexin and the Neuropilin families or complexes thereof (Nakamura et al., 2000; He et al., 2002). Although most emphasis has been placed on the Semaphorins as inhibitory axon guidance molecules due to the presence of the inhibitory Sema domain, they have been shown to have attractive capabilities in some instances (Artigiani et al., 2004).

Vertebrate Sema class 3 secreted molecules are among the most well studied class of Semaphorins. SemIII/D/Collapsin-1 was the first vertebrate Sema to be identified, first in chick (Coll-1), and then in mouse (SemIII/D) (Luo et al., 1993; Kolodkin et al., 1993; Puschel et al., 1995). SemIII/D inhibits the outgrowth of certain cranial and spinal motor neurons, as mice deficient for semIII/D exhibit defects in axon outgrowth of these motoneuron classes (Behar et al., 1996). Two zebrafish homologs of SemIII/D have been isolated, *semaZ1a* and *semaZ1b*. *SemaZ1a* is expressed in dorsal and ventral myotome regions, but is absent in the future horizontal myoseptum, the region which will later demarcate dorsal from ventral muscle. When *semaZ1a* was misexpressed in this region, CaP ventral motor axons stalled just after leaving the spinal cord, indicated an inhibitory role for motor axon outgrowth (Halloran et al., 2000). *SemaZ1b* was found to be expressed in the posterior half of the myotome in each hemisegment. Upon overexpression along with lacZ, *semaZ1b* was found to induce CaP ventral motor axon defects including severe truncation or

complete absence of an axon, indicating once again, an inhibitory role (Roos et al., 1999).

This dissertation work focuses on one class of Semaphorins, vertebrate class 5. Class 5 molecules are unique in that they contain two clusters of type-1 thrombospondin repeats (TSR), 3' to the Sema domain (Fig 3.1c.; Adams et al., 1996; Kantor et al., 2004). In vitro studies have revealed TSR domains mediate attraction to promote axon outgrowth (Neugenbauer, et al., 1991, O'Shea et al., 1991; Osterhout et al., 1992; Rawala et al, 2000; Kruger et al., 2000; Pasterkamp and Kolodkin, 2003; Kantor et al., 2004). The presence of an inhibitory Sema domain and a putatively attractive TSR domain in class 5 molecules lends itself to the idea of a bifunctional molecule. In accordance with that idea, Kantor and colleagues (2004) recently found that murine Sema5a acts as a bifunctional cue in the diencephalon. Using stripe assays with cultured neurons, they found that in the presence of chondroitin sulfate proteoglycans (CSPGs), Sema5a acts as an inhibitory molecule. Conversely, Sema5a mediates attraction in the presence of heparan sulfate proteoglycans (HSPGs). These findings implicated Sema5a as a strikingly complex molecule with a marked ability to both attract and inhibit axon outgrowth. We have cloned the zebrafish homolog of *sema5a*, and show that it is expressed in the ventral myotome coincidental with when and where CaP ventral motor axons extend. Data discussed in chapter 3 demonstrates that Sema5a is functioning as an attractive molecule to promote ventral motor axon outgrowth. Developmental studies in vivo are crucial to our limited understanding

of how axon guidance ligands can switch from being attractive to repulsive in order to guide motor axons to their distal targets.

Mechanisms of motor axon pathfinding

Motor axons must exit the CNS before migrating into the periphery

Motor axons must successfully complete multiple steps in order to reach their final destinations in muscle. First, they must exit the spinal cord on the anterior-posterior axis, as well as extend laterally away from the midline. These decisions are directed by inherently segmented substrates, which vary among organisms (reviewed in Schneider and Granato, 2003). In amniotes including mouse and chick, motor axons exit the spinal cord from the same ventral root in each hemisegment (Keynes and Stern, 1984). Studies concluded that this process is directed by inhibitory guidance cues present in the caudal sclerotome (Oakley and Tosney, 1993; Tannahill et al., 1997). Molecules with expression patterns restricted to the caudal sclerotome include the guidance molecules, semaphorins and ephrins, as well as other molecules including F-spondin and collagen IX (Eickholt et al., 1999; Raper, 2000; Wang and Anderson, 1997; Tzarfati-Majar et al., 2001; Vermeren et al., 2000), suggesting roles in spinal nerve segmentation. However, *in vivo* studies have not confirmed essential roles for these genes in segmental nerve formation. In zebrafish, as in amniotes,

spinal motor axons exit the spinal cord from a common ventral root into each hemisegment; however the substrate essential for migration has been shown to be myotome, not sclerotome (Eisen and Pike, 1991). Support for this came when researchers ablated sclerotome in the somite, and found axon outgrowth to be unaffected (Morin-Kensicki and Eisen, 1997). Further support followed when molecules, Tenascin-C, chondroitin sulfate proteoglycans, and Sema3A2 were found to be restricted to the posterior myotome (Bernhardt et al., 1998; Bernhardt and Schachner, 2000; Roos et al., 1999). Additionally, spinal motor axons in zebrafish mutants, *spadetail* and *you-too*, which exhibit defects in myotome development, fail to extend into the periphery (Eisen and Pike, 1991). From these studies and others, it can be concluded that the cell types axons migrate along are interchangeable, however the cues present in these substrates are crucial for axons to exit the spinal cord and migrate correctly.

Motor axons migrate along common pathways

After motor axons have exited the spinal cord, the next step in the pathfinding process is migrating along common pathways. In both vertebrates and invertebrates, motor axons migrate along common pathways with one another before diverging along unique pathways en route to their unique muscle targets (Landgraf et al., 1997; Westerfield et al., 1986). Coincidental with this process is the presence of a pioneer axon, which is the initial axon to migrate along a common pathway. Later migrating axons, which extend along the same

pathway, either respond to the same local cues, or rely on the pioneer axon to accomplish proper migration. Bodies of evidence have been presented that support each hypothesis. Examples of pioneer axons are the intersegmental (ISN) neuron in grasshopper, and the primary axial motor axons CaP, MiP, and RoP (Rostral Primary) in zebrafish. Zebrafish studies, in which CaP was ablated, revealed that MiP and RoP could pathfind correctly along the common pathway (Eisen et al., 1989; Pike and Eisen, 1990). In contrast, ablation studies in grasshopper demonstrated that axons which follow the ISN require its presence to migrate (du Lac et al., 1986). Although these studies differ in their conclusions, they both suggest there is a necessity for the presence of local cues for axons to exhibit proper migration.

Motor axons encounter intermediate targets

Studies from both vertebrates and invertebrates have shown that axons encounter intermediate targets along their migratory pathways. These regions can be defined as regions where axons either pause, branch, or turn, implying that molecular cues are being imparted to the axon en route to their final destination. There have been several examples in vertebrates where intermediate targets (also referred to as choice points) have been described. One such example that has been well described is the crural and sciatic plexuses in amniotes. In amniotes, the axons of the lateral motor column (LMC) project to the limb. These axons are further subdivided into the lateral (LMC_L) and medial

(LMC_M) LMC axons (Landmesser, 1980). Axons of the LMC_L and LMC_M exit the spinal cord from the same root, but then encounter an intermediate target in the limb bud, referred to as the plexus. Here, axons converge, resort, and then extend into either the dorsal or ventral limb (Hollyday, 1995; Landmesser, 1978; Tosney, 1991). These decisions have been shown at least in part to be controlled by EphA receptors (Eberhart et al., 2000; Helmbacher et al., 2000). Other potential cues may include Semaphorins, N-CAM, L1, and N-cadherin (Kitsukawa et al., 1997; Taniguchi et al., 1997; Allan and Greer, 1998; Landmesser et al., 1988). In zebrafish, muscle pioneer cells that define the horizontal myoseptum (referred to as the first intermediate target or choice point) also acts as an intermediate target (Beattie et al., 2000; Eisen et al., 1986; Melancon et al., 1997). It was shown that CaP axons pause at the first intermediate target and make contact with the muscle pioneers; however, this contact is not required for proper pathfinding (Melancon et al., 1997). Though much is known about the cues that allow axons to exit the spinal cord, migrate along common pathways, and make pathfinding decisions at intermediate targets, there is still a considerable amount of work to be done to identify the full cohort of cues guiding motor axons to their muscle targets. To identify these cues and how they may be functioning, researchers have turned to genetic screens.

Genetic Screens

Drosophila was the first model system in which axon guidance mutants were identified. These studies revealed a complex genetic and biochemical pathway that results in proper guidance of CNS axons at the midline. The *Drosophila* midline is defined by ipsilateral axons that do not cross the midline, and contralateral axons that cross the midline forming a ladder-like structure. In an *ems* mutagenesis screen in 1993, two striking *Drosophila* mutants were revealed that served as the framework for a decade of research defining the way in which axons are guided at the CNS midline (Guthrie, 2001). The Roundabout (*robo*) mutation results in the formation of roundels, where axons cross and recross the midline; while the Commissureless (*comm*) mutation results in a phenotype where there is an absence of commissures (Seeger et al., 1993). Subsequent studies revealed Robo was a receptor for the midline ligand, Slit (Kidd et al., 1999). Briefly, it was found that Slit binds to Robo receptors on the growth cones of commissural axons to repel them from the midline. Comm then acts subsequently to downregulate Robo receptors to allow axons to cross (Keleman et al., 2002; Keleman et al., 2005). Although these genes were identified in an invertebrate system, homologs of Slit and Robo have been identified in vertebrate systems including mouse and human. The exact biochemical roles of these gene products have been shown to be slightly diverged in higher organisms; however, the mechanism defined in *Drosophila* has been crucial in our understanding of these pathways (Guthrie, 2001).

In addition to *Drosophila*, genetic screens designed to uncover genes critical for axon guidance and cell migration have also been successful in *C. elegans* (Zallen et al., 1999; Wightman et al., 1997; Kraut et al., 2001, and Van Vactor et al., 1993). Screens to identify essential genes for nervous system development in mouse have also been conducted (Leighton, et al., 2001). However, there are limitations to large scale screens in mouse as a vertebrate model for axon guidance, such as small numbers of progeny and difficulty visualizing the embryonic nervous system. Therefore, zebrafish has emerged as an excellent vertebrate model for performing small or large scale screens to reveal genes specific for motor axon pathfinding. The zebrafish trunk, composed of axial muscle hemisegments innervated by three primary motoneurons is an ideal model to isolate mutations in genes that affect stereotyped axon outgrowth.

In the mid 1990s, two large scale ENU mutagenesis screens were conducted in zebrafish to isolate mutations with developmental defects. One of these screens looked for motility mutants with defects during the first four days of development (Haffter et al., 1996). Granato et al., 1996 later rescreened those mutants with motility defects with antibodies to visual motor axons. In doing so, they identified two mutations with defects in axon pathfinding, *diwanka* and *unplugged*. In a smaller, more directed, antibody screen designed to isolate mutations affecting motor axon guidance, Beattie et al., 1999 isolated three mutations, *stumpy* and *deadly seven* which affect all three primary motoneurons, and *topped* which specifically affects ventral motor axons (Beattie et al., 2000; Gray et al., 2001; Rodino-Klapac and Beattie, 2004). Recently, Birely et al.,

2005, performed a second, antibody-based screen designed to isolate genes functioning in primary motor axon guidance in zebrafish; and isolated 15 additional mutants, nine of which exhibit axon guidance defects.

Zebrafish as a model for axial innervation

Motor axon pathfinding has been studied extensively in vertebrate limb, however not much is known about axial (body wall) innervation. In the limb, differentially expressed dorsal/ventral cues appear essential for proper motor axon innervation. Studies in mouse revealed that *netrin-1* and *sema3a* specifically repel dorsally extending axons (Varela-Echavarria et al., 1997). Additionally, motor axons in *EphA4* mutant mice can migrate correctly to the plexus, but presumptive dorsal motor axons fail to extend into the dorsal limb and join the ventral nerve (Helmbacher et al., 2000). Moreover, overexpression of *EphA4* also reveals dorsal nerve defects (Eberhardt et al., 2002).

In amniotes, axial motoneurons from the medial motor column (MMC) innervate epaxial (dorsal) and hypaxial (ventral) body wall muscle (Fig 1.2). The target epaxial muscle derived from the dermamyotome is essential for epaxial nerves to form suggesting that guidance or attractive cues are present in the muscle (Tosney, 1987). However, differential cues important for dorsal or ventral axial muscle innervation in amniotes have not been described. To fill this gap in our understanding, zebrafish has emerged as a model system uniquely suited to study axial muscle innervation.

In zebrafish, the vast majority of the motoneurons innervate axial muscles, whereas only a minority of motoneurons innervate the pectoral fins, the evolutionary equivalent of the forelimb. Moreover, there is an entire subset of early developing primary motoneurons that only innervates axial muscle. Each of the three primary motoneurons is uniquely identified by its soma position within the spinal cord, characteristic gene expression, and stereotyped axonal projection (for reviews see Eisen, 1999; Beattie, 2000). CaP motoneurons innervate ventral axial muscle, MiP motoneurons innervate the dorsal axial muscle, and RoP motoneurons innervate the middle muscle territory (see Fig. 2.1). Each of the primary motoneurons exit the spinal cord from the same ventral root before diverged along unique pathways to their target destinations in the developing myotome (Fig. 1.3).

The CaP motoneuron has been studied quite extensively because its soma, in the middle of each spinal cord hemisegment, is relatively easy to visualize, and it has a prominent ventral axon projection. At approximately 18 hours post fertilization (hpf) in each spinal cord hemisegment, the CaP growth cone leaves the spinal cord and extends ventrally until it reaches the first intermediate target, the nascent horizontal myoseptum, which demarcates dorsal from ventral muscle. After pausing for one to two hours, the CaP axon continues past the first intermediate target along the ventral myotome next to the notochord (Fig. 2.1; Eisen et al., 1986; Myers et al., 1986). The ventromedial myotome, composed of fast muscle, has been shown to be crucial for proper CaP axon extension. When the ventromedial cell cluster containing sclerotome and

myotome was ablated, CaP axons displayed a stunted appearance (Morin-Kensicki and Eisen, 1997). This stereotyped axon outgrowth along the ventromedial fast muscle implies the presence of ventrally located guidance cues, but none have yet been identified.

The relative simplicity of the zebrafish nervous system affords researchers with the ability to conduct experiments that are difficult or impossible in other model systems. For example, because zebrafish embryos are optically clear, we can visualize the soma of the primary motor neurons in live embryos. In anesthetized embryos, the cell bodies of the primary motor neurons can be iontophoretically labeled with dye or chemical blocking agents, and the axons can subsequently be visualized over time (Beattie et al., 2000; Eisen et al., 1989; Westerfield, 1995). This technique has revealed dynamic changes in axon outgrowth of CaP, MiP, and RoP in zebrafish axon guidance mutants *stumpy* and *topped* (Beattie et al., 2000; Gray et al., 2001; Rodino-Klapac and Beattie, 2004), where all three primary motor axons in *stumpy* stall at presumptive intermediate targets, and CaP axons stall at the first intermediate target in *topped* mutants.

In addition to labeling motoneurons, transplantation experiments to demonstrate autonomy in zebrafish has greatly contributed to our knowledge of how genes affecting axon guidance may be functioning (Rodino-Klapac and Beattie, 2004; Beattie et al., 2000; Zeller and Granato, 2000; Zhang and Granato, 2000). Blastula transplantation is conducted at the 1000 cell stage of zebrafish development (Ho and Kane, 1990). An electrode is used to transfer cells from a labeled donor embryo into an unlabeled host. This analysis is often used

visualize mutant cells in a wild-type environment, and vice versa, thereby demonstrating the autonomy of a given gene.

Lastly, the relative ease of genetic manipulation of zebrafish has allowed for techniques that were once unique to other model systems. Knock-down of protein expression has been made possible with the advent of Morpholino antisense oligonucleotides (MO) (Nasevicius and Ekker, 2000; Heasman, 2002; Corey and Abrams, 2005). This has allowed for the characterization of countless genes and their potential functions in zebrafish development, including neuromuscular diseases (McWhorter, 2003). Additionally, the production of transgenic fish is now common practice, and more recently Cre-mediated site-specific recombination has been introduced (Udvardia and Linnery, 2003; Thummel et al., 2005). These genes are often tagged with fluorescent reporters, adding to the ease of visualization and characterization of gene function. Therefore, all of the above techniques mentioned, together with the number of progeny, and rapid development of zebrafish, make it a wonderful system for studying nervous system development and axial innervation in particular.

The zebrafish motor axon guidance mutants provide insight into ventral motor axon pathfinding.

Characterization of four zebrafish mutants: *stumpy*, *topped*, *diwanka*, and *unplugged*, that affect primary motor axon pathfinding have greatly impacted our understanding of axial motor axon outgrowth. Analysis of two zebrafish mutants,

diwanka and *unplugged*, have identified cues important for axon guidance that function in slow muscle (Zeller and Granato, 1999; Zhang and Granato, 2000). They have both been shown to function in adaxial cells, a subset of slow muscle cells near the horizontal myoseptum (Devoto et al., 1996). At the onset of its development, slow muscle resides along the medial portion of the somite, next to the notochord. Throughout development, slow muscle migrates laterally through the myotome, before eventually occupying the most lateral portion of the myotome. This process occurs in parallel with axon outgrowth of the primary motor axons, CaP, MiP, and RoP. *Diwanka* function is needed in only 1-3 adaxial cells located between the ventral aspect of the spinal cord and the horizontal myoseptum and is necessary for establishing the common pathway used by all primary motor growth cones (Zeller and Granato, 1999). *Unplugged* function is required in 3 or more adaxial cells in the same region and is necessary for CaP and RoP to make the correct pathway choice at the first intermediate target (Zhang and Granato, 2000). *Diwanka* and *Unplugged*, therefore, appear to function as slow muscle derived signals that affect axon guidance on the fast muscle. More recently, the gene disrupted in *unplugged* mutants was identified and found to encode a homolog of muscle-specific kinase (MuSK) (Zhang et al., 2004). This zebrafish homolog was shown to function differently from its previously demonstrated role in synaptogenesis. The authors demonstrate that *unplugged* activity in the dorsal adaxial cells modulates the ECM next to the adaxial cells at the first intermediate target prior to axon outgrowth. This activity allows two of the primary motoneurons, CaP and RoP to

make the correct pathway decisions. Additionally, Schneider and Granato have revealed that *diwanka* is also a molecule that modulates the ECM near the *adaxial* cells next to the first intermediate target through enzymatic activity (Schneider and Granato, person. comm.).

Another zebrafish mutation, *stumpy* also affects all three classes of the primary motoneurons. *Stumpy* mutants have a very severe phenotype, where all three primary motor axons stall at regions suggested to be intermediate targets (Beattie et al., 2000). Mosaic analysis revealed that *Stumpy* is functioning in both an autonomous and non-cell-autonomous manner with respect to CaP motor axons, suggesting it may be functioning as a homophilic molecule to allow axons to proceed past intermediate targets. This dissertation work includes the characterization of another axon pathfinding mutant, *topped*. *Topped* specifically affects ventral motor axon outgrowth. Moreover, mosaic analysis reveals that *Topped* is functioning in ventromedial muscle cells to promote CaP axon outgrowth. Lastly, we show that *stumpy* and *topped* exhibit a genetic interaction at the first intermediate target, providing evidence for the existence of a complex genetic pathway dictating ventral motor axon outgrowth.

topped, together with the previously characterized mutants that affect CaP axon pathfinding indicate that numerous cues are indispensable for wild-type axon guidance. *diwanka* is needed to set-up the common pathway, *unplugged* is needed for CaP and RoP to make the appropriate choice at the first intermediate target, *stumpy* is needed for axons to proceed past intermediate targets, and *topped* is needed for CaP axons to extend into the ventral myotome. *Topped*

function is unique in that it is the only mutation that specifically affects one class of neurons; those extending into the ventral myotome. Ongoing studies will identify the molecular nature of *topped* and begin to address its biochemical role. Moreover, eventual analysis of *topped* in other species may reveal conserved mechanisms establishing dorsoventral innervation of axial muscle

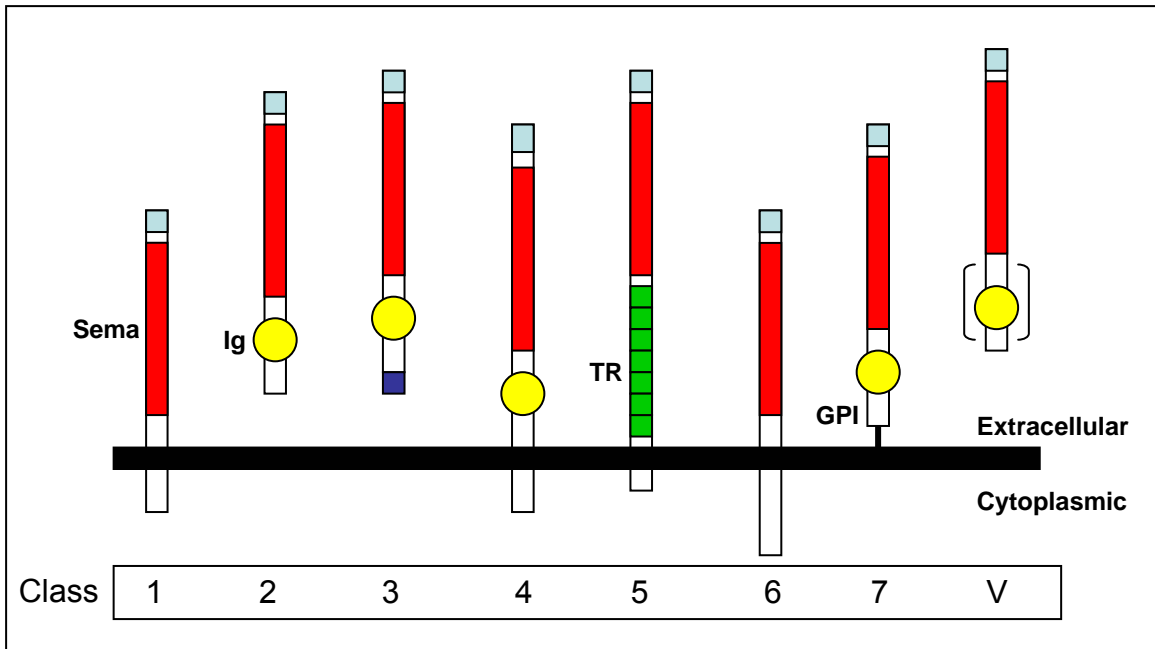


Figure 1.1: The Semaphorin family of axon guidance ligands is comprised of eight classes (adapted from Pasterkamp and Kolodkin, 2003). Class 1 and 2 are invertebrate classes, 3-7 are vertebrate classes, and class V is found in certain neurotrophic DNA viruses.

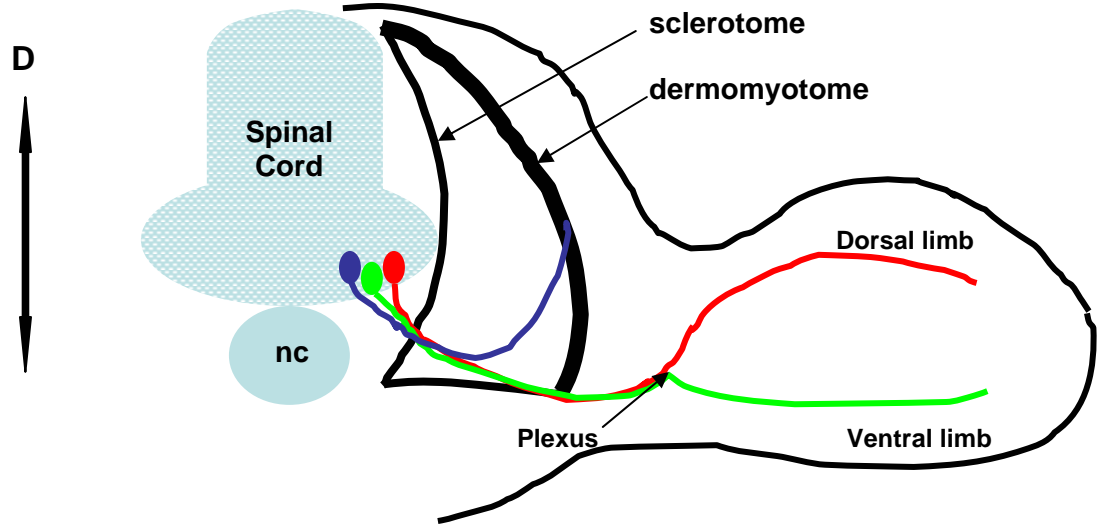


Figure 1.2: Motor axon organization in amniotes. Motor axons exit the spinal cord (sc) from the same root before migrating in common pathways along the sclerotome. Axons that innervate the limb converge at the plexus before resorting and extending into the epaxial (dorsal), or hypaxial (ventral) limb. nc, notochord. Adapted from Schneider and Granato, 2003.

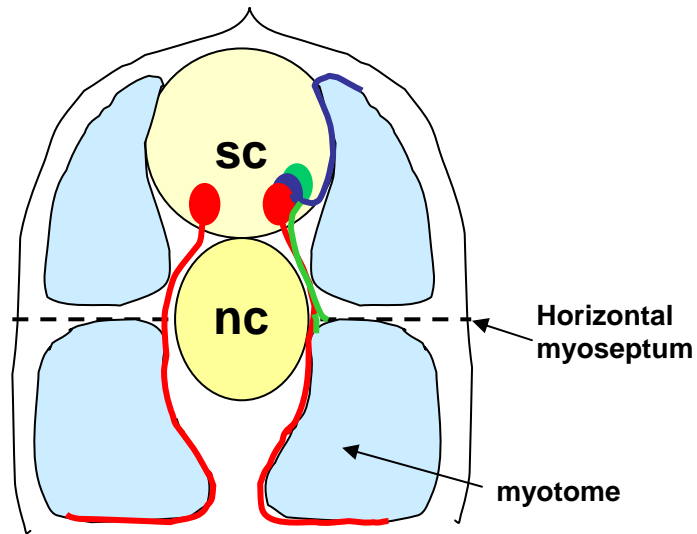


Figure 1.3: Motor axon organization in zebrafish. The primary motor axons exit the spinal cord (sc) from the same ventral root before extending along the common pathway to the 1st intermediate target (horizontal myoseptum). The axons then extend in the space between the notochord (nc) and myotome. CaP (red), MiP (blue), RoP (green).

CHAPTER 2

ZEBRAFISH TOPPED IS REQUIRED FOR VENTRAL MOTOR AXON GUIDANCE¹

Introduction

During vertebrate nervous system development, motoneurons extend their axons in a highly stereotyped manner in order to reach their appropriate target muscles. The specificity of motor axon outgrowth is accomplished by growth cones as they integrate attractive and repulsive environmental cues. In the process of chemoattraction, diffusible/secreted or membrane bound molecules present along axon pathways guide growth cones to both intermediate and distal targets. Identifying the cues critical for formation of motor nerves is essential for understanding neuromuscular development and diseases that may affect this process.

¹ Reprinted from *Developmental Biology*, Vol. 273, No. 1, Louise R. Rodino-Klapac and Christine E. Beattie, *Zebrafish topped* is required for ventral motor axon guidance, Pages No. 308-320, Copyright 2004, with permission from Elsevier.

Motor axon pathfinding has been studied extensively in vertebrate limb and differentially expressed dorsal/ventral cues appear essential for proper motor axon innervation. Studies in mouse revealed that *netrin-1* and *sema3a* specifically repel dorsally extending axons (Varela-Echavarría et al., 1997). Motor axons in *EphA4* mutant mice can pathfind correctly to the plexus, but presumptive dorsal motor axons fail to extend into the dorsal limb and join the ventral nerve (Helmbacher et al., 2000). Overexpression of EphA4 also reveals dorsal nerve defects (Eberhardt et al., 2002). Whereas there is some information about the cues involved in vertebrate limb innervation, almost nothing is known about the cues guiding motor axons to dorsal or ventral axial (body wall) musculature. In chick and mouse, motoneurons from the medial motor column innervate epaxial (dorsal) and hypaxial (ventral) body wall muscle. The target epaxial muscle derived from the dermamyotome is essential for epaxial nerves to form suggesting that guidance or attractive cues are present in the muscle (Tosney, 1987). However, differential cues important for dorsal or ventral axial muscle innervation in amniotes have not been described.

Zebrafish is an excellent model organism to study axial muscle innervation since the vast majority of the motoneurons innervate these muscles with only a minority of motoneurons innervating the pectoral fins, the evolutionary equivalent of the forelimb. Moreover, there is an entire subset of early developing primary motoneurons that only innervates axial muscle. Each of the three primary motoneurons is uniquely identified by its soma position within the spinal cord, characteristic gene expression, and stereotyped axonal projection

(for reviews see Eisen, 1999; Beattie, 2000). Caudal Primary (CaP) motoneurons innervate ventral axial muscle, Middle Primary (MiP) motoneurons innervate the dorsal axial muscle, and Rostral Primary (RoP) motoneurons innervate the middle muscle territory. The CaP motoneuron has been studied quite extensively because its soma, in the middle of each spinal cord hemisegment, is relatively easy to visualize and it has a prominent ventral axon projection. At approximately 18 hours post fertilization (hpf) in each spinal cord hemisegment, the CaP growth cone leaves the spinal cord and extends ventrally until it reaches the first intermediate target, the nascent horizontal myoseptum, which demarcates dorsal from ventral muscle. Intermediate targets are regions along an axon pathway where growth cones pause, branch, or turn implying that information is being imparted. After pausing for one to two hours, the CaP axon continues past the first intermediate target along the ventral myotome next to the notochord (Fig. 2.1; Eisen et al., 1986; Myers et al., 1986). The ventromedial myotome, composed of fast muscle, has been shown to be crucial for proper CaP axon extension. When the ventromedial cell cluster containing sclerotome and myotome was ablated, CaP axons displayed a stunted appearance (Morin-Kensicki and Eisen, 1997). This stereotyped axon outgrowth along the ventromedial fast muscle implies the presence of ventrally located guidance cues, but none have yet been identified.

Mutagenesis screens in zebrafish have begun to uncover mechanisms of axial muscle innervation. The gene *stumpy* appears to function as a cue needed for motor axons to proceed past intermediate targets (Beattie et al., 2000).

Granato and colleagues have identified two cues functioning in slow muscle, *diwanka* and *unplugged*, that are essential for establishing the common pathway shared by all of the primary motor axons and for CaP and RoP to make the correct pathway choices, respectively (Zeller and Granato, 1999; Zhang and Granato, 2000). However, cues have not yet been identified that define axon pathways on the ventral and/or dorsal myotome. Here we characterize the *topped* mutant phenotype. We find that in *topped* mutants, motor axon outgrowth into the ventral myotome is specifically affected. Based on rescue experiments, we reveal that Topped is acting in ventromedial fast muscle to promote ventral axon outgrowth. Our data support the idea of differential dorsal/ventral cues dictating stereotyped motor axon pathways along axial muscle.

Materials and Methods

Fish Strains and Maintenance

Mutant strains were maintained as heterozygous (*topped*^{b458}) lines in the Tubingen long fin (TL)/AB* background. Homozygous mutant *topped* embryos were generated by pairwise mating of *topped* heterozygous fish. Embryos raised from matings were maintained between 25.5 and 28.5°C and staged by converting the number of somites to hours post fertilization (h; Kimmel et al., 1995).

Generation of Mutants

A mutagenesis screen was conducted (Beattie et al., 1999). Briefly, after exposure to 3 mM ethylnitrosourea (ENU) (Solnica-Krezel et al., 1994), adult male fish were outcrossed to wild-type females to create the F₁ generation. F₁ females were screened for mutations by using the early pressure method to examine parthenogenetic diploid F₂ embryos (Streisinger et al., 1981). The embryos were fixed and labeled with antibodies to identify mutants. F₁ females carrying mutations of interest were outcrossed and lines generated.

Genetic Mapping

To map *topped*, mutants in the *AB background were outcrossed to the TL strain to create a polymorphic mapping line. Parthenogenetic F₂ diploid embryos were produced by fertilizing mutant carrier eggs with UV-irradiated sperm (Streisinger et al., 1981). Individual embryos were scored as mutant or wild type based on antibody labeling. Genomic DNA was isolated and PCR was performed with Simple Sequence Length Polymorphic markers to obtain centromeric linkage (Johnson et al., 1995, 1996).

Whole Mount Antibody Labeling

Whole mount antibody labeling was performed as described (Eisen et al., 1989; Beattie et al., 2000). The znp1 monoclonal antibody that recognizes

primary and secondary motor axons (1:100; Trevarrow et al., 1990; Melancon et al., 1997), anti-acetylated tubulin (1:500; Zymed Laboratories, Inc.), 4D9 (1:50; Patel et al., 1989; Devoto et al., 1996), and 3A10 (1:10 Hatta, 1992) were detected using the Sternberger Clonal-PAP system with diaminobenzidine (DAB) as a substrate (Beattie and Eisen, 1997), or with Oregon Green [®] goat anti-mouse IgG (Molecular Probes). Embryos were analyzed with a Zeiss axioplan microscope, and images were captured with Kodak Ektachrome 64Y film or digitally imaged using a BioRad (MRC 1024) confocal microscope.

Whole-mount RNA In Situ Hybridization

Whole-mount RNA in situ hybridization was performed as described by Thisse et al. (1993). An antisense digoxigenin *myoD* riboprobe was synthesized from a plasmid linearized with XbaI and transcribed with T7 (Weinberg et al., 1996). A *robo1* riboprobe was synthesized from the 5' end of a *robo1* clone (Challa et al., 2001). The *crestin* riboprobes was synthesized from a plasmid linearized with EcoR1 and transcribed with T7 (Rubenstein et al., 2000).

Single Cell Labeling

Individual motoneurons were iontophoretically labeled with rhodamine dextran (3 X10³ MW; Molecular Probes) as previously described (Eisen et al., 1989; Westerfield, 1995; Beattie et al., 2000). Labeled cells were visualized with a

Zeiss Axioskop. Images were captured with a Photometrics SPOT camera and were colorized using Photoshop (Adobe).

Blastula Transplants

To generate mosaic embryos, cells were transplanted between wild-type and mutant embryos as described (Ho and Kane, 1990). Donor embryos were injected with rhodamine dextran (3×10^3 MW; Molecular Probes) at the 2-cell stage. Transplantation of blastula cells was conducted from 3 to 3.7 h. Embryos were fixed at 26 hpf for 2 hpf at room temperature in 4% paraformaldehyde. *topped* mutant embryos were identified by immunohistochemistry with znp1 monoclonal antibody, and immunoreactivity was detected with Oregon Green[®] goat anti-mouse IgG (1:200; Molecular Probes). Transplanted cells were visualized using fluorescence microscopy on Zeiss Axioplan and confocal microscopes. For cross sectional analysis of rescued motor axons, embryos were embedded in 1.5 % agar/5 % sucrose and sectioned on a cryostat at 16 μ m. Sections were then processed for immunohistochemistry with znp1 mAb and F310 mAb (Crow and Stockdale, 1986), and immunoreactivity was detected with isotype-specific conjugate secondary antibodies Alexa Fluor[®] 350 IgG1 (F310), and Alexa Fluor[®] 488 IgG2a (znp1) (1:300; Molecular Probes). Sections were analyzed with a Zeiss Axioskop and images were captured with a Photometrics SPOT camera.

Genotyping from Blastulae

Embryos were collected from *topped* heterozygous matings and allowed to develop to 3 hpf. The embryos were then mounted in 4% methyl cellulose in an agar mold. The tray was flooded with embryo medium containing 100 units penicillin and 100 µg streptomycin/ml. Approximately ten cells were removed using a 10 µl electrode (VWR) with a 40 µm diameter opening using a standard blastula transplant apparatus (Ho and Kane, 1990). The cells were then transferred to a sterile staining dish containing 5 µl of a 400 ng/µl ProK/17 µM SDS solution (adapted from Troeger et al., 1999). The solution containing the cells was then transferred to PCR tubes and incubated at 50°C for 1 h and subsequently denatured at 99°C for 30 minutes. To each tube, 25 µl of PCR mix containing dNTPs, MgCl₂, and 25 pM of the closely linked marker z58867 was added and amplified. Mutants were identified as those that segregated with z58867.

Results

topped is a recessive, lethal mutation

In a screen designed to elucidate genes that affect motor axon pathfinding, the *topped*^{b458} (*topped*) mutation was identified (Beattie et al., 1999; 2000). *topped* is an ethylnitrosourea-induced, autosomal recessive mutation, that displays Mendelian inheritance. There is approximately 70% homozygous viability; while the remaining 30% die around 14 days post fertilization (dpf). As a first step towards identifying the molecular nature of the *topped* gene, we placed it onto the genetic map of the zebrafish genome. We used simple sequence length polymorphic markers on early parthenogenetic diploid embryos (EP; Johnson et al., 1995, 1996) to map *topped* to a chromosome. Marker z3399 on chromosome 24 segregated with *topped* in all mutants examined (n=50 EP diploid embryos) indicating that *topped* maps to this linkage group. Fine mapping with haploid *topped* mutant embryos as well as the ratio of mutant:wild-type EP diploid embryos (data not shown) indicated that *topped* is close to the centromere.

CaP axons are delayed entering the ventral myotome in topped mutants

Antibody labeling with the znp1 monoclonal antibody revealed that in *topped* mutants CaP axons stalled at or near the first intermediate target, the nascent horizontal myoseptum, at 26 hpf (Fig. 2.2). This phenotype was penetrant but exhibited some variable expressivity. For example, some F1

heterozygous adults produced mutant embryos with ~74% (100 axons scored in 10 fish) of CaP axons stalling at the first intermediate target with the other 26% extending slightly beyond this region at 26 hpf (Fig. 2.2 C); however, even in these mutants CaP axons never extended into the distal ventral myotome as is seen in wild-type embryos. Other F1 heterozygous adults yielded mutants with 98% (232 axons scored in 43 fish) of CaP axons stalling at the first intermediate target at 26 hpf, while the remaining 2% were located near the ventral edge of the notochord. These breeding pairs were used for all subsequent experiments. For consistency, only axons in hemisegments 6-12 were analyzed.

To analyze the CaP axon defect in more detail, we labeled individual CaP somata in live *topped* mutant embryos and visualized their axon projections over time. Since *topped* mutants have no visible morphological phenotype and can only be identified by their CaP axon phenotype, we extracted 10-20 cells from blastula stage embryos from heterozygous matings and genotyped them using closely linked markers to identify live mutants. These embryos developed properly and at approximately 22 hpf we labeled single CaP motoneurons with a vital fluorescent dye in embryos that were genotypically wild type or mutant (Fig. 2.3). In wild-type embryos at 22 hpf, CaP growth cones had already extended past the first intermediate target (data not shown) and by 25-26 hpf wild-type CaP growth cones had extended into the distal ventral myotome (Fig. 3 A). In *topped* mutants, however, CaP growth cones were still stalled at the first intermediate target at 25-26 hpf (22/23 Fig. 2.3 D). By 30 hpf, however, CaP growth cones in *topped* mutants had extended past the first intermediate target

into the ventral myotome (19/19 Fig. 2.3 E). Interestingly, the axons did not stall at the second putative intermediate target, the myotome adjacent to the ventral edge of the notochord, a phenotype seen in *stumpy* mutants (Beattie et al., 2000). This suggests that the CaP axon stall phenotype in *topped* mutants is not due to defects at all intermediate targets. By 45 hpf, CaP axons in *topped* mutants looked indistinguishable from wild-type CaP axons (14/14 Fig. 2.3 F). These data indicate that *topped* is important for CaP axons to extend into the ventral myotome. The finding that CaP axons eventually recover suggests either that we do not have a null allele or that more than one gene is involved in this process.

Topped is required for the proper outgrowth of ventral motor nerves

A second population of later developing motor axons also extends into the ventral myotome. There are approximately 20-30 secondary motoneurons whose axons fasciculate together with the CaP axon to form the ventral nerve (Myers, 1985; Myers et al., 1986; Pike et al., 1992). Secondary motor axons begin to extend at approximately 26 hpf and continue to emerge until approximately 34 hpf (Myers et al., 1986). Analysis of *topped* mutants at 29-35 hpf revealed that ventral nerve outgrowth was delayed. In wild-type embryos at 30 hpf, approximately 15 secondary motor axons contribute to the ventral nerve and extend to the most ventral aspect of the myotome (Pike et al., 1992). In *topped* mutants at 30 hpf, however, ventral nerves were aberrant with approximately 6% still at the first intermediate target (Fig. 2.4 B arrowhead) and

approximately 52% stalled at the myotome adjacent to the ventral edge of the notochord (Fig. 2.4 B arrow). The remaining nerves extended further ventrally but only 8% of the nerves reached the ventral most aspect of the myotome. This is in contrast to CaP growth cones in *topped* mutants at 29 hpf which are just past the first intermediate target as revealed by single cell labeling (see Fig. 2.3 E). By 34 hpf, 98% the ventral nerves had recovered and reached the ventral most aspect of the myotome. Thus, both populations of ventrally extending motor axons, primaries and secondaries, show delays in entering the ventral myotome in *topped* mutants.

Dorsally projecting axons are unaffected in topped mutants

The finding that growth cones were stalling at the first intermediate target and were delayed entering the ventral myotome suggested that *topped* might function as a ventral axon guidance cue. If this were the case, we would predict that dorsally projecting MiP axons would be unaffected in *topped* mutants. To obtain a detailed analysis of MiP axons in *topped* mutants, we injected somata of MiP motoneurons with a vital fluorescent dye and followed their projections in living *topped* mutant embryos. We found that MiP axons in *topped* mutants were identical to wild-type MiP axons. By 29 hpf, MiPs in *topped* mutant embryos had proceeded into the distal dorsal myotome (8/8 Fig. 2.5 B) and in one case the axon had already turned to extend along the myotome boundary consistent with what is seen in wild-type embryos (Eisen et al., 1986; Myers et al., 1986). By 48 hpf, all mutant MiP axons examined had made their stereotyped projection along

the rostral myotome boundary. We also examined RoP axons, which branch and extend laterally at the first intermediate target, by intracellular dye labeling. While there was some variability in the timing of the appearance of the initial forked branch that forms around 25 hpf, by 30 hpf there was no difference between RoP axons in *topped* mutants and wild-type embryos (Fig. 2.5 C-D). These data indicate that Topped function is only necessary for ventral motor axon guidance.

Other neuronal cell types and myotome are unaffected in topped mutants

To test the specificity of the *topped* mutation for ventral motor axons, we examined the projections and subsequent outgrowth of sensory and interneurons in *topped* mutants. The medial longitudinal fascicle and the lateral longitudinal fascicle contain hindbrain and spinal interneuron axons. We analyzed these large axon tracts with acetylated tubulin antibody at 18, 24, 30, and 36 hpf, and saw no defects in their outgrowth in *topped* mutants. We also examined the hindbrain Mauthner interneuron with 3A10 antibody at 24, 30, and 36 hpf and saw no phenotypic difference in wild-type and *topped* mutant embryos (Fig. 2.6 A, B). The trigeminal ganglia, Rohon-Beard sensory neurons that innervate the peripheral myotome and dermatome (Fig. 2.6 E, F), and the lateral line sensory axons that extend along the length of the embryo (Fig. 2.6 C, D), were all examined at 18, 24, 30, and 36 hpf with acetylated tubulin antibody. All projections from these cells exhibited no delay in their outgrowth and appeared phenotypically wild type in *topped* mutants.

Since growth cone motility is mechanistically similar to cell motility (discussed in Giniger, 2002), we examined the possibility that *topped* is functioning globally in cell migration. Neural crest migration follows the same migratory pathway as primary motor axon growth cones. We examined neural crest migration at 16, 18, and 22 hpf by in situ hybridization with the *crestin* riboprobe that labels migrating neural crest cells (Rubinstein et al., 2000; Luo et al., 2001) in wild-type and *topped* mutant embryos. We saw no abnormalities in neural crest cell migration in *topped* mutants (data not shown). Together, these data indicate that *topped* function is very specific for ventral motor axon outgrowth.

To determine if the ventral motor axon defect in *topped* mutants was due to defects in muscle development or patterning, we examined the patterning and subsequent development of the myotome. Upon visual inspection using Normarski imaging, no difference in morphology was apparent in *topped* mutants compared to wild-type (data not shown). To determine if *topped* myotomes were correctly patterned, we performed in situ hybridization with a *myoD* riboprobe at 14, 16, and 18 hpf (Weinberg et al., 1996; Fig. 2.7 A-B). At all time points analyzed *myoD* expression was identical in wild-type and *topped* mutants. We further examined the specification of the myotome by using separate markers for fast and slow muscle. Using the antibody 4D9 (Patel et al., 1989) that recognizes the engrailed protein in muscle pioneers, a subset of slow muscle (Fig. 2.7 C-D) and the antibody F310 (Crow and Stockdale, 1986) that recognizes fast muscle (see Fig. 10); we saw no difference in expression in wild-

type and *topped* mutant embryos. Lastly, to insure an intact horizontal myoseptum, we examined the lateral line primordium using a *robo1* riboprobe at 24, 30, and 36 hpf (Challa et al., 2001; Fig. 2.7 E-F). We saw no difference in the location or morphology of the primordium in *topped* mutants compared to wild-type embryos. These data suggest that muscle morphology and patterning are not disrupted in *topped* mutants.

Genetic mosaics reveal that Topped function is non-cell-autonomous for CaP axons

Topped could be functioning in CaP axons or in the environment to promote axon growth into the ventral myotome. To address this issue, we used blastula transplantation to create genetic mosaic embryos (Ho and Kane, 1990). We transplanted donor rhodamine labeled cells into age-matched host embryos at 3.3 hpf (high stage). Cells were transplanted from wild-type donors into host embryos obtained from heterozygous *topped* matings. Alternatively, cells from donor embryos obtained from heterozygous *topped* matings were transplanted into wild-type host embryos. After fixation at 26 hpf, the identity of both donor and host was determined by immunohistochemistry with the *znp1* antibody. In wild-type embryos, *topped* mutant CaP motoneurons had axons that exhibited wild-type outgrowth and morphology (Fig. 2.8 A-C; Table 2.1). In the reciprocal experiment, wild-type CaP axons in *topped* mutant host embryos stalled at the first intermediate target; a phenotype consistent with *topped* mutants (Fig. 2.8 D-

F; Table 2.1). These data reveal that *Topped* function is needed in the environment and not in CaP motoneurons.

Topped is required in ventromedial fast muscle

Additional genetic mosaics were generated to determine the precise location of wild-type cells that rescued the *topped* mutant phenotype. For these experiments, blastula stage cells were transplanted from wild-type donors into embryos obtained from a *topped* heterozygous mating. The resulting host embryos were fixed at 26 hpf and stained with znp1 antibody to determine the genotype. We analyzed 281 mosaic *topped* mutant embryos. Analysis of the mosaic *topped* embryos in lateral whole mount revealed that notochord, floor plate, and lateral myotomal cells were not able to rescue CaP axons (Table 2.2). However, in cases where wild-type medial muscle cells were present, CaP axons exhibited rescue (Table 2.2). Interestingly, the dorsoventral location of the transplanted muscle cells was also imperative. CaP axons recovered to the dorsoventral position of the ventral-most wild-type muscle cell (Fig. 2.9 C, F). In addition, CaP axons appeared to be able to extend across two but not three or more mutant muscle cells to reach a wild-type muscle cell (Fig. 2.9 C compare axon 3 and 4). Although we often saw a correlation between rescued axons and wild-type transplanted muscle cells (Fig. 2.9 C), there were cases in which muscle cells were located in the medial ventral myotome and failed to rescue CaP axons (Fig. 2.9 F axon 3 and 4). Subsequent analysis was necessary to resolve these examples.

To further examine the position and identity of wild-type clones that rescued CaP axons in *topped* mutants, we sectioned the mosaic *topped* mutant embryos and used muscle-type specific antibodies (Fig. 2.10). Zebrafish myotome is comprised of fast muscle derived from the lateral presomitic mesoderm and a single layer of lateral slow muscle derived from adaxial cells (Devoto et al., 1996). The F310 antibody was used to confirm the identity of fast muscle (Crow and Stockdale, 1986). Analysis of the rescued axons revealed that wild-type cells that rescued CaP axons in *topped* mutants were ventromedial fast muscle cells (Fig. 2.10 A-H; Table 2.2). Interestingly, the cells had to be located at the most medial location of the fast myotome to rescue mutant CaP axons. To summarize this data, we generated a schematic of the fast muscle cells in the ventral myotome indicating cell position by a number (dorsoventral axis) and letter (medioateral axis; Fig. 2.11 A, B). We saw CaP axon rescue in 45 hemisegments; analyzing a subset of these, we found that in 19/19 cases, the rescuing cells were located in the A position (Fig. 2.11 C). In 17/19 cases, the cell 1A was a wild-type transplanted cell, indicating that this first ventromedial muscle cell is important for Topped to allow CaP axons to enter the ventral myotome. In the remaining two cases, the first rescuing cell was either 2A or 3A. However, in two other cases where cell 3A was the first medial wild-type cell present, we found no rescue and in no cases did we see further ventral cells (e.g. 4A-6A) rescue. Moreover, while we saw gaps of one or two cells still rescue (Fig. 2.11 C examples 3, 4, 5), gaps of more than two cells never rescued mutant

axons. These data indicate that two cells is the limit that wild-type cells, and thus topped Function, can act.

Wild-type muscle cells that failed to rescue support the hypothesis that Topped is functioning specifically in ventromedial fast muscle cells. We found that even though transplanted cells were located in row 1 or 2, they were not able to rescue in any letter position other than A. For example we examined twelve cases where cells were located in positions 1B or 2B and none of the CaP axons were rescued. This precise juxtaposition was supported by an example where CaP was rescued in one hemisegment, while remaining truncated in the corresponding hemisegment (Fig. 2.10 E-H). Both hemisegments contained wild-type fast muscle cells in the 1A position, however the non-rescued side contained a wild-type cell in position 3B, while in the rescuing hemisegment the cell was in the position 4A suggesting that this medial A location is essential for wild-type cells to rescue. We were also able to resolve examples where we saw ventral muscle in lateral views but saw no rescue. We found in these cases that the muscle cells were not in the most medial A position. For example, we examined axons 3 and 4 from Fig. 2.9 F in cross section and found that wild-type muscle cells in positions 2B, 2C, and 3B were present in the same section as axon 3, while cells 3B and 4B were present in the section with axon 4.

That other myotome cells did not rescue supports the idea that the location of Topped function is critical for ventral motor axon outgrowth. We found that even large numbers of wild-type lateral fast muscle were unable to rescue CaP axons in *topped* mutants (Fig. 2.10 I-L; Table 2.2). Additionally, slow

muscle was also unable to rescue the axon defect (2.10 M-P; Table 2.2). Even the presence of three slow muscle cells at the first intermediate target did not rescue mutant CaP axons (Fig. 2.10 P). Taken together, these results indicate that Topped is functioning very specifically in ventromedial fast muscle to allow for CaP axon outgrowth into the ventral myotome.

Discussion

In *topped* mutants CaP axons stall at the first intermediate target at the nascent horizontal myoseptum, a region that demarcates the boundary between dorsal and ventral muscle. Genetic mosaic analysis reveals that Topped function is required in ventromedial fast muscle for CaP axons to extend ventrally. Furthermore, the degree of rescue is dependent upon the ventral extent of wild-type muscle cells. Taken together, our analysis suggests that Topped functions either as a short range or membrane bound cue in medial fast muscle that defines the ventral motor axon pathway.

Ventral motor axon outgrowth is specifically affected in topped mutants

The only defect found in *topped* mutants is delayed axon outgrowth into the ventral myotome. Because this mutant was found in an immunohistochemistry screen designed to uncover defects in primary motor axons (Beattie et al., 1999), it is not surprising that such a subtle mutation was

found. The finding that these axons eventually extend into the ventral myotome suggests that this mutation may not be a null allele; alternatively, there may be redundant cues in the ventral myotome. Both primary and secondary motor nerves were delayed entering the ventral myotome in *topped* mutants suggesting either that secondary motor axons defects are due to the defects in the primary motor axons (see Pike et al., 1992) or that both populations of ventrally extending motor axons respond to the same cues. Zeller et al. (2002) showed that both primary and secondary motor axons were aberrant in *diwanka* mutants and that the secondary motor axons defects did not directly follow the primary motor axon defects suggesting that both populations were responding to pathfinding cues in the myotome. Moreover, we found that secondary motor axons had extended further ventrally at 30 hpf than primary motor axons. Therefore, data from mutant analysis thus far supports the idea that both primary and secondary motor axons are responding to myotomally derived pathfinding cues.

We found no other defects in *topped* mutant embryos suggesting that *Topped* specifically functions to promote ventral motor axon outgrowth along the ventral myotome. In particular, we did not find defects in the MiP axons, which project dorsally. Another zebrafish axon guidance mutant, *unplugged*, affects CaP and RoP motor axon pathway choice at the horizontal myoseptum leaving MiP unaffected (Zeller and Granato, 1999). These data support the idea that the different primary motoneurons are responding to unique cues that enable the formation of their stereotyped axonal projections.

Fast muscle and ventral axon outgrowth

Like other vertebrates, zebrafish have both fast and slow muscle fibers. The origins of these muscle fibers are unique as are their developmental properties. The majority of the cells in the zebrafish somite will give rise to the myotome with only a small region of the ventromedial somite giving rise to sclerotome (Morin-Kensicki and Eisen, 1997). Slow muscle starts as a group of approximately 20 cells adjacent to the notochord, referred to as adaxial cells, and fast muscle comprises the remainder of the myotome. At about 18 hpf all but 3-6 slow muscle cells begin to migrate dorsally and ventrally and then radially through the developing fast muscle and ultimately reside as the most lateral cells in the myotome (Devoto et al., 1996; reviewed in Stickney et al., 2000). The slow muscle cells that fail to migrate are located at the horizontal myoseptum and are referred to as muscle pioneer cells (Felsenfield et al., 1991; Devoto et al., 1996). After slow muscle migration, fast muscle becomes the most medially located muscle type in the myotome. The timing of CaP axon outgrowth coincides with the radial migration of slow muscle cells (Zeller and Granato, 1999) such that CaP growth cones extend along ventromedial fast muscle as it is exposed by the migrating slow muscle.

Analysis of two zebrafish mutants, *diwanka* and *unplugged*, have identified cues important for axon guidance that function in slow muscle (Zeller and Granato, 1999; Zhang and Granato, 2000). *Diwanka* function is needed in only 1-3 adaxial cells located between the ventral aspect of the spinal cord and the horizontal myoseptum and is necessary for establishing the common pathway

used by all primary motor growth cones (Zeller and Granato, 1999). Unplugged function is required in 3 or more adaxial cells in the same region and is necessary for CaP and RoP to make the correct pathway choice at the first intermediate target (Zhang and Granato, 2000). Diwanka and Unplugged, therefore, appear to function as slow muscle derived signals that affect axon guidance on the fast muscle.

Our analysis of *topped* mutants reveals that fast muscle cells also contain cues essential for directed growth cone migration. The finding that the extent of CaP axon rescue in the genetic mosaics depended on the dorsoventral location of the transplanted wild-type cells and that gaps of 3 or more wild-type medial fast muscle cells failed to rescue mutant CaP axons suggests that Topped may function as a contact mediated or short range attractive cue. We found no evidence of abnormal muscle development suggesting that *topped* does not function in fast muscle maturation (Fig. 2.7). The finding that MiP axons are unaffected in *topped* mutants suggests that Topped does not function as an inhibitory molecule for non-ventrally extending axons.

topped, together with the previously characterized mutants that affect CaP axon pathfinding indicate that numerous cues are indispensable for wild-type axon guidance. *diwanka* is needed to set-up the common pathway, *unplugged* is needed for CaP and RoP to make the appropriate choice at the first intermediate target, *stumpy* is needed for axons to proceed past intermediate targets, and *topped* is needed for CaP axons to extend into the ventral myotome. Topped function is unique in that it is the only mutation that specifically affects one class

of neurons; those extending into the ventral myotome. Studies underway will identify the molecular nature of *topped* and begin to address its biochemical mechanism of action. Moreover, eventual analysis of *topped* in other species may reveal conserved mechanisms establishing dorsoventral innervation of axial muscle.

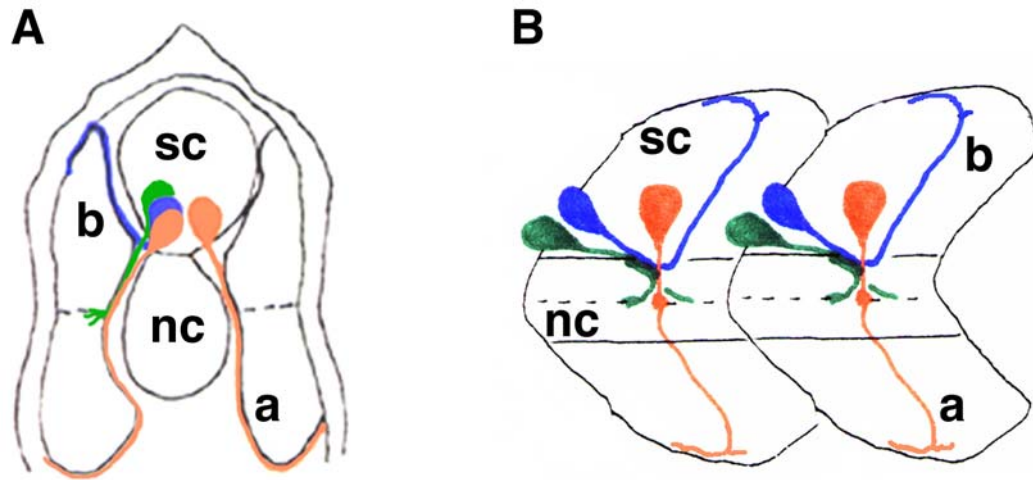


Figure 2.1: Schematic diagram of the primary motor axon pathways at 26 h. (A) Cross-sectional view of the three primary motoneurons. (B) Lateral view of spinal cord hemisegments. The CaP (orange), MiP (blue), and RoP (green) cell bodies are located in stereotyped positions in the ventral spinal cord. CaP growth cones exit the spinal cord at approximately 18 hpf, and extend ventrally until they reach the first intermediate target, the nascent horizontal myoseptum (dashed line), where they pause for 1-2 h. The CaP axon then continues ventrally along the ventromedial myotome (a). MiP axons extend along the dorsomedial myotome (b), and RoP axons extend through the horizontal myoseptum. Due to the normal variability in axon outgrowth at 26 hpf, schematics are representative. sc, spinal cord; nc, notochord.

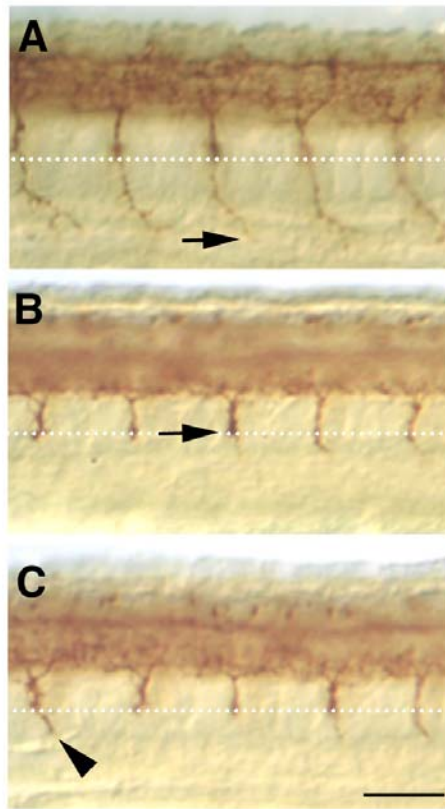


Figure 2.2: CaP axons in *topped* mutants exhibit a stall phenotype at the first intermediate target. Lateral views of whole-mount antibody labeling with znp1 of 26 hpf *topped* wild-type sibling (A) strong homozygous (B) and weak homozygous (C) mutants. The dashed line denotes the first intermediate target. Arrows indicate CaP growth cone position. Arrowhead indicates a CaP axon extending past the first intermediate target. Bar, 35 μm .

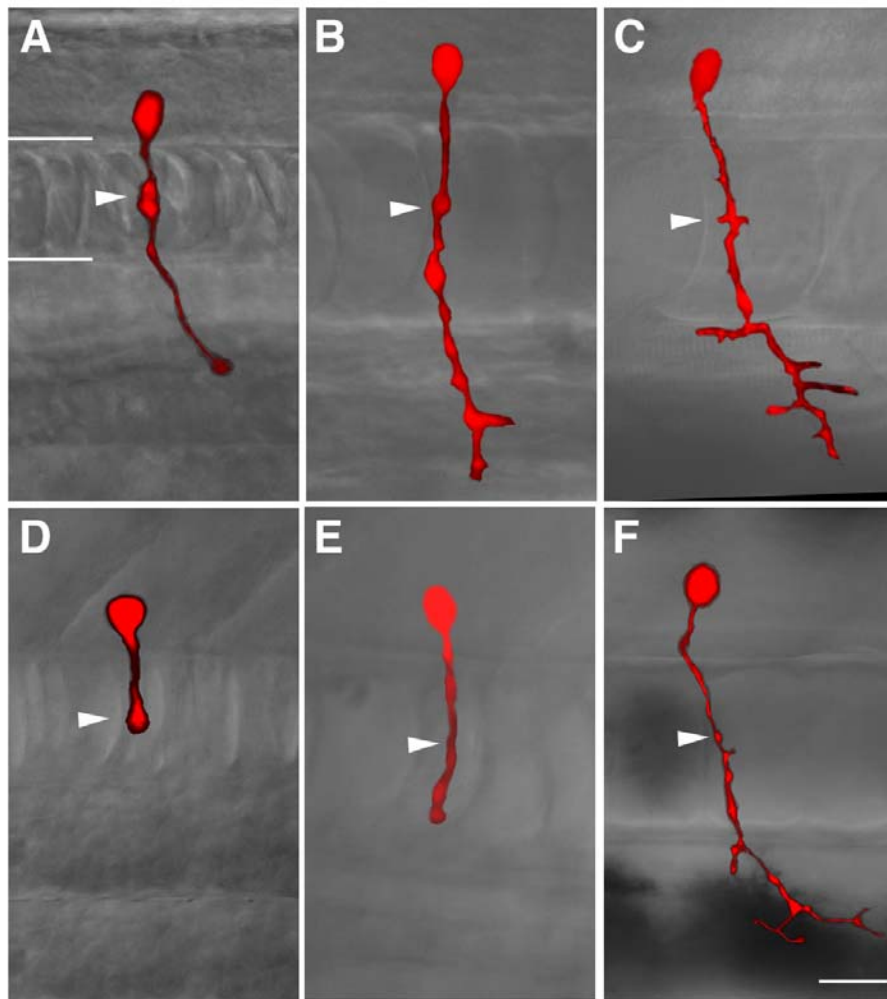


Figure 2.3: CaP axons are delayed entering the ventral myotome in *topped* mutants. Individual CaP cell bodies were iontophoretically labeled in living wild-type (A-C) and *topped* mutants (D-F) with rhodamine dextran and imaged at approximately 25 hpf (A, D), 29 hpf (B, E), and 45 hpf (C, F). Axons were imaged along the medial pathway. Arrowheads denote the first intermediate target. White lines indicate the dorsal and ventral aspects of the notochord. Bar, 25 μ m.

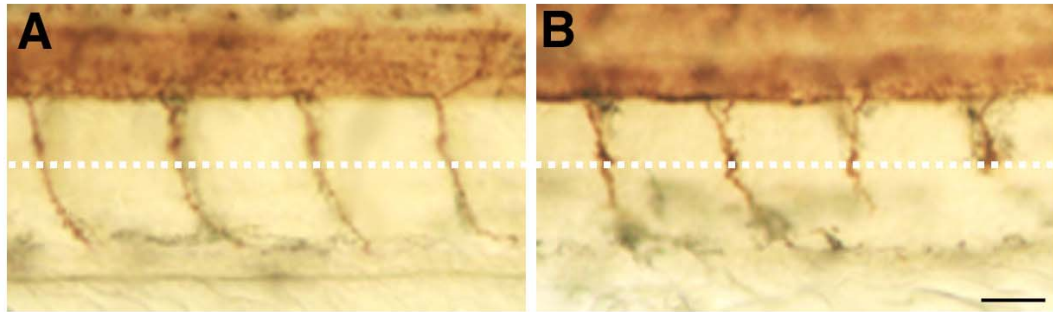


Figure 2.4: Formation of ventral nerves is delayed in *topped* mutants. Wild-type (A) and *topped* mutant (B) embryos labeled with *znp1* at 30 hpf. The first intermediate target is denoted by the white dashed line. The arrowhead indicates a nerve stalled at the first intermediate target, and the arrow indicates a nerve stalled at the myotome adjacent to the ventral edge of the notochord. Bar, 20 μm .

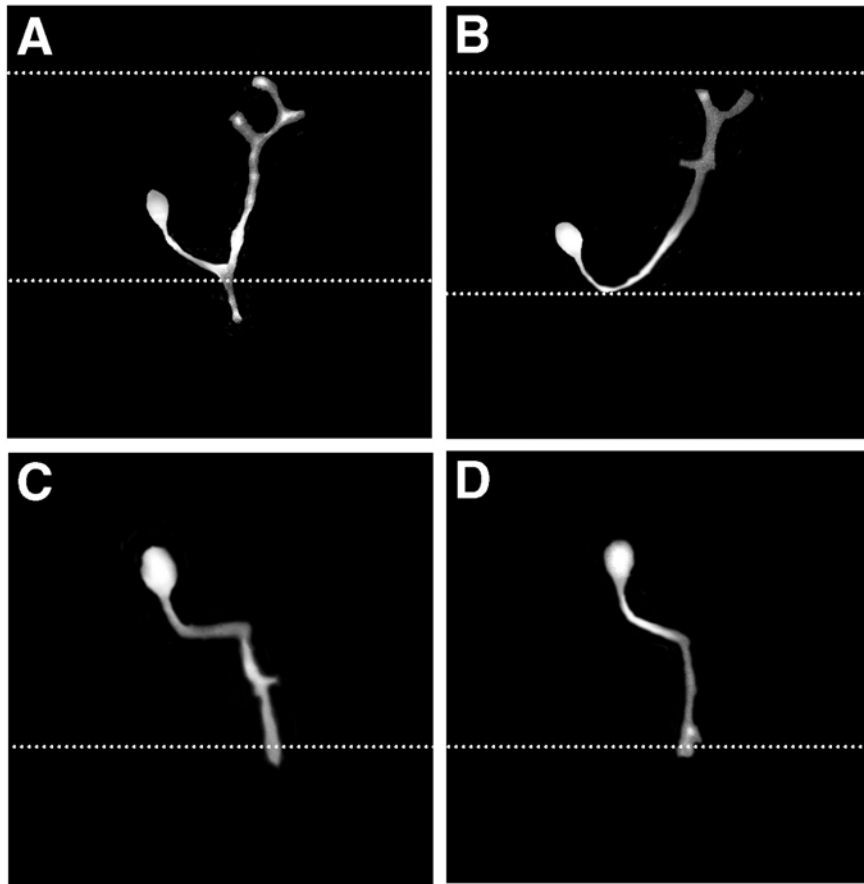


Figure 2.5: MiP and RoP axons are unaffected in *topped* mutants. Iontophoretically labeled MiP motoneurons in living wild-type (n=6; A) and *topped* mutants (n=8; B) at 29 hpf. Dashed lines in A and B indicate the dorsal and ventral aspects of the spinal cord. RoP motoneurons were labeled in living wild-type (n=5; C) and *topped* mutants (n=5; D) and imaged at 30 hpf. Dashed line in C and D indicates the first intermediate target. Bar, 20 μ m.

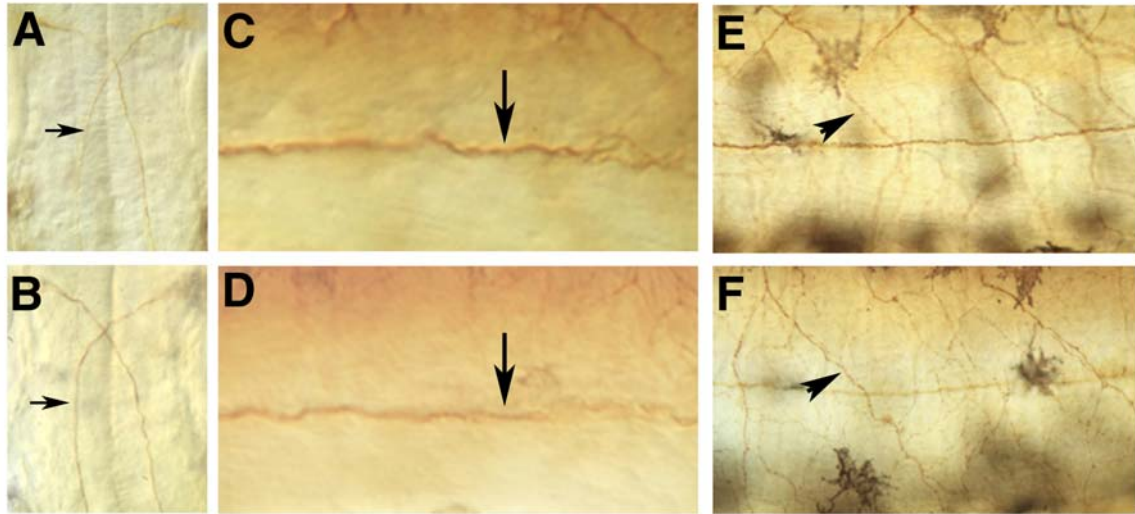


Figure 2.6: Other neuronal cell types are unaffected in *topped* mutants.

Dorsal view of the hindbrain Mauthner interneuron cell bodies and axons (arrowhead) stained with 3A10 at 30 hpf in wild-type (A) and *topped* mutants (B). Lateral view of the lateral line sensory neurons (black arrow) stained with acetylated tubulin antibody at 30 hpf in wild-type (C) and *topped* mutants (D). Lateral view of Rohon-Beard sensory axons (arrowheads) stained with acetylated tubulin antibody at 36 hpf in wild-type (E) and *topped* mutants (F).

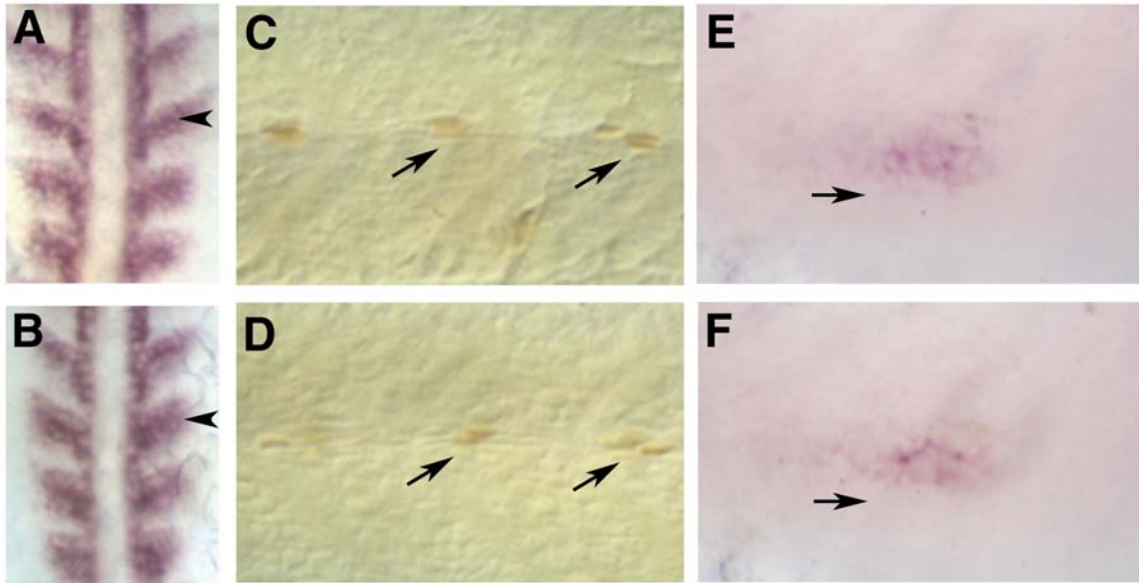


Figure 2.7: Myotome is unaffected in *topped* mutants. Dorsal view of 14 hpf in situ hybridization of *myoD* in wild-type (A) and *topped* mutants (B). Arrowheads indicate intact somite boundaries. Lateral views of 24 hpf wild-type (C) and *topped* mutants (D) stained with 4D9 antibody. Arrows indicate muscle pioneer cells; a subset of slow muscle. Lateral views of 30 hpf in situ hybridization of *robo1* in wild-type (E) and *topped* mutants (F). Arrows indicate the lateral line primordium.

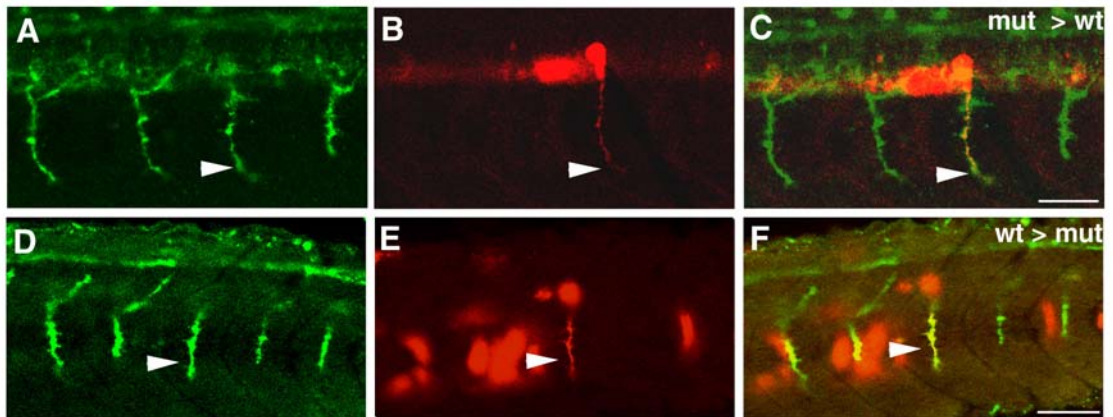


Figure 2.8: Topped acts non-cell-autonomously with respect to CaP. (A, D) FITC image of *znp1* labeled CaP axons. (B, E) Transplanted rhodamine labeled cells. (C, F) Merged images. (A-C) Lateral views of 27 hpf wild-type host embryo containing transplanted cells derived from a rhodamine labeled *topped* mutant donor (B). White arrows indicate a mutant CaP with a wild-type morphology. (D-E) Lateral view of a 27 hpf *topped* mutant embryo containing transplanted cells derived from a wild-type donor. White arrows indicate a wild-type CaP exhibiting a stall phenotype in a *topped* mutant. (A-C) Bar, 20 μm . (D-E) Bar, 40 μm .

Donor genotype	Host genotype	Result
wild-type	wild-type	14/14 wild-type (100%)
<i>topped</i> ^{-/-}	wild-type	12/12 wild-type (100%)
wild-type	<i>topped</i> ^{-/-}	12/12 mutant (100%)

Table 2.1: Topped is non-cell-autonomous for CaP motoneurons. Donor embryos were labeled with rhodamine dextran. Cells were transplanted from wild-type donors into embryos collected from a heterozygous *topped* mating and vice versa to obtain the above scenarios. Donor and host embryos were fixed at 26 hpf and antibody labeled to determine genotype. The embryos were then examined for the presence of rhodamine labeled transplanted CaP motoneurons. The result indicates the number and percentage of the indicated phenotype of the transplanted CaP axons.

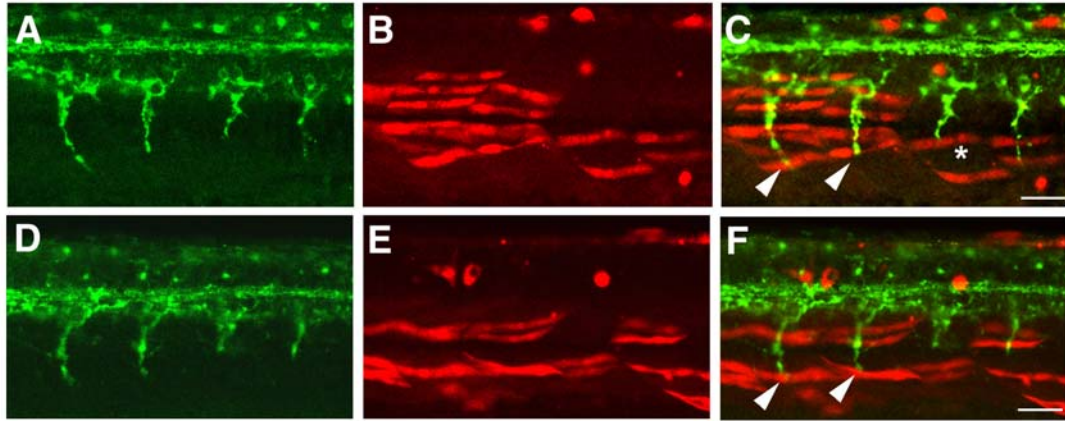


Figure 2.9: Wild-type muscle rescues the CaP axon defect in *topped* mutants. Wild-type rhodamine labeled cells were transplanted into *topped* mutant host embryos. (A, D) Lateral view of a *znp1* labeled 27 hpf *topped* mutant embryo containing transplanted wild-type rhodamine-labeled muscle cells (B, E). (C, F) Merged image indicating that the transplanted wild-type muscle is able to rescue the CaP axon defect in *topped* mutants. Arrowheads indicate that CaP axons are rescued to the location of the most ventral muscle cell; asterisk in C indicates a space the width of three muscle cells does not allow rescue of the CaP axon. Bar, 20 μm .

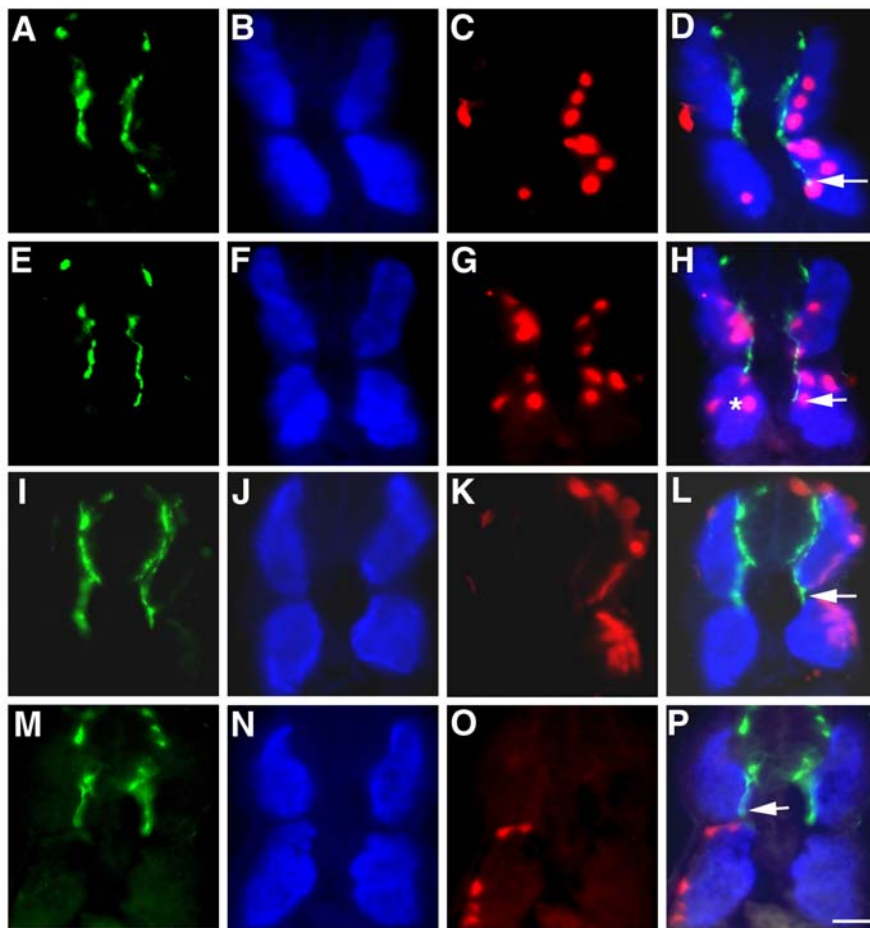


Figure 2.10: Topped is functioning in ventromedial fast muscle to promote CaP axon outgrowth into the ventral myotome. Wild-type rhodamine-labeled cells were transplanted into *topped* mutant host embryos. Using cross-sectional analysis, we determined the position of the transplanted muscle (red); (C, G, K, O) and the corresponding position of F310 labeled fast muscle cells (B, F, J, N) in *topped* mutants as shown by antibody labeling with *znp1* (A, E, I, M). Merged image of rhodamine, FITC, and DAPI images indicates the juxtaposition of the CaP axon and the transplanted wild-type muscle (D, H, L, P). Purple cells in (D, H, L) indicate doubly labeled fast muscle cells. Only ventromedial fast muscle was able to rescue the CaP axon defect in *topped* mutants (A-D) and (E-H). White arrows denote where CaP axons are rescued to the location of transplanted wild-type fast muscle cells. Asterisk in H indicates that a fast muscle cell in roughly the same dorsoventral position as the one in the corresponding hemisegment is not able to rescue the CaP axon defect due to its more lateral position. (I-L) The presence of ventrolateral fast muscle cells or slow muscle cells at the horizontal myoseptum (P) fail to rescue the CaP axon defect in *topped* mutants. Bar, 30 μ m.

Cell type	<i>n</i>	% Rescue
Medial fast muscle	45 (25)	100
Lateral fast muscle	46 (23)	0
Slow muscle	17 (14)	0
Notochord	33 (15)	0
Floor plate	18 (10)	0

Table 2.2: Topped is required in ventromedial fast muscle. Wild-type cells were transplanted into *topped* mutant embryos and the ability of particular cell types to rescue CaP axons was determined. To determine the type and position of transplanted muscle, a subset of the embryos were sectioned. Numbers for notochord and floor plate were counted only when the entire hemisegment contained transplanted cells (approximately 3 cells per hemisegment). *n* = the number of hemisegments where the various cell types were present and the number in parenthesis corresponds to the number of embryos

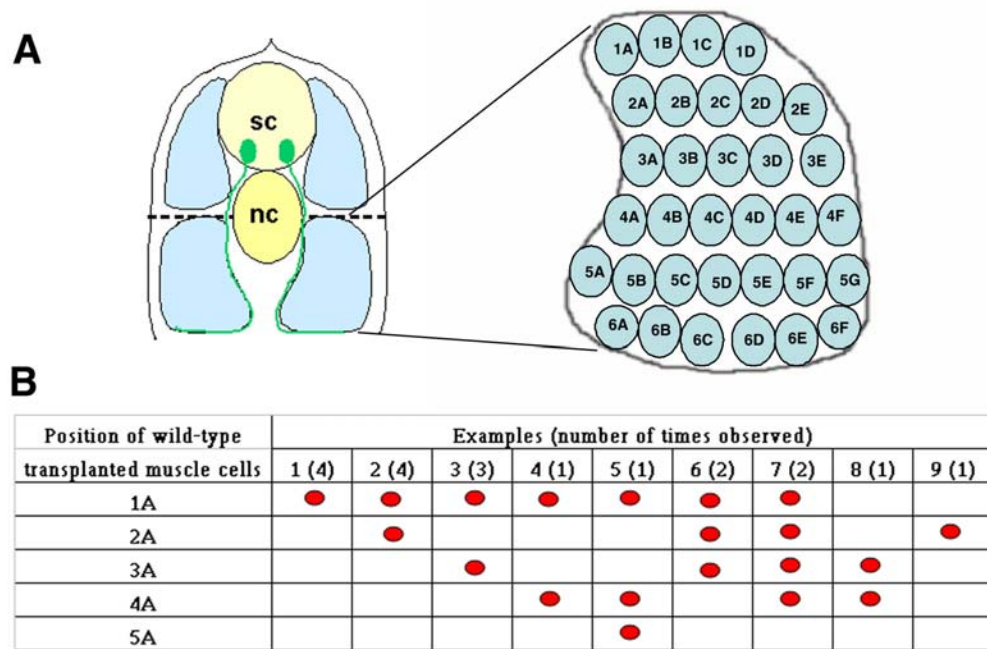


Figure 2.11: Schematic depiction of wild-type muscle cells that rescue CaP axons in *topped* mutants. (A) Cross section of the mid trunk of a 26 hpf embryo. Fast muscle is indicated in blue, wild-type muscle in red, and CaPs in green. For clarity, CaP cell bodies and axons are the only primary motoneurons shown. (B) A representative ventral myotome hemisegment where each myotome cell is given a number and letter designation. (C) Graph exhibiting a detailed description of position of rescuing cells (red). In each example, CaP axons were rescued to the ventral most wild-type muscle cell. *n* refers to the number of hemisegments. sc, spinal cord; nc, notochord.

CHAPTER 3

POSITIONAL CLONING OF TOPPED AND THE IDENTIFICATION AND CHARACTERIZATION OF ZEBRAFISH SEMAPHORIN 5A

Introduction

Zebrafish forward genetic analysis in which genetic mutations are induced is powerful because the embryo conveys what genes are important for specific developmental processes; in the case of this thesis work, ventral motor axon pathfinding. However, identifying the genes that contain the lesions responsible for the mutant phenotypes is a difficult and timely process. In the 1990s, the emergence of zebrafish as a developmental model system in which forward genetics could be conducted readily sparked the necessity of successful cloning methods. Zebrafish researchers built on previously known positional cloning methods and developed a zebrafish linkage map, radiation hybrid maps, and fish specific positional cloning techniques (Knapik, et al., 1996; Knapik et al., 1998; Talbot and Schier, 1999; Amamiya et al., 1999; Geisler et al., 1999)

Positional cloning is a process whereby mutations are revealed based on their linkage to a particular region using markers that recognize polymorphisms in

the genome. Mutations are induced in one strain of fish and then outcrossed to another strain that is polymorphic to that strain. Polymorphisms are base pair differences present throughout the genome that do not change amino acid sequences but are detectable via different PCR methods. Simple Sequence Length Polymorphisms (SSLP) markers are designed based on these differences and were used to create a standard zebrafish genetic linkage map to which any mutation could be mapped (Knapik et al., 1996; Shimoda et al., 1999). The use of zebrafish Bacterial Artificial Chromosome (BAC) and P1 Artificial Chromosome (PAC) clones further advanced the process by creating physical maps onto which mutations could be placed (Amemiya et al., 1999).

In zebrafish, the use of the early pressure method (EP) to create parthenogenic diploid embryos allowed researchers to not only link their mutation to a chromosome, but also determine genetic distance from the centromere (Streisinger, 1981). In this method, eggs are fertilized with UV irradiated sperm and then subjected to pressure using a French press to suppress the second meiotic division, thus creating maternally diploid embryos. Since the second meiotic division is suppressed, the region of the chromosome between the centromere and the mutation cannot be recombined; therefore centromeric markers can be used for each chromosome to assign linkage to a mutation. In addition, the equation [distance in cM = 50 (1-(2 x mutant number/total number of embryos))] can be used to calculate genetic distance from the centromere. For example, if the ratio of progeny obtained from a heterozygous female was 50 wild type:25 mutant, then the mutant would be located approximately 16 cM from the

centromere. Fine mapping, where the precise location of mutation is revealed by analyzing recombination frequencies, was advanced through the use of haploid embryos. In this case, eggs from a heterozygous female are fertilized with UV irradiated sperm to create maternally haploid embryos. UV irradiation of the sperm destroys the paternal DNA, but does not diminish the sperms capacity to fertilize. Both wild-type and mutant progeny are kept as individuals and processed for PCR. Chromosome specific markers are then used to test all the individuals to identify recombination events. The more closely linked a mutation and a marker are to one another, the more infrequent recombination; therefore genetic distance is determined based on recombination frequency where the number of recombinants/total number of individuals equals distance in cMs (centiMorgan). This allows researchers to narrow down the genomic region containing the mutation and identify candidate genes.

Most recently, the zebrafish genome sequencing project by the Sanger Center has made the process of positional cloning slightly easier. Now, Sanger has mapped BAC clones onto their genome map and provides gene predictions, allowing researchers to identify candidate genes more readily. Although positionally cloning mutations in zebrafish is a difficult process, the rewards of analyzing gene function in an in vivo model greatly outweigh the difficulties. As discussed in this chapter, I have undertaken a positional cloning approach to uncover the molecular lesion in *topped* mutants. Although this journey has been difficult, my efforts have resulted in a win-win situation, in which I have either

identified the gene affected in *topped* mutants or an additional gene functioning in ventral motor axon pathfinding.

Materials and Methods

Fish Strains and Maintenance

Mutant strains were maintained as heterozygous and homozygous (*topped*^{b458}) lines in the Tubingen long fin (TL)/ *AB background. Homozygous mutant *topped* embryos were generated by pairwise mating of *topped* heterozygous or homozygous fish. Embryos raised from matings were maintained between 25.5 and 28.5°C and staged by converting the number of somites to hours post fertilization (hpf; Kimmel et al., 1995).

Generation of Mutants

A mutagenesis screen was conducted (Beattie et al., 1999). Briefly, after exposure to 3 mM ethylnitrosourea (ENU) (Solnica-Krezel et al., 1994), adult male fish were outcrossed to wild-type females to create the F₁ generation. F₁ females were screened for mutations by using the early pressure method to examine parthenogenetic diploid F₂ embryos (Streisinger et al., 1981). The embryos were fixed and labeled with antibodies to identify mutants. F₁ females carrying mutations of interest were outcrossed and lines generated.

Genetic Mapping

To map *topped*, mutants in the *AB background were outcrossed to the TL strain to create a polymorphic mapping line. Parthenogenetic F₂ diploid embryos were produced by fertilizing mutant carrier eggs with UV-irradiated sperm (Striesinger et al., 1981). Individual embryos were scored as mutant or wild type based on antibody labeling. Genomic DNA was isolated and PCR was performed with SSLP markers to obtain centromeric linkage (Johnson et al., 1995, 1996). For fine mapping, haploid embryos were generated from polymorphic heterozygous *topped* females. Polymorphic SSLP and EST markers were then used to identify recombinants to determine physical distance from the *topped* mutation.

Genomic Cloning and Sequencing

The zebrafish *semaphorin5a* gene was isolated by reverse transcription PCR (Qiagen One-Step RT-PCR kit) using total RNA from 24 hpf pooled AB* or homozygous mutant *topped*^{b458-/-} embryos. Gene specific primers were designed based on predicted *semaphorin5a* coding sequence from the Sanger Ensemble database (www.ensembl.org/Danio_rerio) (Table 3.2). RT-PCR products were cloned using the Invitrogen Topo TA Cloning kit. Resulting colonies derived from either AB* or mutant RNA were sequenced with either SP6 or T7 primers.

BAC and Heterologous RNA Rescue

For genomic rescue, *danio rerio* BAC clones CH211-277N6, CH211-112I15, DKEY-8B6, and DKEY-96N22 (RZPD Deutsches Ressourcenzentrum für Genomforschung GmbH, Heubnerweg 6, D-14059 Berlin, Germany) were injected at a concentration of 100 ng/ul at the one cell stage into homozygous mutant *topped* embryos. Injected embryos and uninjected controls were fixed at 26 hpf and stained with znp1 antibody. For heterologous RNA rescue, the full-length rat *sema5a* gene (Kantor et al., 2003) was cloned into the PCS2 vector. Capped polyA *sema5a* mRNA was transcribed using the mMessage mMachine (Ambion) SP6 kit and injected at the one cell stage into homozygous mutant *topped* embryos at 333 ng and 500 ng doses. Injected embryos and uninjected controls were fixed at 26 hpf and stained with znp1 antibody.

Morpholino Analysis

For antisense oligonucleotide morpholino mediated knockdown of *Sema5a*, a splice blocking morpholino was designed to the splice donor site of exon 6 (Gene Tools, LLC: CTTCTTTACTTACACATTACTGGTG). 18 ng of morpholino was injected at the one cell stage. Embryos were allowed to develop to 26 hpf, and subsequently stained with znp1 or used to isolate total RNA for RT-PCR analysis. To test the efficiency of the morpholino, RT-PCR was performed using the One-Step RT-PCR kit (Qiagen). *Sema5a* transcript specific primers flanking the targeted morpholino site were used to amplify an 1100 bp fragment in uninjected controls and an 850 bp fragment in MO injected embryos.

Whole Mount Antibody Labeling

Whole mount antibody labeling was performed as described in Eisen et al., (1989) and Beattie et al., (2000). The znp1 monoclonal antibody that recognizes primary and secondary motor axons (Trevarrow et al., 1990; Melancon et al., 1997) was detected using the Sternberger Clonal-PAP system with diaminobenzidine (DAB) as a substrate (Beattie and Eisen, 1997), or with Oregon Green goat anti-mouse IgG (Molecular Probes). Embryos were analyzed with a Zeiss axioplan microscope.

Whole-mount In Situ Hybridization

Whole-mount in situ hybridization was performed as described by Thisse et al. (1993). An antisense digoxigenin *sema5a* riboprobe was synthesized from a plasmid linearized with HindIII and transcribed with T7.

Results

Positional cloning of zebrafish topped

We previously mapped the *topped* locus near the centromere of chromosome 24 (Rodino-Klapac and Beattie, 2004). Subsequently, I undertook a fine mapping approach with haploid mutant *topped* embryos using SSLP markers and expressed sequence tags (EST) markers to determine physical

distance from the *topped* locus. For fine mapping, both wild-type and mutant haploid embryos were obtained from the same heterozygous *topped* female and kept as individuals. Subsequently, I performed PCR on genomic DNA isolated from each embryo using SSLP and EST markers on chromosome 24. The number of recombinant events between the various markers and the mutation were scored, based on the fact that the more closely linked the mutation is to each marker, the more infrequent recombination will be. Markers on opposing sides of the mutation (5' vs. 3') generated a different set of recombinants. From these data, a recombinant panel was generated and the region of interest was narrowed by identifying markers with fewer and fewer recombinants on either side of the mutation. Closely linked flanking markers were identified as z9321 with 1/79 recombinants and z3399 with 2/85 recombinants yielding genetic distances of 1.3cM and 2.3cM respectively (Fig. 3.1). A cM (centiMorgan) in zebrafish averages 625 kb, but is highly variable and could actually be 100kb or 1mb depending on whether you are working in a region of compression, where recombination is infrequent (Postlethwait et al., 1994). The cM distances for z9321 and z3399 indicate that *topped* is located more closely to the 5' end of the interval; however the sample size is small, due to difficulties obtaining polymorphic markers and accurately identifying *topped* mutant haploids. In addition, the *topped* mutation is located close to the centromere where recombination is suppressed; therefore the cM distance may not be an accurate reflection. For all these reasons, we decided to look at annotated genes and ESTs in this region to see if any candidate genes were present. At the time, the

zebrafish genome was partially sequenced and annotated by the Sanger Center; therefore I located markers z9321 and z3399 on the genome website (www.ensembl.org) and looked for predicted open reading frames in this region (Table 3.1). Scanning the list of candidate genes, the predicted *semaphorin 5a* gene was intriguing. Semaphorins are a large family of axon guidance molecules that can function as either inhibitory or attractive cues. Based on our previous prediction that Topped was functioning as an attractive ventral cue, *Sema5a* was a good candidate to test above the other candidates listed.

Cloning of zebrafish sema5a

The *sema5a* gene was partially annotated by Sanger with predictions for the first 14 exons. In addition, an EST 3' to this exhibited homology to the 3' end of *sema5a*. Using Sanger's prediction for the 5' portion of the *sema5a* gene and the EST fi41a04 for the 3' end of the gene, I designed primers and performed RT-PCR on wild-type RNA to isolate these regions of the *sema5a* cDNA (Table 3.2). Initially, I cloned the cDNA in three pieces using primer sets 1, 2; 3, 4; and 7, 8 from Table 3.2 corresponding to exons 1-14 and 17-20 (Fig. 3.2, Table 3.3). However, the middle portion of *sema5a* corresponding to exons 15 and 16 were absent from Sanger's prediction. To isolate this portion of the cDNA, I designed a forward primer in exon 14 and a reverse primer in exon 17. I successfully isolated the cDNA which exhibited homology to mouse and human *sema5a* exons 15 and 16. To determine the intron/ exon boundaries, I aligned the cDNA

sequence with the zebrafish genomic database and deduced the proper boundaries by comparing cDNA and genomic sequence (Table 3.3). In total, the zebrafish *sema5a* gene is composed of 20 exons spanning a genomic region of over 200kb with large introns in the 5' end of the gene (Fig 3.3). The coding region identified thus far is approximately 3.1 kb.

Alignments of zebrafish *sema5a* cDNA with mouse, rat, human, and chimp revealed that *sema5a* is highly conserved among those species (Fig. 3.4). Zebrafish *sema5a* is approximately 75% similar to mouse *sema5a* and 71% similar to human *sema5a* (Fig. 3.5). Analyzing the *sema5a* cDNA in relation to the other species revealed I had cloned the entire cDNA including the stop codon, with the exception of the first part of exon one containing the start codon (Fig 3.4). The alignment revealed that there is an additional 87 bp upstream of zebrafish *sema5a* exon 1 in the other species which is part of exon 1 in those species. I then blasted this 87 bp region against the zebrafish genome and against BACs that contain the *sema5a* gene (see below), and found no sequence homology. 5' RACE (Rapid Amplification of cDNA ends) PCR will be conducted to reconcile the exact sequence of exon 1 in zebrafish including the start site and consensus sequences.

In other vertebrates, there are two Semaphorin class 5 molecules, A and B. To determine if zebrafish also has two forms of this gene, I scanned the zebrafish genome for *sema5b* to verify the gene I had cloned was the homolog of *sema5a*. I found the predicted homolog of *sema5b* to be located on chromosome 9. *Sema5b* was annotated more completely; therefore alignment of

sema5a and *sema5b* was relatively simple. Overall, *sema5a* and *sema5b* are 46% identical, with a higher degree of homology in the Sema domain (74%) and the Thrombospondin domain (71%) (Fig. 3.6).

Analysis of sema5a as a candidate for topped

The juxtaposition of *sema5a* within the *topped* critical region, along with the Semaphorins having known roles as axon guidance molecules made it a priority candidate for *topped*. I undertook a multi-faceted approach to determining if *topped* is a mutation in *sema5a*; including sequencing, expression analysis, rescue experiments, and knock-down analysis. Due to the large size of the *sema5a* gene, the sequencing was done in parallel to the other qualitative experiments.

I began the difficult task of sequencing the *sema5a* gene in *topped* mutants to look for a molecular lesion by sequencing the *sema5a* cDNA obtained by isolating RNA from both wild-type and *topped*^{-/-} 24 hpf pooled embryos. The resulting PCR products were cloned into the TOPO vector and sequenced using SP6 and T7 primers. The resulting sequences were aligned with the ClustalW (EBI) program and looked for consistent base pair changes in *topped* mutants versus wild type. As previously mentioned, the cDNA I cloned was complete with the exception of the 5' region of exon one. I found no mutations in the coding region in *topped* mutants thus far. Next, I sequenced the splice acceptor and donor sites flanking each exon by sequencing from intron to intron across each exon. For exon one, I sequenced 137 bp upstream of where the exon was

predicted to begin. Within this region is a potential ATG in frame, but no consensus RNA POLII binding site. There were no mutations found in these regions. Further characterization of the 5' end of the *sema5a* gene will be necessary to conclude that there are no mutations in *topped* mutants in the *sema5a* coding region.

Zebrafish sema5a is expressed in the ventral myotome

CaP motor axons begin to extend out of the spinal cord at 18 hpf, and complete their outgrowth along the medial pathway by 24 hpf, thus we would predict guidance cues functioning in this process would be expressed during these time points. To examine the expression pattern of *sema5a* in zebrafish, I conducted RNA in situ hybridization at 18 and 24 hpf. I generated antisense probes from four different *sema5a* fragments from non-overlapping regions. *sema5a* transcript was detected in the ventral myotome at both time points. Looking laterally, at 18 hpf, *sema5a* transcript levels were higher in the rostral ventral myotome (Fig. 3.7 A). By 24 hpf, the expression had progressed more caudally, and was detected throughout the ventral myotome (Fig. 3.7 A). At all time points analyzed, I was unable to detect any measurable differences in the levels of *sema5a* expression in wild-type versus homozygous *topped* mutant embryos (Fig. 3.7 A). I also sectioned wild-type embryos and looked at *sema5a* expression, and found it to be expressed in the ventromedial myotome (Fig. 3.7

B). This was very intriguing due to the fact that we previously showed *Topped* was functioning specifically in those cells.

To verify that *sema5b* is not compensating for *sema5a* function, I also conducted in situ hybridization with *sema5b*, and found the expression pattern was non-overlapping with that of *sema5a*. At 18 hpf, *sema5b* transcript was detected exclusively in the head, with expression in the ventricles of the developing brain and in the midline (Fig. 3.8 A). At 24 hpf, *sema5b* expression continued in the ventricles, but also at low levels in the notochord (Fig. 3.8 A, B). From this data it can be concluded that *sema5a* and *sema5b* have functionally independent roles in the embryo.

BAC Rescue Analysis

From the expression analysis, I concluded that the *sema5a* transcript was present at the right place and time to be functioning like *topped*, as a ventral cue. Therefore, I went on to see if I could rescue the *topped* mutant phenotype with *sema5a*. The first approach I took was to obtain BAC clones in the *topped* critical region that contained *sema5a*. Using the Sanger Center zebrafish ensemble, I scanned for BAC clones that mapped to this region. Clones CH211-277N6, CH211-112I15, DKEY-8B6, and DKEY-96N22 mapped within the critical interval. I injected these BACs at the single cell stage at 100ng/ul and found I could rescue the *topped* phenotype to varying extents (Table 3.4). PCR analysis with *sema5a* exon specific primers revealed that portions of the *sema5a* gene were present on each BAC clone (Table 3.4). All of the BACs contained the

Sema domains, and at least a portion of the TSR domain, while, CH211-112I15 and DKEY-96N22 contained the entire TSR domain and the transmembrane domain. I saw a higher degree of rescue with these BACs, suggesting the membrane bound forms of Sema5a were able to rescue the *topped* phenotype to a greater extent.

Heterologous RNA rescue with rat sema5a

Based on the finding that four BAC clones containing *sema5a* were able to rescue the *topped* CaP axon guidance phenotype, I asked whether the *sema5a* transcript could also rescue the *topped* phenotype. Since our cDNA was missing a portion of the 5' end, I performed rescue experiments with a full-length rat *sema5a* transcript generously provided by Dr. Alex Kolodkin (Kantor et al., 2004). I subcloned this cDNA into the PCS2 vector and generated capped PolyA rat *sema5a* RNA and injected it into *topped*^{b458} mutant embryos at the single cell stage. After whole-mount antibody labeling with znp1, the mutants were scored for rescue. Ten CaP axons per side (20 per embryo) were scored for growth cone position. Axons were considered rescued if their growth cones had proceeded past the myotome adjacent to the ventral edge of the notochord. I found that CaP axons were rescued in 40% of the hemisegments, with only 30% stalled at the first intermediate target (Fig. 3.9 B, C). This data lends evidence that the *topped* phenotype could result from a decrease in functional Sema5a protein. However, the possibility that Sema5a has a compensatory role for Topped in the ventral myotome cannot be ruled out.

Knockdown of zebrafish sema5a phenocopies the topped mutant phenotype

If *topped* were a mutation in *sema5a*, you would expect by knocking down *Sema5a* in wild-type embryos, you would see the same phenotype. To test this, I first employed SI antisense oligos. SI oligos are primers designed to your gene of interest with the first three and next to the last three bases modified with a sulfur group (Fig 3.10 B). I designed three SI oligos within the first six exons of *sema5a* and injected them at the single cell stage. After antibody staining with znp1, I scored CaP axons for growth cone position. I found 5% of CaP axons were stalled at or near the first intermediate target as in *topped* mutants (Fig. 3.10 A, C)

To test this further, more efficient knock-down approach, splice-blocking antisense morpholino oligonucleotides (MO). I designed a morpholino (Gene Tools) to the splice donor site of *sema5a* exon 6 to preferentially result in the excision of exon 7 causing a frameshift mutation in the *Sema5a* protein. I injected 18 ng of the morpholino at the one cell stage, and subsequently fixed and stained the embryos at 26 hpf. I scored 10 axons per side (20 per embryo) for growth cone position, and observed a stall phenotype in 52.6% of the hemisegments with growth cones located at either the first intermediate target or near the ventral edge of the notochord compared to 0% in wild type (Fig. 3.11 B, C). To verify that the morpholino was knocking down *Sema5a*, I conducted RT-PCR using total RNA obtained from both MO injected embryos, and uninjected wild-type siblings. Using gene specific primers, I amplified an 1100 bp *sema5a*

fragment in wild type and an approximately 850 bp *sema5a* fragment in MO injected embryos, consistent with a loss of exon 4 (Fig. 3.11 E). In my hands, I found the morpholino to be extremely efficient, as I was only able to amplify the fragment lacking exon 7 in the morpholino injected embryos. Subsequent sequence analysis confirmed the 820 bp fragment did not contain exon 7 in the Sema domain, causing a frameshift in the remainder of the protein (Fig. 3.11F).

To determine if further reducing functional Sema5a levels in *topped* mutants could exacerbate the CaP axon phenotype, I injected the Sema5a MO into homozygous mutants at the single cell stage. Since the *topped* phenotype can not be made worse at 26 hpf, I fixed and stained the embryos at 30 hpf and 36 hpf; time points when the phenotype is partially recovered. I found an exacerbation of the *topped* phenotype at both time points. Using the same method of scoring, at 30 hpf, I found 73.1% of CaP axons stalled at the first intermediate target in mutants compared to 37% in wild type (Fig. 3.12 B, E). Additionally, at 36 hpf, I found 17.1% in of CaP axons in mutants stalled at the first intermediate target compared to 1.5% in wild-type (Fig. 3.12 D, F). Taken together, these data show that knocking down Sema5a in a wild-type background can phenocopy the *topped* phenotype, and further reducing Sema5a levels in a *topped* mutant background can exacerbate the CaP axon phenotype. We can infer from these data, that *topped* is either a mutation in *sema5a*, or a gene functioning in the same pathway. The exacerbation of the *topped* phenotype by reducing levels of Sema5a suggests either that *topped* is a hypomorphic allele of *sema5a*, or as previously mentioned, an interacting gene.

Overexpression of sema5a results in aberrant ventral motor axons

To gain insight into how *Sema5a* may be functioning, I performed overexpression analysis. I injected the rat *sema5a* RNA at 500pg/nl at the single cell stage in wild-type embryos. In this technique, RNA is expressed at high levels in most cells. After antibody staining at 26 hpf, I scored CaP axons for position and overall morphology. I found 50% of embryos had branched axons that did not follow the normal pathway (Fig. 3.13 A). In addition, 20% of the embryos contained axons in which CaP axons on opposing sides of the embryo did not follow the same pathway as we see in wild-type embryos (Fig. 3.13 B, C; compare with wild type in Fig. 2.2 A). Lastly, 30% of the embryos showed no defects. The axon defects that presented support the hypothesis that *Sema5a* is functioning as an attractive cue. By overexpressing *sema5a* in regions it normally is not or above threshold levels, the axons may be attracted to these regions in an aberrant fashion, resulting in misrouted axon trajectories.

Sema5a function in ventral motor axon pathfinding

Previous mosaic analysis of the *topped* mutant phenotype, along with studies in other systems with *Sema5a* have alluded to potential functions of *Sema5a* in ventral motor axon pathfinding (Rodino-Klapac and Beattie, 2004; Kantor et al., 2004). We've previously hypothesized that *topped/sema5a* may be functioning as an attractant in the ventromedial myotome for CaP motor axons to

enter the ventral myotome (Rodino-Klapac and Beattie, 2004). To address this question, I tested a *sema5a* construct containing only one functional domain. Since *Sema5a* contains an inhibitory Sema domain, and a putative attractive TSR domain, I obtained a rat construct containing the TSR domain independently along with the transmembrane domain (Kantor et al., 2004). I generated capped Poly A mRNA and injected it into homozygous *topped* mutants. In the presence of the rat *sema5a* RNA containing only the TSR domain, I saw no rescue in *topped* mutants (n=75 embryos, 1500 axons). This data suggests that the *Sema5a* TSR domain alone is not sufficient to rescue the *topped* phenotype in vivo.

Discussion

The stereotyped outgrowth of ventral axial motor axons is dependent upon the presentation and proper integration of the appropriate guidance cues in the ventral myotome. Here we show that zebrafish *topped*, specifically affecting ventral motor axons, is phenocopied by the knock-down of *Sema5a*, a guidance cue expressed in the ventral myotome. In addition, the *topped* phenotype can be rescued either by injection of BAC clones containing portions of the *sema5a* gene or with RNA generated from a heterologous rat *sema5a* cDNA. Together, these results and others greatly support the hypothesis that the *topped* mutation

is most likely a mutation in *sema5a*. A mutation of this nature will not only be the first viable *sema5a* mutant, but will also be the first zebrafish Semaphorin mutation. Recently, a mouse knock-out of *Sema5a* was generated and found to be lethal at day E11 (Embryonic day) (Fiore et al., 2005). The only defects found were slightly less arborization of the cranial vasculature at E10.5. However, the homozygotes died prior to axial motor axon outgrowth; therefore these axons could not be characterized. As a result, a viable zebrafish *sema5a* mutant would be a powerful tool in understanding *Sema5a* function in ventral motor axon outgrowth, as well as its putative involvement in other developmental processes.

The topped critical mapping region contains other predicted genes

The topped critical region defined by fine mapping was not precise enough to solely indicate one candidate gene. The reasons for this were difficulty finding polymorphic markers, proximity to the centromere, and difficulty accurately scoring haploid *topped* mutants in all cases, thereby limiting sample size. Therefore, the possibility can not be ruled out that *topped* may be a mutation in another gene in this region. Looking at the other genes outlined in Table 3.1, *sema5a* is the most obvious candidate, however the remaining candidates cannot be disregarded. For example, there is an unnamed gene present with a homologous domain to Fibronectin III, a domain that is found in cell adhesion and/or axon guidance molecules. In addition, *tif2* is a transcription factor, and could likely affect a host of downstream genes. Although mounting evidence that

topped is *sema5a* resounds, until a mutation is identified, these other genes cannot be ruled out.

Isolation of a mutation in the sema5a gene in topped mutants

At this point, the majority of the *sema5a* open reading frame and splice junctions for each exon have been sequenced from *topped* mutants without the identification of a consequential mutation. As discussed earlier, the 5' end of exon one including the functional start codon have not been identified. Defining this region is critical not only for the identification of a mutation, but also for identifying the complete zebrafish *sema5a* transcript, as this gene has not previously been described. It is possible that the 5' end of the zebrafish homolog of *sema5a* is diverged significantly, and may include an additional coding exon. If this were the case, then a mutation could lie in this region in *topped* mutants. Given the fact that most mutations are found in coding regions, this possibility is most favorable for determining if *topped* is *sema5a*.

It is also reasonable to predict that a mutation exists within a *sema5a* genomic regulatory region that is affecting the *sema5a* transcript or protein product in *topped* mutants. Although more infrequent and more difficult to isolate; mutations of this nature can prove just as vital to the understanding of gene function. Non-coding mutations may produce changes in transcript levels either at the transcriptional or post-transcriptional stability level. To determine if this is the case in *topped*, several steps will be taken. In situ hybridization is not

quantitative, therefore Real-Time PCR will be utilized to analyze whether *sema5a* transcript levels are reduced in *topped* mutants. If we find transcript levels are reduced, this would indicate a mutation may exist that is affecting transcription or RNA stability. In addition, an antibody will be generated to an unconserved region of *Sema5a*. This antibody will be used in western analysis to examine whether *Sema5a* levels are decreased in *topped* mutants. The identification of additional *topped* alleles will increase the probability of isolating a mutation in the coding region, thus providing concrete proof as to whether *topped* is a mutation in *sema5a*.

Sema5a is expressed in the ventral myotome

In situ hybridization analysis revealed that *sema5a* is expressed in the ventral myotome of zebrafish embryos. The transcript is present at 18 hpf when primary motor axons just begin to extend out of the spinal cord and persists in the ventral myotome until 26 hpf when CaP motor axons have completed their journey along the medial pathway. After 26 hpf, *sema5a* expression becomes more diffuse throughout the myotome. The hypothesis that *Sema5a* is functioning as an attractive ventral cue is supported by the finding that *sema5a* transcript is present in the ventral myotome at the time when CaP ventral motor axons are extending into the ventral myotome. After these axons have completed their extension along the medial pathway at approximately 26 hpf, the cue is no longer needed, and transcript levels decrease.

Zebrafish sema5a and sema5b have non-overlapping expression patterns

Zebrafish *sema5a* and *sema5b* presented different expression patterns. *Sema5a* was found to be expressed in the ventral myotome, most distinctly between 18 and 26 hpf. Conversely, *sema5b* is expressed early at the midline and in the brain ventricles, and later at low levels in the notochord. These complementary expression patterns provide evidence against the hypothesis that these two class members play redundant roles in ventral motor axon pathfinding. Given that fact that motor axons recover in *topped* mutants, we are faced with two possibilities: redundant cues or a hypomorphic allele. The expression pattern of *sema5b* eliminates it as a potential redundant cue for *Sema5a*.

Topped may be a hypomorphic allele of sema5a

We found that we could exacerbate the *topped* mutant phenotype by further reducing levels of *sema5a* in *topped* mutants. This data supports the hypothesis that the *topped*^{b458} allele is a hypomorph with some functional protein still present allowing the phenotype to recover. However, we are unable to rule out the possibility that *sema5a* and *topped* are two genes functioning in the same pathway. By reducing *sema5a* levels in a *topped* background, we could be revealing a genetic interaction rather than additive non-complementation. Perhaps, *topped* and *sema5a* biochemically interact, and by knocking down two components of the same genetic pathway, we are witnessing an exacerbation of

the phenotype. This possibility will not be eliminated until we definitely show that *topped* is or is not *sema5a*.

Sema5a may be modulated by proteoglycans in the myotome or CaP axon growth cones

Kantor and colleagues (2004) recently identified that murine Sema5a is functioning in the diencephalon to promote that proper guidance of an axon tract called the fasciculus retroflexus. These axons extend from the habenular nucleus through the diencephalon to their final target in the interpenduncular nucleus (Kantor et al., 2004). Sema5a along with CSPGs out in the diencephalon acts as an inhibitory cue to keep axons from straying off their pathway. In addition, Sema5a along with HSPGs acts as an attractant along the FR pathway and keeps axons tightly bundled (Kantor et al., 2004). Zebrafish Sema5a may be functioning in a similar manner in the ventromedial myotome. We have previously shown that Topped is needed in only the most ventromedial myotome cells to promote CaP axon outgrowth (Rodino-Klapac and Beattie, 2004; Fig.8). Sema5a may be functioning as an attractant in those cells to promote ventral motor axon outgrowth, and in addition to as well as later, be functioning as an inhibitor in the remainder of the myotome to promote the outgrowth of a stereotyped and tightly fasciculated ventral nerve. The overexpression data where CaP axons migrated to improper regions of the myotome supports this hypothesis. This function may or may not be coincidental with the interaction with HSPGs and CSPGs. Future genetic and biochemical experiments with

Sema5a and the proteoglycans will undoubtedly impact our understanding of the genetic pathway dictating ventral motor axon outgrowth in zebrafish.

Sema5a is functioning in ventral motor axon pathfinding

Regardless of whether *topped* is *sema5a*, I have shown that Sema5a is playing a role in CaP axon outgrowth. By knocking down Sema5a in an otherwise wild-type background, CaP axons were stalled. This alone suggests that when Sema5a is not present, CaP axons cannot proceed into the ventral myotome correctly. Taken together with the fact that *sema5a* is expressed in the ventral myotome, we can hypothesize that Sema5a is acting as an attractive ventral cue for CaP motor axons. Future experiments will include a detailed characterization of *sema5a* morphants (morpholino injected embryos) including the analysis of other axon tracts, as well as other processes such as vasculogenesis and cell migration. These experiments will indicate whether Sema5a is functioning specifically in CaP axon outgrowth or whether it is playing multiple roles in development.

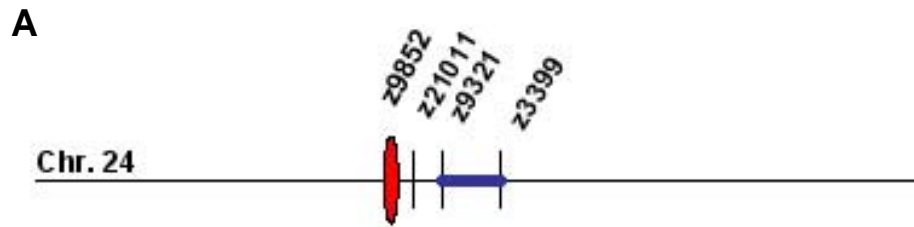


Figure 3.1: Genetic linkage map of *topped*. (A) The *topped* locus was found to be closely linked to flanking markers z9321 and z3399 on Chr. 24.

Name	Type transcript	Comments
Z9321 5'		
<i>sema5a</i>	Ensemble Transcript	Exons 1-14 annotated
fi41a04	EST	3'Sema5a Exons 17-20
Interleukin receptor precursor	Novel transcript	
Unnamed	Genescan predicted	Domain with homology to Fibronectin domain
Q7T140	Novel transcript	Similar to vertebrate Junctophilins
Q7T141	Novel transcript	Similar to trypsin inhibitor
<i>tif2</i>	Zfish gene	Transcriptional intermediary factor 2
<i>tram1</i>	Genescan predicted	Homology to <i>tram1</i>
Unnamed	Genescan predicted	Contains ankyrin repeat
<i>ccnd1</i>	Genescan predicted	Cyclin D1
Z3399 3'		

Table 3.1: Predicted transcripts in *topped* critical region. Transcripts present on Sanger Ensemble Database (www.ensembl.org) between markers SSLP markers z9321 and z3399.

Figure 3.2: Zebrafish *sema5a* cDNA sequence 5'-3' obtained from RT-PCR analysis using primers designed from Sanger Ensemble Database for the predicted *sema5a* gene (www.ensembl.org). See Table 3.2 for primer sequences.

5'

TGCCACAGAGCTGAACACCCGCTCATCTCTCACACAGATATTGAGCCGTGG
ATCCACCGGTTTCAGAGCTGAAGGCACTGTTCGATTATTCACAGCTGACCTTTG
ACCCTGGCCAAAATGAACTCATCGTGGGTGCAAGAAATCATCTCTTCAGGC
TACATTTAGAGGATCTTTCACTGATCCAGGAGGCAGAATGGCATTGTGATGA
GTTTACCAAAGGAGCCTGTTTCAGTCGTGGGAAATCAGAGGAGGAGTGCCA
GAATTACATCCGTGTCCTCCTCGTCAATGGTGACAGGCTGTTTACCTGCGG
AACAAATGCATTCACTCCTATTTGCACCAATCGCACGCTGACTAACCTGACT
GAGGTCCATGATCAAATCAGTGGGATGGCACGGTGCCCTATAACCCTCTG
CATAATTCCACCGCCCTCATCACTTCCAGTGGAGAACTGTATGCTGCAACTG
CAATGGACTTTTTAGGCAGAGACCCAGCCATCTACCGCAGCTTGGGAGGG
CTTCCACCTCTGCGTACTGCTCAGTACAACCTCCAAATGGCTCAATGAGCCCA
ACTTCGTCTCCTCCTATGACATCGGCAACTTCACGTA CTCTTCTTCCGTGA
AAATGCTGTGGAGCACGACTGCGGCAGGACTGTTTTCTCTCGGGCTGCCCCG
CGTCTGCAAGAATGATATCGGGGGCCGTTTCCTTCTGGAGGACACCTGGAC
TACCTTTATGAAAGCCCGGCTCAACTGCTCACGGCCTGGCGAGATCCCATT
CAACTACAATGAGTTGCAGGGAACCTTCTTTCTGCCTGAGCTCGAGCTCCTC
TATGGGATTTTACCACCTAATGTTAACAGTATTGCGGCCTCAGCAGTGTGTG
CCTTCAATCTGAGCGCTATTACCAAGTGTTTCAGCGGCCCTTTCAAGTACCAA
GAGAACTCGCGCTCTGCTTGGCTTCCCTTACCCCAATCCTAACCCCGACTTC
CAGTGTGGTACTATAGATTTTGGCTCGTATGTGAACTTAACGGAGAGGAATC
TGCAGGATGCTCAGAAGTTCATCCTGATGCATGAGGTGGTGCAGCCTGTGG
TTCCTGTGCCGTATTTTCATGGAGGACAATGTGCGCTTCTCTCATGTGGCTGT
GGACGTGGTGCAGGGCAAAGACATGCTTTACCACATCATTTATCTGGCAAC
AGATTACGGCACCATTAAGAAGGTGCTCTCCCCTCTCAACCAGACCACGGG
CAGCTGCTTGCTGGACGAGATTGAGCTTTTCCCCCTGAAGAAGAGGCAGCC
AATTCGTAGCCTGCTCATCCTTCACAGCCAAGTGAGCTATTTGTAGGAGTCA
GAGAGCAGGTCATCAAATCCCCCTGATGCGCTGCAACTTCCACAAGTCTA
GAGAAGCCTGTGTGGGGGCCAGAGATCCATACTGCGGCTGGGATCTGGTG
CTCAAGAAATGCACCACGCTGGAAGAGAGCGTCAGCATGAGCCAATGGGA
GCAGAGCATTACACGCTGTCCTGTGAGAAACGTGACTGTAGATGGTCATTA
TGGAGCCTGGTCAGGGTGGAAAACCTTGTAGTCACAGTGTGGTGGCAGTGT
GGGTTTCGTGCCAGTGTGGAACCCGAGCGTGTGACAGTCCAAGTCTCAATG
TGGCGGACAGCCTTGCCAAGGAATCAGTGTTGAAGTGGCAAACCTGCTCCAG
AAATGGGGCATGGACACCGTGGACTGCCTGGGCTCCATGCAGCACCAGCT
GTGGGATTGGATTCCAGGTTCCGGCAGCGTTCCTGCAGTAACCCCACTCCCA
GACATGGAGGACGCGTCTGTGTGGGCCAGAACCGAGAGGAGAGATACTGC
AATGAACACCTGCCGTGTCCTCCGCATGTCTATTGGTCAGCTTGGTCTCCTT
GGGAGCGCTGCACAGTTCCTTGCAGTGGAGGAATCCAGTCACGGCGAAGA
ACGTGTGAGAATGGAATGAATGCCCTGGATGCAGCACTGTATGTAACAAT
AATCAGGACAGGGCTGGATGTTGCAGAGGGCCTCTTCAGTATGCAAACCCA
GGCAGATGTCACCTCCATAGGCAGGTGGAGGGTTGTTACAGGAGCGTGTG
CGCATGTAATGGCCTCCGCCGCATGTCACTGAGCATTTCGACCAAGGTGAC

CAGCACGACCAGCTCCCGTCCACTGGACATGGTGTGGTATTGCACTCCTGG
AACTCTTGGGCTGGCCCGAGGCAGGTAATTCCTCCATACTTGGGTTTGGGG
TTGGAGCAGGTGCGTTTTCGATTTCGGACACCTGAGCTACAGTCTCGACTA
CACTGGCTCCAGGGGCCCCAGACGGACCAGCCTCATTACTGTCAATCCA
GTGATACGTCCAGAACGCAGCAAATCTCCGTGTACAGAGAGCTGGTCTGAT
TGGTCAGAATGGTCCCCCTGTGACTCATCAGGGTCTCAGGTTTCGCCTCCGG
CATTGTGACGTCTTGTTTCCCACCGGCAACCAGTGCTCTGGCAACAGCAGT
GAAACTCGTGCCTGTCTGCCCATCTCCAACTTCATCCCAGAAACGTCTGTTG
CACGTTCAAGTCAGGAGGAAAGATGGTGTGGAGACTTCAATGTGTTCCACA
TGATCGCCGTGGGTCTGAGCAGCTCCATACTCGGCTGCTTGGTCACTTTAC
TGGTGTACACATACTGCCAGAGATACCAGCAGCAATCCCATGATGCCACAG
TCATCCATCCTATCTCTGCTGCCCCGCTCAACACCAGCATCAGCAACCATAT
CAACAAACTGGACAAGTATGACTCAGTTGAAGCCATTAAGGCTTTCAATAAG
AATAACTTGATCCTGGAGGAAAGAAATAAGTATT 3'

Primer Name	Sequence	Sema5a exon location
Sema5aexon1for	TTACAGGAGGCAGAATGGC	1
Sema5aintrev	TCCCAGCCGCAGTATGGATC	11
Sema5aintfor	GCCACAGTGAGCTATTTGTAGG	10
Sema5aencode	ACCGTCAGTGGAGCAGCCC	14
Sema5aTSRfor1	CCTGCTGGAAGTTGGACGA	14
fi41a04startrev	GACCAATCAGACCAGCTCT	17
fi41a04for	GAGCTGGTCTGATTGGTC	17
fi41a04rev	GTCGTCGTATGTGTTGACG	20

Table 3.2: Primers used to clone the zebrafish *sema5a* gene from reverse transcribed cDNA. Primers were designed based on Sanger Ensemble Database (www.ensembl.org) for the predicted portions of the *sema5a* gene. The entire *sema5a* cDNA was cloned in four pieces using listed primer pairs 1 and 2, 3 and 4, 5 and 6, and 7 and 8, respectively.

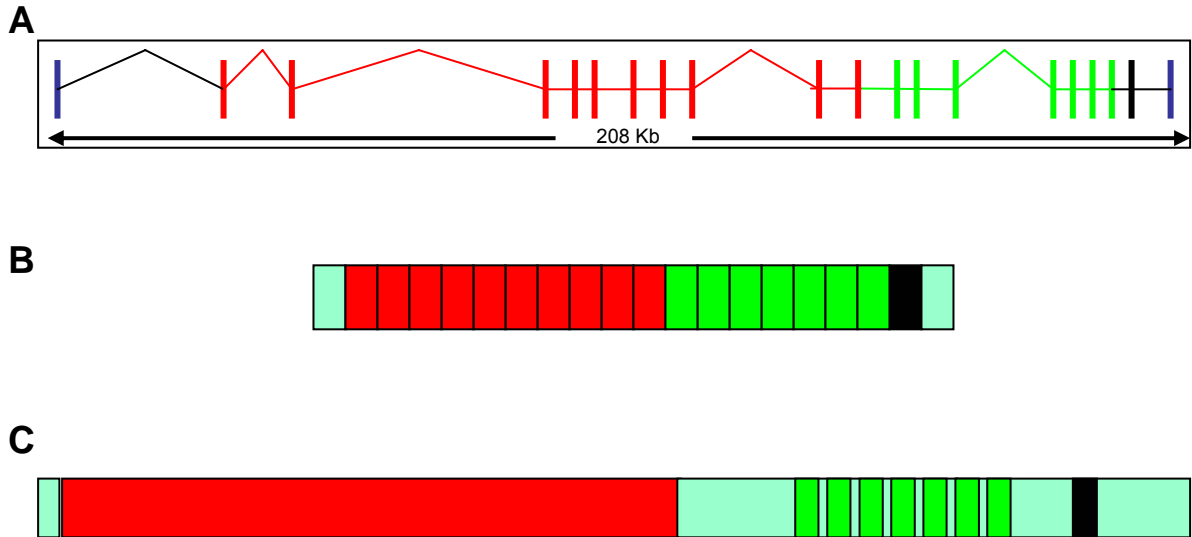


Figure 3.3: Genomic organization of zebrafish *sema5a*. (A) The *sema5a* gene is encoded by 20 exons spanning over 200 kb of genomic sequence and gives rise to an approximately 3.1kb coding region (B) yielding a 1019 amino acid protein (C) containing a Sema domain (red), a TSR domain (green), and a transmembrane domain (black).

Table 3.3: Exon sequences for zebrafish *sema5a*. Sequences are annotated by Sanger Ensemble Database (www.ensembl.org) for exons 1-14, and 17-20. Exons 15 and 16 were annotated by aligning *sema5a* cDNA sequence obtained from with the zebrafish database genomic sequence.

Exon #	Size (bp)	Sequence
1	37	TGCCACAGAGCTGAACACCCGCTCATCTCTCACACAG
2	100	ATATTGAGCCGTGGATCCACCGGTTTACAGAGCTGAAGG CACTGTCGATTATTCACAGCTGACCTTTGACCCTGGC CAAATGAACTCATCGTGGGTGCAAG
3	46	AAATCATCTCTTCAGGCTACATTTAGAGGATCTTTCAC TGATCCAG
4	63	GAGGCAGAATGGCATTGTGATGAGTTTACCAAAGGAG CCTGTTTCAGTCGTGGGAAATCAGAG
5	99	GAGGAGTGCCAGAATTACATCCGTGTCCTCCTCGTCA ATGGTGACAGGCTGTTTACCTGCGGAACAAATGCATT CACTCCTATTTGCACCAATCGCACG
6	214	TGACTAACCTGACTGAGGTCCATGATCAAATCAGTGG GATGGCACGGTGCCCCTATAACCCCTCTGCATAATTCC ACCGCCCTCATCACTTCCAGTGGAGAACTGTATGCTG CAACTGCAATGGACTTTTCAGGCAGAGACCCAGCCAT CTACCGCAGCTTGGGAGGGCTTCCACCTCTGCGTACT GCTCAGTACAACCTCAAATGGCTCAATG
7	286	AGCCCAACTTCGTCTCCTCCTATGACATCGGCAACTT CACGTA CTCTCTTCCGTGAAAATGCTGTGGAGCAC GACTGCGGCAGGACTGTTTTCTCTCGGGCTGCCCGC GTCTGCAAGAATGATATCGGGGGCCGTTTCCTTCTGG AGGACACCTGGACTACCTTTATGAAAGCCCGGCTCAA CTGCTCACGGCCTGGCGAGATCCCATTCAACTACAAT GAGTTGCAGGGAACTTCTTTCTGCCTGAGCTCGAGC TCCTCTATGGGATTTTCACCACTAATGT
8	136	TAACAGTATTGCGGCCTCAGCAGTGTGTGCCTTCAAT CTGAGCGCTATTACCCAAGTGTTTCAGCGGCCCTTTCA AGTACCAAGAGA ACTCGCGCTCTGCTTGGCTTCTTA CCCAATCCTAACCCCGACTTCCAG
9	205	TGTGGTACTATAGATTTTGGCTCGTATGTGAACTTAAC GGAGAGGAATCTGCAGGATGCTCAGAAGTCATCCTGA TGCATGAGGTGGTGCAGCCTGTGGTTCTGTGCCGT ATTTTCATGGAGGACAATGTGCGCTTCTCTCATGTGGC TGTGGACGTGGTGCAGGGCAAAGACATGCTTTACCAC ATCATTATCTGGCAACAG
10	208	ATTACGGCACCATTAAGAAGGTGCTCTCCCCTCTCAA CCAGACCACGGGCAGCTGCTTGCTGGACGAGATTGA GCTTTTCCCCTGAAGAAGAGGCAGCCAATTCGTAGC CTGCTCATCCTTACAGCCACAGTGAGCTATTTGTAG GAGTCAGAGAGCAGGTCATCAAATCCCCCTGATGCG CTGCAACTTCCACAAGTCTAGAGA
11	118	AGCCTGTGTGGGGGCCAGAGATCCATACTGCGGCTG GGATCTGGTGCTCAAGAAATGCACCACGCTGGAAGA GAGCGTCAGCATGAGCCAATGGGAGCAGAGCATTAC ACGCTGTCCT
12	182	GTGAGAAACGTGACTGTAGATGGTCATTATGGAGCCT

		GGTCAGGGTGGAAAACCTTGTAGTCACAGTGATGGTG GCAGTGTGGGTTTCGTGCCAGTGTCTGAACCGAGCGTG TGACAGTCCAAGTCCTCAATGTGGGGACAGCCTTGCC AAGGAATCAGTGTTGAAGTGCAAACCTGCTCCAG
13	144	AAATGGGGCATGGACACCGTGGACTGCCTGGGCTCC ATGCAGCACCAGCTGTGGGATTGGATTCCAGGTTCCG GCAGCGTTCCTGCAGTAACCCCACTCCCAGACATGGA GGACGCGTCTGTGTGGGCCAGAACCGAGAGGAGAG
14	163	ATACTGCAATGAACACCTGCCGTGTCTCCGCATGTC TATTGGTCAGCTTGGTCTCCTTGGGAGCGCTGCACAG TTCCTTGCGGTGGAGGAATCCAGTCAGCGAAGAACGT GTGAGAATGGAAATGAATGCCCTGGATGCAGCACTGT ATGTAACAATAAT
15	174	CAGGACAGGGCTGGATGTTGCAGAGGGCCTCTTCAG TATGCAAACCCAGGCAGATGTCACCTCCATAGGCAGG TGGAGGGTTGTTACAGGAGCGTGTGCGCATGTAATG GCCTCCGCCGCATGTCACTGAGCATTTCGACCAAGGT GACCAGCACGACCAGCTCCCGTCCACTG
16	210	GACATGGTGTGGTATTGCACTCCTGGAACCTTGGGGC TGGCCCGAGGCAGGTAATTCCTCCATACTTGGGTTTG GGGTTGGAGCAGGTGCGTTTTGCGATTTCCGGACACCT GAGCTACAGTCTCGACTACACTGGCTCCAGGGGCC CAGACGGACCAGCCTCCATTTACTGTCAATCCAGTGA TACGTCCAGAACGCAGCAAATCTCCG
17	163	TGTACAGAGAGCTGGTCTGATTGGTCAGAATGGTCCC CCTGTGACTCATCAGGGTCTCAGGTTCCGCTCCGGCA TTGTGACGTCTTGTTCACCGGCAACCAAGTGCTCT GGCAACAGCAGTGAACCTCGTGCCTGTCTGCCCATCT CCAACTTCATCCAG
18	45	AAACGTCTGTTGCACGTTCAAGTCAGGAGGAAAGATG GTGTGGAG
19	212	ACTTCAATGTGTTCCACATGATCGCCGTGGGTCTGAG CAGCTCCATACTCGGCTGCTTGGTCACTTTACTGGTG TACACATACTGCCAGAGATAACCAGCAGCAATCCCATG ATGCCACAGTCATCCATCCTATCTCTGCTGCCCGCT CAACACCAGCATCAGCAACCATATCAACAAACTGGAC AAGTATGACTCAGTTGAAGCCATTAAG
20	46	GCTTTCAATAAGAATAACTTGATCCTGGAGGAAAGAAA TAAGTATT

A

```

Rat      AAGACACGTTCCAGAGTCGGAGACCCCTTGCCACCATGAAGGGAGCCTGCATCCTTGC 97
mouse   AAGACACGTTCCAGAGTCAGAGACCCCTTGCCACCATGAAGGGAGCCTGCATCCTTGC 150
human   AAGACACGTGCCAGAGTCAGAGGCCCTTGCCACCATGAAGGGAACCTGTGTTATAGC 660
chimp   -----ATGAAGGGAACCTGTGTTATAGC 23
zfish   -----

Rat      ATGGCTGTTCTCAAGCCTGGGAGTGTGGAGACTTGCTCGGCCTGAGACCCAGGACCCCTGC 157
mouse   ATGGCTGTTCTCAAGCCTGGGAGTGTGGAGACTTGCTAGGCCCGAGACCCAGGACCCCTGC 210
human   ATGGCTGTTCTCAAGCCTGGGGCTGTGGAGACTCGCCACCCAGAGGCCAGGGTACGAC 720
chimp   ATGGCTGTTCTCAAGCCTGGGGCTGTGGAGACTCGCCACCCAGAGGCCAGGGTANNNC 83
zfish   -----

Rat      CAAGTGCCAGAGAGCTGAGCACCCCGTCGTCCTCTCAAAAGAAATTGGCCCTGGTTACG 217
mouse   CAAGTGCCAGAGAGCTGAGCACCCCTGTCGTCCTCTTACAAAGAAATTGGCCCTGGTTACG 270
human   TCAGTGCCAGAGAACCAGCATCCAGTCATCTCCTATAAAAGAAATTGGCCCTGGTTACG 780
chimp   TCAGTGCCAGAGAGCCGAGCATCCAGTCATCTCCTATAAAAGAAATTGGCCCTGGTTACG 143
zfish   ----TGCCACAGAGCTGAACACCCGCTCATCTCTCACACAGATATTGAGCCGTGGATCCA 56
          ***** ** * ** * ** * ** * ** * ** * ** * ** * ** * ** *

Rat      GGAATTCAGAGCCGAGAATGCTGTGGATTTCTCGAGGTTAACATTTGACCCAGGACAGAA 277
mouse   GGAGTTCAGAGCCGAGAATGCTGTGGATTTCTCGAGGTTAACATTTGACCCAGGACAGAA 330
human   GGAGTTCAGAGCGAAGAATGCTGCGGATTTCTCGCAGTTAACATTTGACCCAGGACAGAA 840
chimp   GGAGTTCAGAGCGAAGAATGCTGTGGATTTCTCGCAGTTAACATTTGACCCAGGACAGAA 203
zfish   CCGGTTTCAGAGCTGAAGGCACTGTGATTTATTCACAGCTGACCTTTGACCCAGGACAAA 116
          ***** * ** * ** * ** * ** * ** * ** * ** * ** * ** *

Rat      AGAACTTGTCGTAGGAGCAAGAACTATCTCTTCAGACTACAGCTCGAGGATCTGTCTCT 337
mouse   AGAACTTGTCGTAGGAGCGAGAACTATCTCTTCAGATTAGAGCTTGAGGATCTGTCTCT 390
human   AGAACTTGTTGTAGGAGCAAGAACTACCTCTTCAGGTTACAGCTTGAGGATCTGTCTCT 900
chimp   AGAACTTGTTGTAGGAGCAAGNAACTACCTCTTCAGGTTACAGCTTGAGGATCTGTCTCT 263
zfish   TGAACTCATCGTGGGTGCAAGAAATCATCTCTTCAGGCTACATTTAGAGGATCTTTCACT 176
          ***** * ** * ** * ** * ** * ** * ** * ** * ** * ** *

```

B

Cladogram

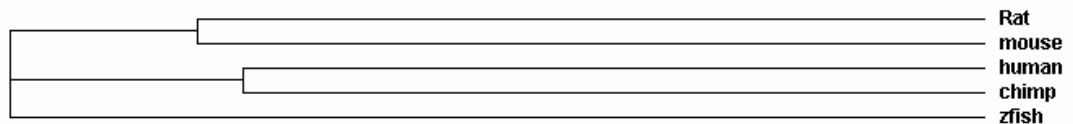


Figure 3.4: Cross species homology of *sema5a* cDNA. (A) cDNA alignment of 5' end of *sema5a* in rat, mouse, human, chimp, and zebrafish. ATG start site in mouse, rat, human, and chimp underlined (red). Exon 1 is highlighted in blue. Note: zebrafish *sema5a* exon 1 is smaller and does not contain a ATG start site. (B) Cladogram indicating relatedness of *sema5a* transcript in indicated species using ClustalW program (www.ebi.ac.uk/clustalw).

Figure 3.5: Sema5a protein cross species alignment. ClustalW alignment of Sema5a in human, mouse, rat, chimp, and zebrafish. Sema domain (Red), Thrombospondin domain (Green), and Transmembrane domain (Blue). Note: Zebrafish Sema5a protein sequence ends with a stop codon; however, the other species contain additional protein sequence 3' of this stop.

Figure 3.6: cDNA alignment of zebrafish *sema5a* and predicted *sema5b* sequence from Sanger Ensemble Database (www.ensembl.org). ClustlW program was used to generate alignment (www.ebi.ac.uk/clustalw). Asterisks indicate exact base pair matches.

```

sema5a      ---TGCCACAGAGCTGAACACCCGCTCATCTCTCACACAGATATTGAG-CCGTGGATCCA 56
sema5b      GAGTGTAACAGATTAGAGCACCTGTGCTCTC-CATTCAAGCTCTAAGTCCTTTGATCTC 59
          **   ***   *   *****   *   *****   *   *   *   *   *   *   *   *   *   *   *   *   *   *

sema5a      CCGGTTTCCAGAGCTGAAGGCACTGTGCGATTATTCACAGCTGACCTTTGACCCCTGGCCAAAA 116
sema5b      CTCTTTTCTCGCATCCTGGTGTAAAGGATTATTCAGCTGACCTTTGACCTTAACCAGGAA 119
          *   **   *   *   *   *   *   *   *   *   *   *   *   *   *   *   *   *   *   *   *   *   *

sema5a      TGAACTCATCGTGGGTGCAAGAAATCATCTCTTCAGGCTACATTTAGAGGATCTTTCACT 176
sema5b      TGAACCTATAGTCGGAGCAAGAACTACCTCTTCAGACTAAATCTCAGCAACATTTCACT 179
          *****   *   *   *   *   *   *   *   *   *   *   *   *   *   *   *   *   *   *   *

sema5a      GATCCAGGAGGCAGAAATGGCATTGTGATGAGTTTACCAAAGGAGCCTGTTTTAGTCGTGG 236
sema5b      AATTCAAGCAACGGAATGGGGCCAGACGAAGACACCAGGAGTCTGTCAAAGCAAGG 239
          **   ***   *   *****   *   *   *   *   *   *   *   *   *   *   *   *   *   *

sema5a      GAAATCAGAGGAGGAGTGCCAGAATTACATCCGTGTCTCCTCGTCAATGGTGACAGGCT 296
sema5b      GAAGACGAGCTGGAGTGTCAAATACATCCGGTGTCTGTGTCAACAAGACAGAGGT 299
          ***   *   ***   *****   *   *   *   *   *   *   *   *   *   *   *   *   *   *

sema5a      GTTTACCTGCGGAACAAATGCATTCACTCCTATTTGCACCAATCGCACGCTGACTAACCT 356
sema5b      GGTCACCTGCGGGACAAATGCCTTCCAGCCTCTTTGCATCACCAGAGAGGCAGGGAACAT 359
          *   *   *****   *****   *   *   *   *   *   *   *   *   *   *   *   *   *   *

sema5a      GACTGAGGTCCATGATCAAATCAGTGGGATGGCACGGTGCCTTATAACCCCTCTGCATAA 416
sema5b      GAGCAGAGTGTGGAGAGGGTGAACGGAGTGGCCCGTGTCCCTATGACCCCGTCATAA 419
          **   **   **   *   *   *   *   *   *   *   *   *   *   *   *   *   *   *   *

sema5a      TTCCACCGCCCTCATCACTTCCAGTGGAGAAGTGTATGCTGCAACTGCAATGGACTTTTC 476
sema5b      CTCCACAGCGGTGGTACTGAAAGTGGAGAGCTGTACGCTGCCACGGTCACTGATTTCTC 479
          *****   **   *   *   *   *   *   *   *   *   *   *   *   *   *   *   *   *

sema5a      AGGCAGAGACCAGCCATCTACCGCAGCTTGGGAGGGCTTCCACCTCTGCGTACTGTCTCA 536
sema5b      TGGACGGGACCCTGTCTATCTACCGCAGCCTTGGAGGAATGCCGCCTTTGCGGACCGCCA 539
          **   *   *****   *   *****   *   *   *   *   *   *   *   *   *   *   *

sema5a      GTACAACCTCAAATGGCTCAATGAGCCCAACTTCGTCTCCTCTATGACATCGGCAACTT 596
sema5b      GTACAACCTCAAATGGCTTAATGAGCCTCACTTCATCTCGGCTTATGATGTGGGTCTTTT 599
          *****   *****   *****   *****   *   *****   *   **   **

sema5a      CACGTACTTCTTCTTCCGTGAAAATGTGTGGAGCAGACTGCGGCAGGACTGTTTTTCTC 656
sema5b      CACCTTCTTCTTCTTGGAGGAGAACGAGTGGAGCATGACTGCGGTAACGCGGTGTACTC 659
          ***   *   *****   *   *   *   *   *   *   *   *   *   *   *   *   *   *

sema5a      TCGGGCTGCCCGCGTCTGCAAGAAATGATATCGGGGGCCGTTTCTTCTGAGGACACCTG 716
sema5b      ACGGGTGGCGCGGTGTGTAATAAATGACATTTGGAGGCCGATTCTGTCTGAGGACACGCTG 719
          *****   **   *   *   *   *   *   *   *   *   *   *   *   *   *   *   *   *

sema5a      GACTACCTTTATGAAAGCCCGCTCAACTGCTCACGGCTGGCGAGATCCCATTCAACTA 776
sema5b      GACCACTTTTACGAAGCCCGACTCAACTGCTCGCGGTGAGGAGAAATCCCTTTCTACTA 779
          ***   **   *****   *   *   *   *   *   *   *   *   *   *   *   *   *   *

sema5a      CAATGAGTTGCAGGGAACCTTCTTCTGCTGAGCTCGAGCTCCTCTATGGGATTTTTCAC 836
sema5b      TAATGAGCTACAAGCACCTTCTACCTGCCGGAACAGGACCTCATCTATGGGATTTTTCAC 839
          *****   *   *   *   *   *   *   *   *   *   *   *   *   *   *   *   *

sema5a      CACTAATGTAAACAGTATTGCGGCCCTCAGCAGTGTGTGCCCTCAATCTGAGCGCTATTAC 896
sema5b      CACCAATGTGAACAGCATTTGCTGCCCTGTCAGTTTGCAGTACAACCTCAGCGCAATCAC 899
          ***   *****   *****   *****   *****   *   *   *   *   *   *   *   *

sema5a      -CAAGTGTTCAGCGGCCCTTTCAAGTACCAAGAGAACTCGCGCTCTGCTTGGCTTCCTTA 955
sema5b      ACAGGCTTTCAAGGGCCCTTCCGCTCCAGGAGAACCTCGCTCCAGTGGCTGCCAC 959
          *   *   *****   *   *   *   *   *   *   *   *   *   *   *   *

sema5a      CCCCATCTAACCCGACTTCCAGTGTGGTACTATAGATTTTG---GCTCGTATGTGAA 1012
sema5b      CCCCACCCATCCCCAAGTGTGGGACCATAGATGAAGAAGGGCCATATGAAAG 1019
          *****   **   *   *****   *****   *   *****   *   *   *   *

```



```

sema5b      CTCCAAGTGGGCAAGCGTAAGGTGGAGACACGCTTCTGTCC-CAATGACGGGATGGTA-- 2094
             ** **** * * * ** * **** * ** * * * *
sema5a      ACCTCCATAGGCAGGTGGAGGTTGTTACAGGAGCGTGTGCGCATGTAATGGCCCTCCGCC 2117
sema5b      ACCTGCG-AAACAGACTCTC--TTGTTG-AGGAGCTTCTCAGAATGCC-TGGTGTCCGAC 2149
             **** * * * **          ***** ***** * * * ** * * * *
sema5a      GCAT-GTCACTGAGCATTTTCGACCAAGGTGACCAGCAGCAGCAGCTCCCCTCCACTGGAC 2176
sema5b      TCTCAGGCAC TGG----CTGGTCATCATGGGAGATGTGGTCAGCTTGCAGCTCAG-GAAT 2203
             * * ***** * ** ** * * * **** * ** * *
sema5a      ATGGTGTGG--TATTGCACTCCTGGA-ACTCTGGGGTGGCCCGA--GGCAGGTAATTC 2231
sema5b      GTGCCAAAGGCTACCGCACTCGCAAACGCAGCTGCACCAACACAGATGGCAAACATAC 2263
             ** * * * ***** * * ** * * * **** * * *
sema5a      TCCATACTTGGGTTTGG--GGTGGAGCAGGT-GCGTTTGCATTTTCGGACACC--TGAG 2286
sema5b      CCACTGCCTGTGCGGGATCGCTGTAGAATATCAGGACTGCAATCCTCAGCCCTGTCCAG 2323
             * * * * * * * * * * * * * * * * * * * *
sema5a      CTACAGTCTC--GACTACACTGGCTCCAGGGGCCCCAGACGGACCAGCCTCCATTTA--C 2342
sema5b      TTAAAGGCGCCTGGTCTTGGTGGTCATCATGGTCGCAG-TGTTGCGTTCCTGTGGAGGC 2382
             * * * * * * * ***** * * * * * * * * * * *
sema5a      TGTCAAT-CCAGTGA-TACGTCCA-GAACGCAGCAAATCTCCGTGTACAGAGAGCTGGTC 2399
sema5b      GGACACTACCAACGAACACGCACATGTACAAGCCCTGCCCTGCCAATGGAGGGGACATC 2442
             * * * * * * * * * * * * * * * * * * * * *
sema5a      TG-ATTGGT-----CAGAATGGTCCCCCTGTGAC-----TCATCAGGGTCTCAGG 2443
sema5b      TGCATCGGCTTGACACAGAGGAGGCTCTTTGCAACACGCATACTTGTGATGGTGGCTGG 2502
             * * * * * ***** * * * * * * * * * * * * *
sema5a      TTCGCCT--CCGGCATGT--GACGTCCTTGTTCACCACGGCAACCA-GTGCTCTGGCA 2497
sema5b      ATGGCCTGGTCTGTGTGGTCTGAGTGTGATGATTCAGGCCTGCAGCTGCGCAGTTCGAGTG 2562
             * **** * * * * * * * * * * * * * * * * *
sema5a      ACAGCAGTGAAGTCTGTCGTC--TGTCCTG-----CCCATCTC-----CAACTTC 2538
sema5b      TGTGGAGCTCAATCCATGCCATGTGCGGGAAACAGCTCCAGCACAGAGACTGCAATGAG 2622
             * * * * * * * * * * * * * * * * * * * *
sema5a      ATCCAGAAACGCTGTGTCACGTTCAAGTCAGGAGGAAAGATGGTGTGAGACTTCAAT 2598
sema5b      ATCCAGCCATTCTTCCGGCATCCAGCTATGAGAAGGACCAGCAGTGTGGAGGGTCACT 2682
             ***** * * * * * * * * * * * * * * * *
sema5a      GTGTTCACATGATCGCGTGGGTCTGAGCAGCTCCATACTCGGCTGCTTGGTCACTTTA 2658
sema5b      CTGCTCCACCTGATAGCGACAGGTGTGTGTTTCTTGGTGCCGGTCTGTGTCTTTC 2742
             * * * * * * * * * * * * * * * * * * * *
sema5a      CTGGTGTACACATACTGCCAGAGATACCAGCAGCAATCCCATGATGCCACAGTCATCCAT 2718
sema5b      CTGGTGTATGTTTACTGTGTCAGCGGTTCCACAAGCCCTCGCAGGAGTCTGCCATCATCCAT 2802
             ***** ***** * * * * * * * * * * * * *
sema5a      CCTATCTCTGCTGCCCCGCTCAACACCAGCATCAGCAACCATATCAACAACTGGACAAG 2778
sema5b      CCCACCACTCCCAACCCTCAACTACAAGGGCAACA-CCACACAAAGAATGAGAAATA 2861
             * * * * * * * * * * * * * * * * * * * *
sema5a      TATGACTCAGTTGAAGCCATTAAGGCTTTCAATAAGAATAACTTGATCCTGGAGGAAAGA 2838
sema5b      CAC-ACCCA--TGGAGT--TCAAGACTTGAATAAGAACAATCTCCTGCCAGACGAGAGG 2916
             * * * * * * * * * * * * * * * * * * * *
sema5a      AATAAGTATT----- 2848
sema5b      ACAAACTACTTCCCTTCACCGCTTCAGCAGACCAACGCTACACCACCAGTACTACCC 2976
             * * * * *
sema5a      -----
sema5b      ACAGGACTGGGCAAATACGACTACCGGCCGACTCCTCACCC 3018

```

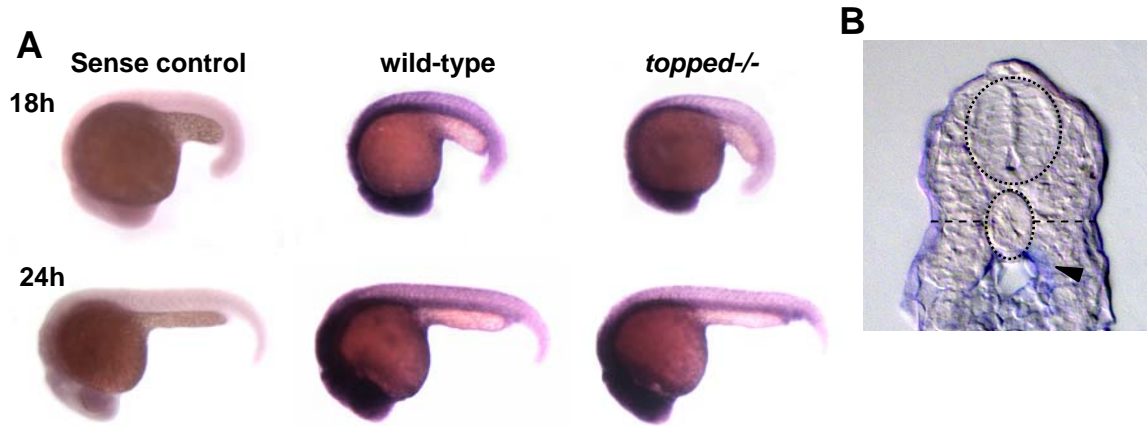


Figure 3.7: zebrafish *sema5a* is expressed in the ventral myotome. (A) In situ hybridization with *sema5a* sense and antisense riboprobes at 18hpf (top) and 24 hpf (bottom) in wild-type and *topped* mutant embryos. (B) *sema5a* in situ hybridization cross-section of a 24 hpf wild-type embryo. Arrow indicates expression in the ventromedial myotome.

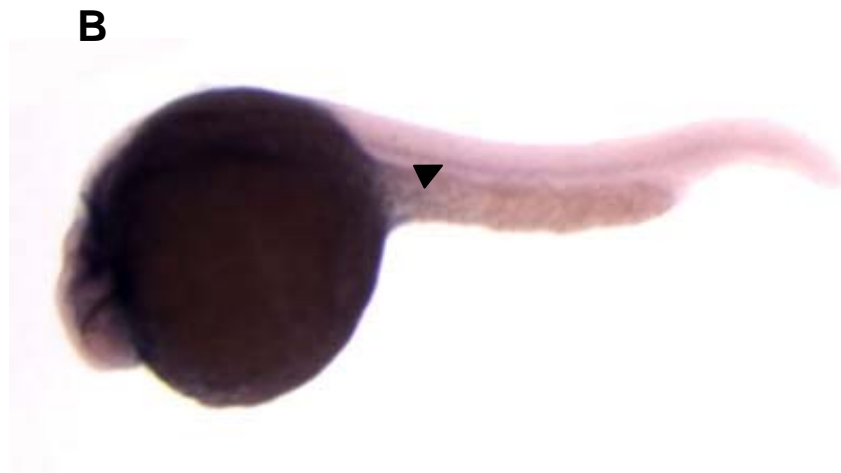


Fig. 3.8: zebrafish *sema5b* is expressed in the brain and notochord. In situ hybridization with antisense *sema5b* riboprobe at 24 hpf. (A) *sema5b* is expressed in the brain ventricles (white arrows, dorsal view with anterior to the left) and notochord (lateral view, arrowhead) (B).

<u>Sema5a Exons Present</u>	<u>Injected Construct</u>	<u><i>topped</i>^{458/-} Embryos with rescue</u>	<u>Axons rescued</u>
0	J2495Q8 (Control)	0/74 (0%)	0/1480 (0%)
	DKEY-8B6	12/106 (11.3%)	25/2120 (1.2%)
	CH211-277N6	16/107 (14.9%)	46/2140 (2.2%)
	DKEY-96N22	49/94 (52.1%)	111/1880 (5.9%)
	CH211-112I15	48/98 (48.9%)	109/1960 (5.5%)

Table 3.4: Zebrafish BAC clones containing portions of the *sema5a* gene rescue the *topped* phenotype. PCR analysis was performed on each BAC with *sema5a* gene specific primers to identify which exons were present. Each BAC was injected into *topped* homozygous embryos at the single cell stage at 100ng/ μ l. Rescue is reported as the number of embryos with any rescue, and also as the total number of axons rescued where axons 5-14 were scored on both sides of the embryos. Axons were considered rescued if the axons had grown past the ventral edge of the notochord.

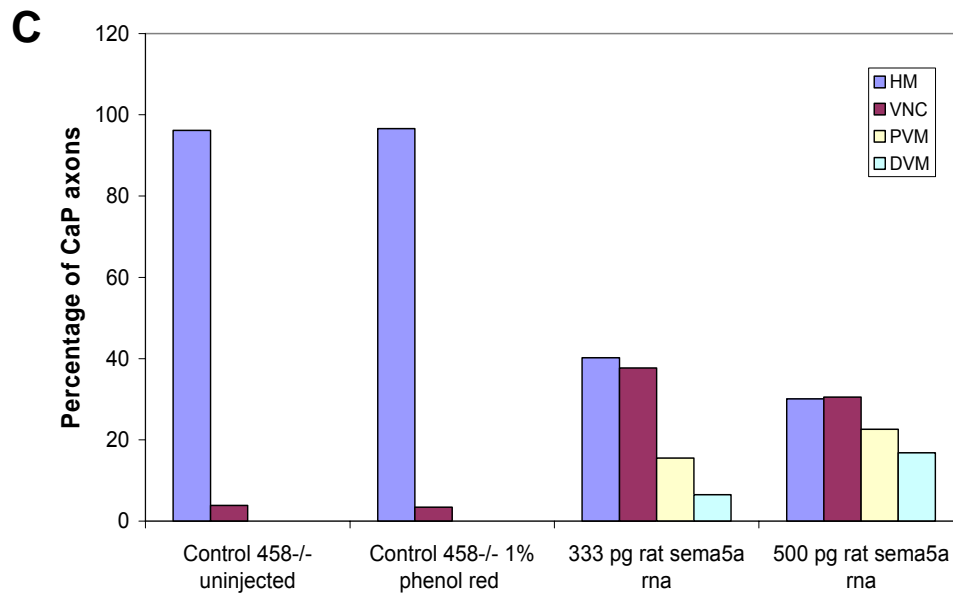
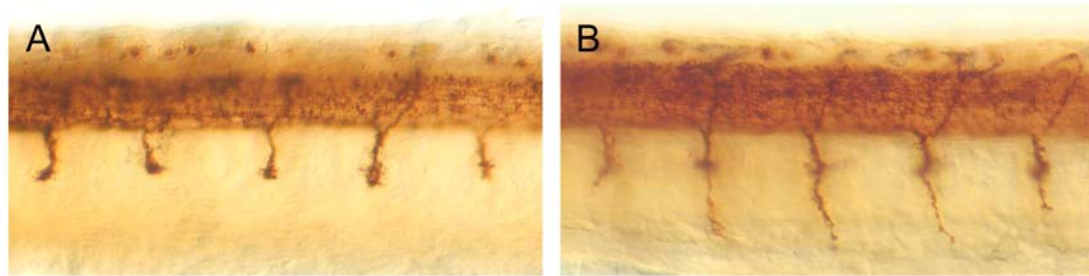


Figure 3.9: Heterologous rescue of CaP axons in *topped* mutants with rat full-length *sema5a* RNA. Lateral views of 26 hpf *topped* mutant (A) and *topped* mutant injected with 500pg of rat *sema5a* RNA (B). (C) CaP axon positions were counted in hemisegments 5-14, $n= 1220, 1000, 1240,$ and 1060 axons in 61, 50, 62, and 53 embryos respectively in control uninjected, dye injected, 333pg *sema5a* RNA, and 500pg *sema5a* RNA. Axon positions were scored as HM (horizontal myoseptum), VNC (ventral edge of notochord), PVM (proximal ventral myotome), DVM (distal ventral myotome).

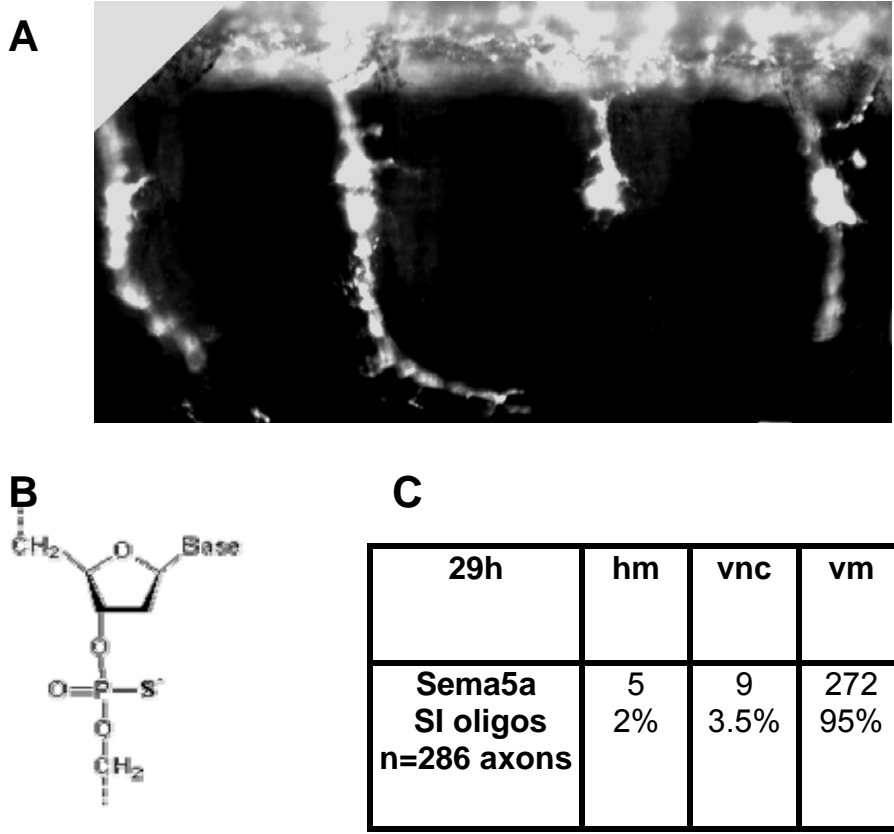
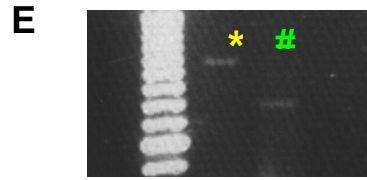
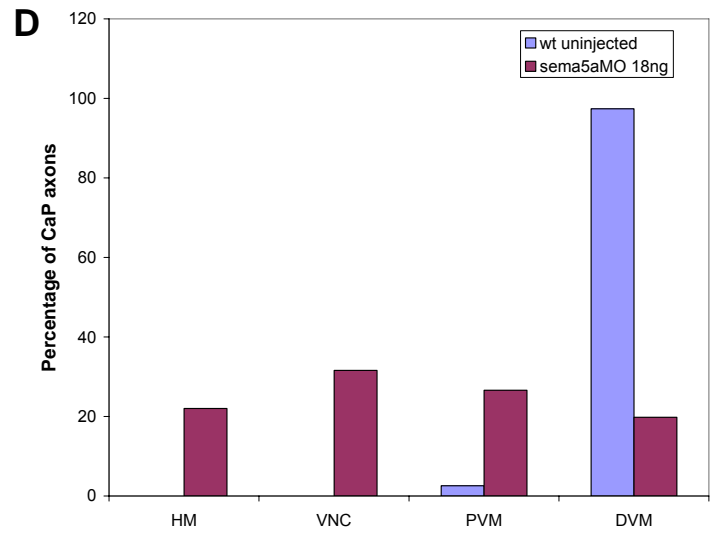
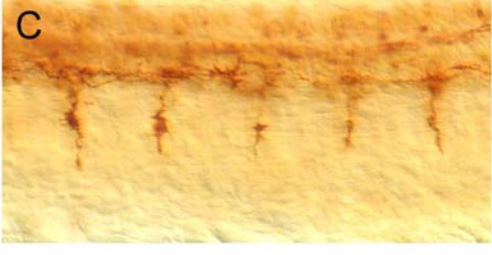
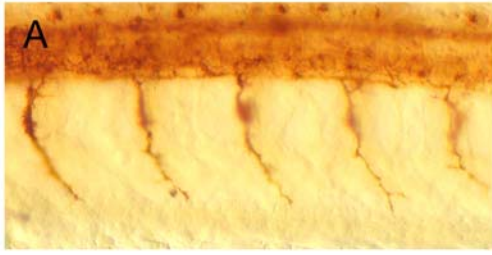


Figure 3.10: Knock-down of Sema5a with SI antisense oligos. (A) Lateral view of znp1 antibody staining of wild-type embryo at 26 hpf injected with antisense oligos to *sema5a*. (B) Antisense oligos are modified with a sulfur group. (C) Quantitation of CaP axon location after injection with *sema5a* antisense oligos.

Figure 3.11: Knockdown of zebrafish *Sema5a* with antisense oligonucleotide morpholinos phenocopies the *topped* mutant phenotype. Lateral views of 26 hpf wild type (A) and *Sema5a* morpholino injected embryos (B, C). (C) CaP axon positions were counted in hemisegments 5-14, $n= 612$ and 800 axons in 32 and 40 embryos respectively in wild-type uninjected and *Sema5a* MO injected embryos. Axon positions were scored as HM (horizontal myoseptum), VNC (ventral edge of notochord), PVM (proximal ventral myotome), and DVM (distal ventral myotome). (E) RT-PCR confirmed an 1100bp band (*) in wild type and an 850bp (#) band in *Sema5a* MO injected embryos. (F) ClustalW sequence alignment of wild-type *sema5a* and *Sema5a* MO injected embryos indicating the absence of exon 7.



F

```

WTsema5a      GAGGCAGAATGGCATTGTGATGAGTTTACCAAAGGAGCCTGTTTCAGTCGTGGGAAATCA 60
Sema5aMO      GAGGCAGAATGGCATTGTGATGAGTTTACCAAAGGAGCCTGTTTCAGTCGTGGGAAATCA 60
*****

WTsema5a      GAGGAGGAGTGCCAGAATTACATCCGTGTCTCCTCGTCAATGGTGACAGGCTGTTTACC 120
Sema5aMO      GAGGAGGAGTGCCAGAATTACATCCGTGTCTCCTCGTCAATGGTGACAGGCTGTTTACC 120
*****

WTsema5a      TGC GGAACAAATGCATTCACTCCTATTGACCAATCGCACGCTGACTAACCTGACTGAG 180
Sema5aMO      TGC GGAACAAATGCATTCACTCCTATTGACCAATCGCACGCTGACTAACCTGACTGAG 180
*****

WTsema5a      GTCCATGATCAAAATCAGTGGGATGGCACGGTGCCCTATAACCCTCTGCATAAATCCACC 240
Sema5aMO      GTCCATGATCAAAATCAGTGGGATGGCACGGTGCCCTATAACCCTCTGCATAAATCCACC 240
*****

WTsema5a      GCCCTCATCACTTCCAGTGGAGAACTGTATGCTGCAACTGCAATGGACTTTTCAGGCAGA 300
Sema5aMO      GCCCTCATCACTTCCAGTGGAGAACTGTATGCTGCAACTGCAATGGACTTTTCAGGCAGA 300
*****

WTsema5a      GACCCAGCCATCTACCCGAGCTGGGAGGGCTTCCACCTCTGCGTACTGCTCAGTACAAC 360
Sema5aMO      GACCCAGCCATCTACCCGAGCTGGGAGGGCTTCCACCTCTGCGTACTGCTCAGTACAAC 360
*****

WTsema5a      TCCAATGGCTCAATGAGCCCAACTTCGTCTCCTCCTATGACATCGGCAACTTCACGTAC 420
Sema5aMO      TCCAATGGCTCAATG----- 376
*****

WTsema5a      TTCTTCTTCCTGAAAATGCTGTGGAGCAGACTGCGGCAGGACTGTTTTCTCTCGGGCT 480
Sema5aMO      -----

WTsema5a      GCCCGCGTCTGCAAGAAATGATATCGGGGGCCGTTTCCTTCTGGAGGACACCTGGACTACC 540
Sema5aMO      -----

WTsema5a      TTTATGAAAGCCCGGCTCAACTGCTCACGGCCTGGCGAGATCCCATTCAACTACAATGAG 600
Sema5aMO      -----

WTsema5a      TTGCAGGGAACCTTCTTTCTGCCTGAGCTCGAGCTCCTCTATGGGATTTTCACCCTAAT 660
Sema5aMO      -----

WTsema5a      GTTAACAGTATTGCGGCCTCAGCAGTGTGTGCCTTCAATCTGAGCGTATTACCCAAGTG 720
Sema5aMO      --TAACAGTATTGCGGCCTCAGCAGTGTGTGCCTTCAATCTGAGCGTATTACCCAAGTG 434
*****

WTsema5a      TTCAGCGGCCCTTTCAAGTACCAAGAGAACTCGCGCTCTGCTTGGCTTCCTTACCCCAAT 780
Sema5aMO      TTCAGCGGCCCTTTCAAGTACCAAGAGAACTCGCGCTCTGCTTGGCTTCCTTACCCCAAT 494
*****

WTsema5a      CCTAACCCCGACTTCCAGTGTGGTACTATAGATTTTGGCTCGTATGTGAACCTAACGGAG 840
Sema5aMO      CCTAACCCCGACTTCCAGTGTGGTACTATAGATTTTGGCTCGTATGTGAACCTAACGGAG 554
*****

WTsema5a      AGGAATCTGCAGGATGCTCAGAAGTTCATCCTGATGCATGAGGTGGTGCAGCCTGTGGTT 900
Sema5aMO      AGGAATCTGCAGGATGCTCAGAAGTTCATCCTGATGCATGAGGTGGTGCAGCCTGTGGTT 614
*****

WTsema5a      CCTGTGCCGTATTTCAAGGAGACAATGTGCGCTTCTCTCATGTGGCTGTGGACGTGGTG 960
Sema5aMO      CCTGTGCCGTATTTCAAGGAGACAATGTGCGCTTCTCTCATGTGGCTGTGGACGTGGTG 674
*****

WTsema5a      CAGGGCAAAGACATGCTTTACCACATCATTATCTGGCAACAGATTACGGCACCATTAAG 1020
Sema5aMO      CAGGGCAAAGACATGCTTTACCACATCATTATCTGGCAACAGATTACGGCACCATTAAG 734
*****

WTsema5a      AAGGTGCTCTCCCTCTCAACCAGACCACGGGAGCTGCTTGTGGACGAGATTGAGCTT 1080
Sema5aMO      AAGGTGCTCTCCCTCTCAACCAGACCACGGGAGCTGCTTGTGGACGAGATTGAGCTT 794
*****

WTsema5a      TTCCCCCTGAAGAAGAGGC 1099
Sema5aMO      TTCCCCCTGAAGAAGAGGC 813
*****

```

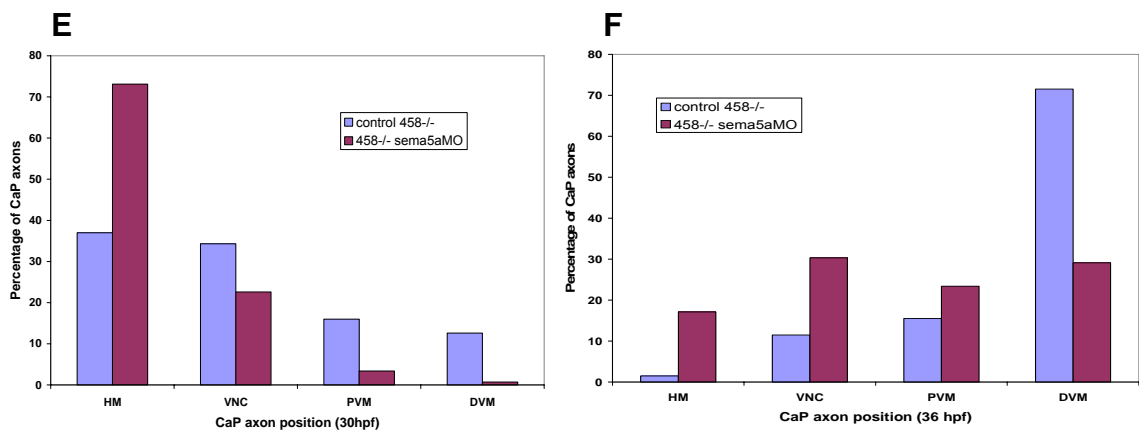
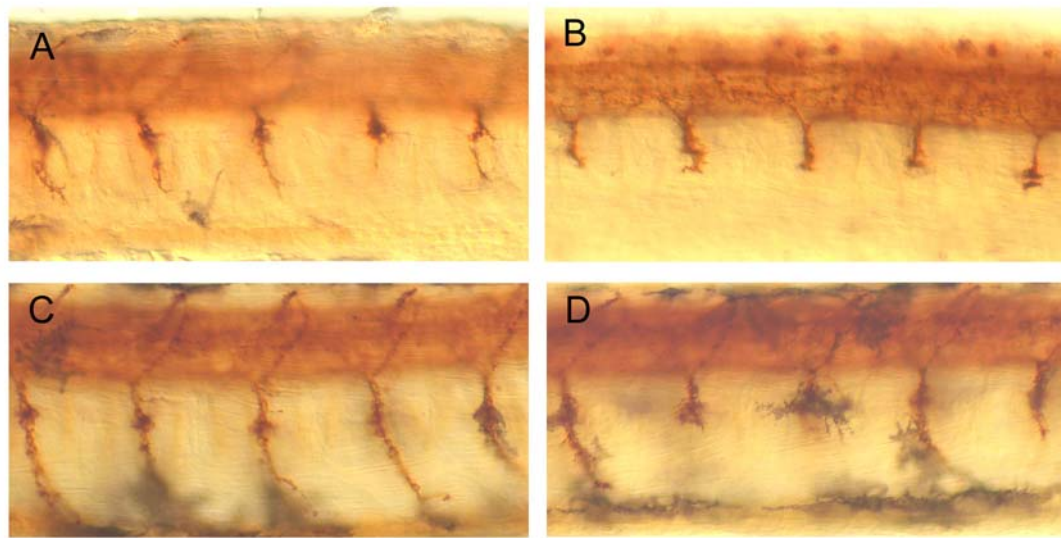


Figure 3.12: Knock-down of Sema5a in *topped* mutants exacerbates the *topped* phenotype. Lateral views of 30 hpf (A, B) and 36 hpf (C, D) *topped* mutant (A, C) and *topped* mutant injected with Sema5a MO (B, D) embryos. (E, F) CaP axon positions were counted in hemisegments 5-14, $n= 300, 760, 200,$ and 560 axons in $15, 38, 10,$ and 28 embryos respectively in *topped* uninjected and *topped*^{-/-} Sema5a MO injected embryos at 30hpf and 36 hpf. Axon positions were scored as HM (horizontal myoseptum), VNC (ventral edge of notochord), PVM (proximal ventral myotome), DVM (distal ventral myotome).

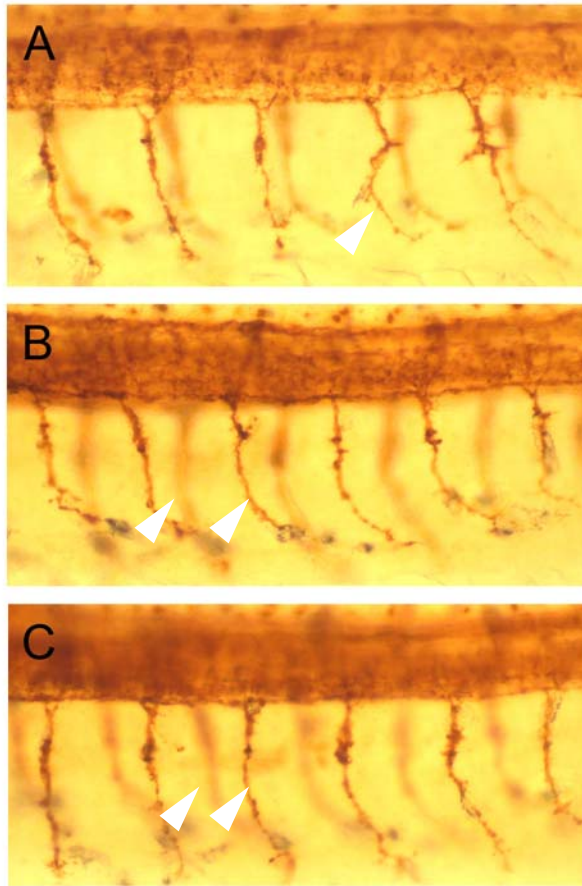


Fig. 3.13: Overexpression of *sema5a* transcript induces CaP axon defects. (A, B, C) Three examples of lateral views of antibody labeling with znp1 at 26 hpf of wild-type embryos injected with 500ng/ul of rat *sema5a* RNA. Compare with wild-type from Fig. 2.2A. Arrow in A indicating a branched axon, arrows in B and C indicates CaP axons are staggered on opposing lateral sides of the embryo.

CHAPTER 4

GENETIC DISSECTION OF VENTRAL AXIAL MOTOR AXON PATHFINDING IN ZEBRAFISH

Introduction

Mutational analysis has proven to be a critical tool in uncovering the genetic pathways that control cellular and developmental processes. Genetic screens designed to uncover genes critical for axon guidance and cell migration have been successful in *Drosophila* and *C. elegans* (Seeger et al., 1993; Zallen et al., 1999; Wightman et al., 1997; Kraut et al., 2001, and Van Vactor et al., 1993). Screens to identify essential genes for nervous system development in mouse have also been conducted (Leighton, et al., 2001). However, there are limitations to large scale screens in mouse as a vertebrate model for axon guidance, including small numbers of progeny and difficulty visualizing embryonic motor axons. Therefore, zebrafish has emerged as a vertebrate model for performing small or large scale screens to reveal genes specific for motor axon pathfinding.

In three independent ENU mutagenesis screens, several mutants were revealed with defects in ventral primary motor axon pathfinding (Beattie et al., 1999; Granato et al., 1996; Birely et al., 2005). The well characterized mutants include *stumpy*, *topped*, *diwanka* and *unplugged*. Diwanka and Unplugged have been shown to function early in CaP axon pathfinding; Diwanka is important for axons to exit the spinal cord and Unplugged is important for CaP axon pathway selection (Zeller and Granato, 1999; Zhang and Granato, 2000). Stumpy and Topped have been shown to function later in CaP axon guidance. We found Topped is functioning as a ventral cue in the ventromedial myotome to promote CaP axon outgrowth, while Stumpy is functioning at intermediate target regions along the CaP axon pathway, where decisions to turn, branch, or extend are decided (Rodino-Klapac and Beattie, 2004; Beattie et al., 2000). Here we have shown that *stumpy* and *topped* interact genetically at the first intermediate target, which is the entry point into the ventral myotome. We have also identified three additional mutants, *OS4*, *OS11*, and *OS12* that genetically interact with *stumpy*. The molecular identification of these genes along with *stumpy* and *topped* will help to define the genetic pathway that guides CaP motor axons into the ventral myotome. Defining this pathway has important implications for understanding motor nervous system development and motoneuron disease processes in higher vertebrates.

Materials and Methods

Fish Strains and Maintenance

Mutant strains were maintained as heterozygous lines in the AB*/WIK background. Homozygous mutant embryos were generated by pairwise mating of OS4, 11, and 12 heterozygous fish. Embryos raised from matings were maintained between 25.5 and 28.5°C and staged by converting the number of somites to hours post fertilization (hpf; Kimmel et al., 1995).

Generation of Mutants

stumpy and *topped* mutants were generated by Beattie et al., 1999. Briefly, after exposure to 3 mM ethylnitrosourea (ENU) (Solnica-Krezel et al., 1994), adult male fish were outcrossed to wild-type females to create the F₁ generation. F₁ females were screened for mutations by using the early pressure method to examine parthenogenetic diploid F₂ embryos (Streisinger et al., 1981). The embryos were fixed and labeled with antibodies to identify mutants. F₁ females carrying mutations of interest were outcrossed and lines generated. OS4, OS11, and OS12 mutants were generated from gamma-irradiated fish. Briefly, sperm from P₀ males was irradiated with gamma rays. F₁ eggs were then obtained from

P₀ females and fertilized with the irradiated sperm. F₁ heterozygous progeny were raised to adulthood, and then crossed to *stumpy*^{393+/-} fish.

Whole Mount Antibody Labeling

Whole mount antibody labeling was performed as described (Eisen et al., 1989; Beattie et al., 2000). The znp1 monoclonal antibody that recognizes primary and secondary motor axons (1:100; Trevarrow et al., 1990; Melancon et al., 1997), was detected using the Sternberger Clonal-PAP system with diaminobenzidine (DAB) as a substrate (Beattie and Eisen, 1997). Embryos were analyzed with a Zeiss axioplan microscope.

Results

topped and stumpy function in the same genetic pathway

To examine whether the known zebrafish mutations that affect CaP axon guidance are functioning in a genetic pathway, I first generated transheterozygotes with *stumpy* and *topped*. In *stumpy* mutants, motor axons stall at intermediate targets and fail to extend into distal myotome regions (Beattie et al., 2000). *topped* heterozygotes do not have a phenotype and *stumpy*^{b393} heterozygotes display a mild-stall phenotype (Beattie et al., 2000; Fig 4.1 B). If *topped* and *stumpy* were in the same genetic pathway, then we would predict that lacking one copy of both *stumpy* and *topped* would cause a more

pronounced stall phenotype at the first intermediate target than that seen in *stumpy*^{b393} heterozygotes.

To do this, I collected progeny from heterozygous crosses of *stumpy* and *topped* and performed antibody staining with znp1 to visualize the motor axons. Ten CaP axons per side (20 per embryo; hemisegments 5-14), were scored for growth cone position (Fig 4.1 D). I subsequently genotyped the embryos using closely linked SSLP markers to the *stumpy* and *topped* loci. Those embryos that were heterozygous for both *stumpy* and *topped* were scored as transheterozygotes and directly correlated with those embryos with axons stalled at the first intermediate target (Figure 4.1 C, D). I found that *stumpy*^{b393+/-}; *topped*^{+/-} embryos had a more severe stall phenotype at the first intermediate target than *stumpy*^{b393} heterozygous embryos (Fig. 4.1). There was a 92% increase in the number of CaP axons stalled at the first intermediate target in the transheterozygotes versus *stumpy* heterozygotes at 26 hpf. By 48 hpf CaP axons in the double heterozygotes had recovered suggesting that the transheterozygous phenotype is less severe than the *stumpy* homozygous phenotype (see Beattie et al., 2000). Therefore, partially eliminating *topped* can worsen the CaP stall phenotype in *stumpy* heterozygote. The same interaction was observed using a recessive, lethal allele of *stumpy*, *stumpy*^{b398}.

The trans-heterozygote analysis was also characterized at 36 hpf and 48 hpf, time points when *topped* homozygous mutants are unaffected and *stumpy* homozygous mutants remain affected. *Stumpy* heterozygotes remain partially affected at 36 hpf (40% of axons at hm), while *topped* heterozygotes exhibit no

phenotype. Neither mutants exhibit heterozygous phenotypes at 48hpf, therefore if we saw an interaction it would suggest that lacking one copy of both genes can delay CaP axons longer than with either mutant alone. At 36 hpf, 40% of CaP axons were stalled at the horizontal myoseptum in *stumpy*^{b393+/-}; *topped*^{+/-}, (*n*=1100 axons) compared to 50% in *stumpy*^{b393+/-} (*n* = 500 axons) (Fig. 4.2). At 48 hpf, CaP axons had completely recovered in both *stumpy*^{b393+/-} and *stumpy*^{b393+/-}; *topped*^{+/-}, indicating that partial deficiency for these genes is insufficient to stall CaP axons permanently.

I also asked whether altering *topped* dosage in a *stumpy* homozygous background could exacerbate the *stumpy* phenotype. At 26, 36, and 48 hpf, I saw no significant difference in CaP axon location in *stumpy*^{-/-} vs *stumpy*^{-/-}; *topped*^{+/-} or *topped*^{-/-}, suggesting that *stumpy* may lie upstream in the genetic pathway.

To address whether this interaction was unique to *stumpy* and *topped*, I generated transheterozygotes with another mutation that affected CaP axons, *unplugged*. In *unplugged* mutants CaP and RoP axons fail to undergo appropriate pathfinding at the first intermediate target (Zhang et al., 2000). I found no evidence of a genetic interaction in *stumpy*; *unplugged* or *topped*; *unplugged* transheterozygotes. These data support the idea that *topped* and *stumpy* act in the same genetic pathway to promote CaP axon outgrowth into the ventral myotome.

OS4, OS11, and OS12 genetically interact with stumpy

As a preliminary step towards identifying the relevant genes in the CaP axon pathway, I performed a small scale deletion screen to look for genes that are allelic to or interact with *stumpy*. To identify putative mutations, I crossed heterozygous *stumpy*^{b393} fish with heterozygous F₁ gamma irradiated fish and screened the resulting progeny by antibody labeling at 26 hpf to score CaP motor axons. I identified three mutations that displayed a “*stumpy-like*” phenotype when trans-heterozygous with *stumpy*, which include *OS4*, *OS11*, and *OS12* (Fig. 4.3). I subsequently generated an F₂ generation of each line by outcrossing each mutation to WIK mapping background. Interestingly, I saw no CaP axon phenotype, from 18 hpf to 26 hpf, in any of the mutations when homozygous embryos were generated by crossing the F₂ heterozygous progeny. To confirm the mutations were not lost, the F₂ heterozygotes were crossed once again to *stumpy* heterozygotes. These crosses confirmed the trans-heterozygous phenotype yielding a “*stumpy-like*” phenotype. To test the specificity of the interaction, *OS4*, *OS11*, and *OS12* heterozygotes were crossed with *topped* heterozygotes to generate trans-heterozygotes. I saw no phenotype in any of the trans-heterozygotes, suggesting the interactions between *stumpy* and *OS4*, *OS11*, and *OS12* are specific. These data suggest that *OS4*, *OS11*, and *OS12* are genes which genetically interact with *stumpy* to promote CaP axon outgrowth.

OS4, OS11, and OS12 exhibit homozygous lethality

To determine if the deletions present in *OS4*, *OS11*, and *OS12* result in embryonic lethality, I mated heterozygotes for each mutation and analyzed the progeny. I found that each mutation was embryonic lethal. *OS4* and *OS11* homozygous mutants died 10 days post fertilization (dph) from undetermined causes, while *OS12* homozygous mutants died of more pleiotropic defects, including adema at 3 dpf. The deletions responsible for the “stumpy” axon phenotype may result in the loss of multiple genes; therefore the lethality cannot be directly correlated to the CaP axon phenotype.

Discussion

Genetic pathways as revealed by mutant analysis

The genetic interaction between *stumpy* and *topped* strongly supports that these two genes function in the same genetic pathway. The data do not, however, discern between a direct and an indirect interaction, meaning a physical interaction versus two molecules functioning in parallel pathways affecting the same process. Using transheterozygotes to analyze genes involved in axon guidance at the midline in *Drosophila* revealed that *roundabout (robo)* and *ablesen protein tyrosine kinase (abl)* interact genetically and subsequent biochemical analysis showed that this interaction was direct (Bashaw et al., 2000; Wills et al., 2002). Since *stumpy* is needed in both a CaP cell-autonomous

and non-cell autonomous manner (Beattie et al., 2000), it has been difficult to determine where in the environment *stumpy* function is required. Since *stumpy* and *topped* show a genetic interaction, it is possible that *stumpy* is also required in the ventromedial myotome. However, we can hypothesize as to how *stumpy* and *topped* may be interacting. Beattie et al., (2000) demonstrated that Stumpy was functioning at intermediate target regions. If we just consider the first intermediate target, both *stumpy* and *topped* CaP axons stall there. Stumpy and Topped may be functioning in parallel pathways in which Stumpy is needed for CaP axons to proceed past the first intermediate target, and Topped is needed for CaP axons to enter the ventral myotome resulting in an additive effect. Alternatively, Topped may be modulating Stumpy in the ventral myotome. The reverse scenario where Stumpy modulates Topped is diminished by the finding that *topped* could not exacerbate the *stumpy* mutant phenotype, suggesting that *stumpy* is genetically upstream of *topped*. However, given the fact that only ventral motor axons are delayed in *topped*, and all three primary motor axons are delayed in *stumpy*, for Topped function to simply be to modulate Stumpy seems unlikely. Cloning these genes and analysis of their proteins will allow us to build upon this genetic interaction with biochemical data, and therefore determine the exact nature of the interaction.

Identifying the deletion responsible for the OS4, OS11, and OS12 CaP axon phenotype

OS4, OS11, and OS12 may be independent genes, or could represent alleles of one or two genes. Mapping the break points that define the gamma induced deletions is critical for determining which of these two possibilities is correct. This would entail looking for the absence of chromosomal markers in the mutants vs wild-type siblings, indicating a loss of a distinct genomic region. The caveat is the absence of a homozygous phenotype in OS4, OS11, and OS12. Without a homozygous phenotype, linkage analysis is difficult. There are two options to circumvent this problem. First, OS4, OS11, and OS12 homozygous mutants could be identified as they are dying at characteristic time points we defined, and subsequently used for mapping analysis. However, there is the potential for misscoring mutants as this is also the time point when wild-type embryos exhibit a higher percentage of lethality. The second option is to map the OS4, OS11, and OS12 mutations in a *stumpy* heterozygous background. In this case the mutation would be present on only one chromosome, while traditional mapping is conducted on homozygous loci. Although there are caveats to each approach, identifying the deletions is necessary to determine the molecular identity of the genes and how they may be functioning in CaP axon outgrowth along with *stumpy*.

CaP motor axon outgrowth is defined by a complex genetic pathway

Previous work based on zebrafish motor axon guidance mutants has shown that at least four genes are functioning in CaP ventral motor axon outgrowth.

Diwanka and Unplugged are functioning early on in the pathway for CaP axons to exit the spinal cord and make the correct pathway selection. Topped is needed in ventromedial muscle cells to promote CaP axon outgrowth into the ventral myotome. Lastly Stumpy is needed at critical intermediate targets along the CaP axon pathway where decisions are made in order for CaP to complete its outgrowth into the ventral myotome. *OS4*, *OS11*, and *OS12* may be modulating Stumpy's activity in these regions via genetic or biochemical interactions by acting as enhancers. It is possible that *OS4*, *11*, and *12* do not exhibit a homozygous phenotype because of redundant cues or redundancy for one another. Then, when placed in trans with *stumpy*, the relationship becomes apparent. Since the *stumpy* heterozygous phenotype is somewhat variable, reducing levels of a genetic enhancer may be just enough to stall CaP axons completely at the first intermediate target. Whereas, when Stumpy function is normal, the enhancers can compensate for one another. Identifying the molecular identity of *stumpy* and *OS4*, *11*, and *12* will be crucial in defining the nature of this interaction, and the seemingly complex genetic pathway guiding CaP motor axons.

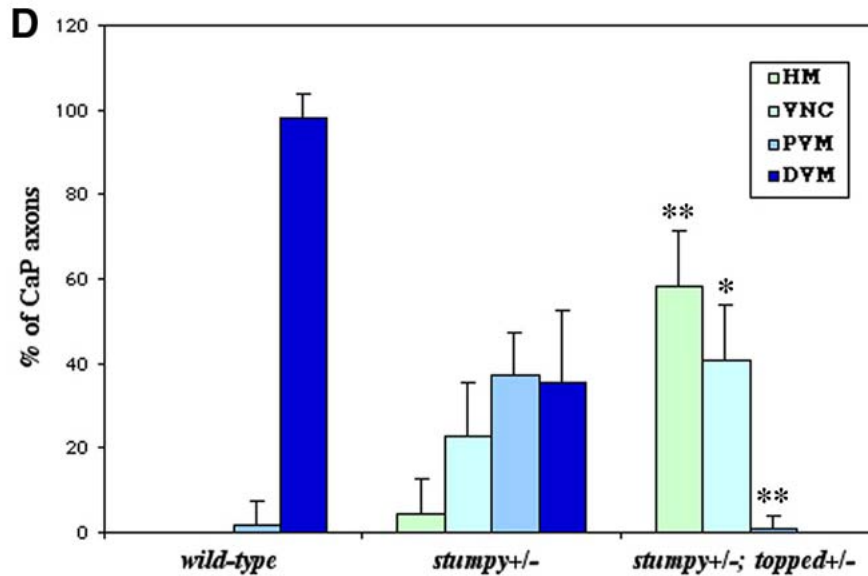
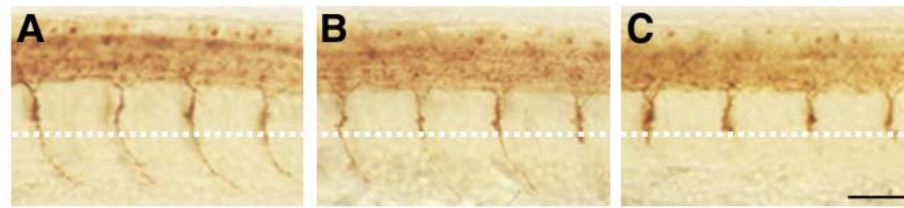


Figure 4.1 *topped* and *stumpy* genetically interact. (A) Lateral view of a 26 hpf wild-type embryo. *stumpy*^{393^{-/-}} fish were mated with *topped*^{+/-} fish to generate *stumpy*^{393^{+/-}}; *topped*^{+/-} transheterozygotes (C) and *stumpy*^{393^{+/-}} siblings (B). White dashed line denotes the first intermediate target. (D) CaP axon position was counted in hemisegments 8-12; n=110 CaP axons in 11 embryos for wild-type, *stumpy*^{393^{+/-}}, and *stumpy*^{393^{+/-}}; *topped*^{+/-} embryos. Axon positions were scored as follows: HM (horizontal myoseptum), VNC (ventral edge of notochord), VM (ventral muscle) and plotted as mean \pm 95% confidence interval. The statistical difference in growth cone position between *stumpy*^{393^{+/-}} and *stumpy*^{393^{+/-}}; *topped*^{+/-} embryos was determined by Student's *t* test with *, $P = 0.01-0.001$; **, $P < 0.001$. Bar, 35 μ m.

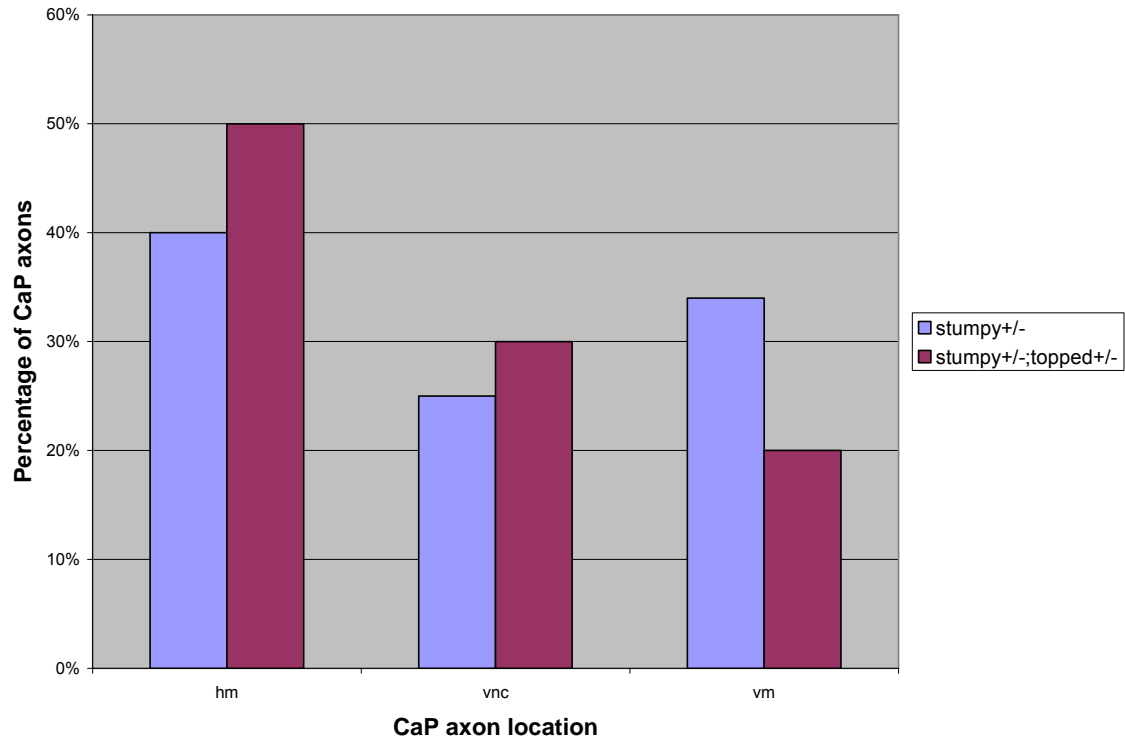


Figure 4.2: *Stumpy*^{+/-}; *topped*^{+/-} transheterozygotes remain affected at 36 hpf. CaP axon position was counted in hemisegments 8-12; n=500 CaP axons in *stumpy*^{393+/-}, and n=1100 in *stumpy*^{393+/-}; *topped*^{+/-} embryos. Axon positions were scored as follows: HM (horizontal myoseptum), VNC (ventral edge of notochord), and VM (ventral muscle).

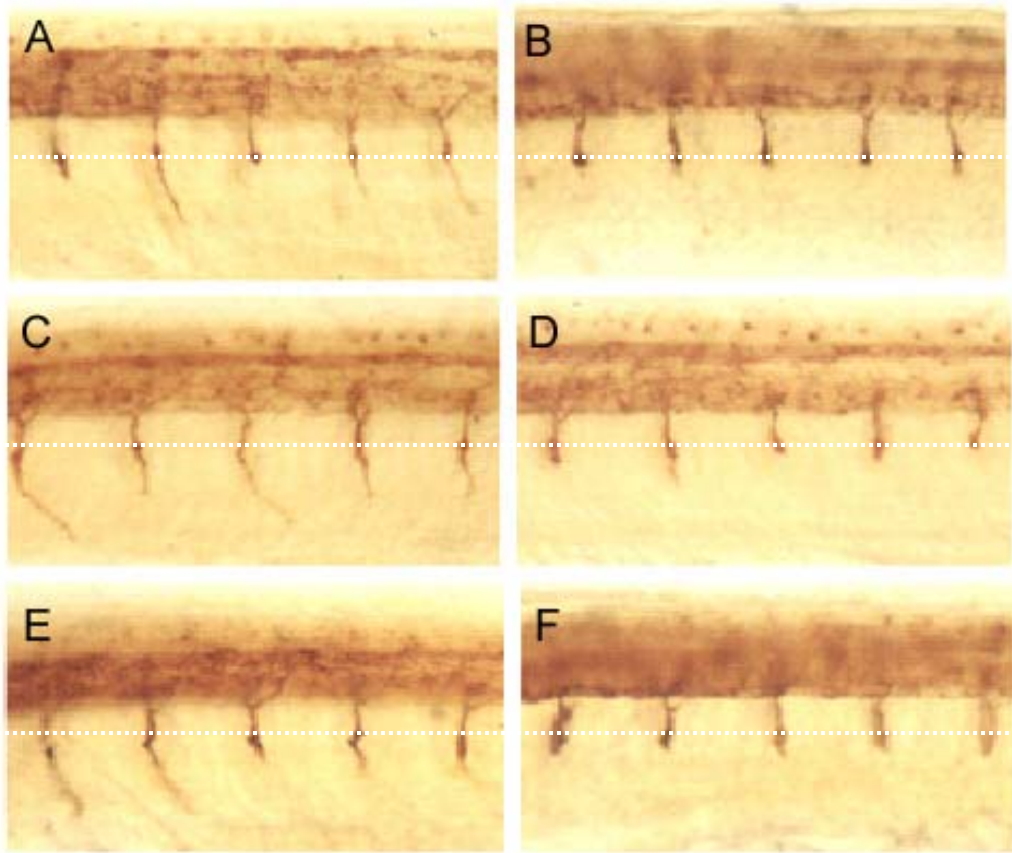


Figure 4.3: OS4, OS11, and OS12 exhibit a transheterozygous interaction with *stumpy*. Lateral views of 26 hpf whole-mount antibody staining with znp1 of *stumpy* heterozygous siblings (A, C, E), and *OS4;stumpy*^{+/-} (B), *OS11;stumpy*^{+/-} (D), and *OS12;stumpy*^{+/-} (F) trans-heterozygous embryos. White dashed line indicates the first intermediate target.

CHAPTER 5

DISCUSSION

The zebrafish model system affords researchers with the opportunity to study nervous system development at the genetic, molecular, and cellular levels. Taking advantage of that, this dissertation work has dissected ventral motor axon pathfinding using all three approaches. Forward genetic analysis has identified several genes, including *topped*, that affect ventral axon outgrowth.

Furthermore, cellular studies revealed a requirement for Topped function in ventromedial myotome cells to promote CaP axon outgrowth. Lastly, molecular analyses have revealed that the zebrafish homolog of vertebrate Sema5a is also functioning in ventral motor axon outgrowth. Taken together, this work has shown that myotomally derived cues present along the CaP motor axon pathway are functioning in a genetic pathway to promote ventral motor axon outgrowth.

The identification of the zebrafish mutant, *topped*, was ideal in that it specifically affects ventral motor axon pathfinding, thereby allowing me to address the mechanism of axon outgrowth specific to the CaP axon pathway. In

topped mutants, CaP axons stall at the first intermediate target at the nascent horizontal myoseptum, a region that demarcates the boundary between dorsal and ventral muscle. This allowed me to begin to address the question of what cues allow an axon to extend ventrally versus dorsally. Genetic mosaic analysis revealed that *Topped* function is required in ventromedial fast muscle for CaP axons to extend ventrally. Furthermore, the degree of rescue is dependent upon the ventral extent of wild-type muscle cells. Taken together, this analysis has suggested that *Topped* functions either as a short range or membrane bound cue in medial fast muscle that defines the ventral motor axon pathway.

In this work, I also demonstrated that *topped* is phenocopied by the knock-down of the guidance cue, *Sema5a* which is expressed in the ventral myotome. In addition, the *topped* phenotype can be rescued either by injection of BAC clones containing portions of the *sema5a* gene or with RNA generated from a heterologous rat *sema5a* cDNA. Together, these results and others support the hypothesis that the *topped* mutation is most likely a mutation in *sema5a*. A mutation of this nature will not only be the first viable *sema5a* mutant, but will also be the first zebrafish Semaphorin mutation, affording *topped* as a powerful tool in understanding Semaphorin function and its roles in ventral motor axon guidance.

Serendipitously, this work has also revealed a novel role for *Sema5a* in axial motor axon pathfinding. Previously, studies in mouse and rat have only focused on the role of *Sema5a* in the habenular system in the diencephalon, and the retinotectal system. It will be interesting to see whether *Sema5a* is

functioning via a conserved mechanism in each of these axon tracts. Moreover, analysis of zebrafish *sema5a* in the habenula and retinotectal system may indicate organism specific roles for Sema5a. Sema5a may or may not be functioning in these processes in fish. In addition, future work will include the search for the Sema5a receptor. In zebrafish, putative receptors can be initially screened with morpholinos to look for the same phenotype that we see with Sema5a knockdown, thereby expediting the process as well as narrowing down the list of candidates. Additional studies to identify physical interactions will then confirm the receptor. Knowing the identity of both the ligand and receptor will be important for understanding how the axon pathfinds to its targets in muscle, where the signal in the muscle (Sema5a) is correctly interpreted by the receptor on the growth cone, and converted to a message for the axon to extend.

To summarize, forward genetic analysis in zebrafish has allowed us to uncover genes involved in ventral motor axon pathfinding. We have and are on the verge of identifying the molecular identity of these genes, which will allow us to look for biochemical interactions to shed light on how they are interacting to promote ventral motor axon outgrowth.

LIST OF REFERENCES

- Adams, RH, Heincih, B, and Puschel, AW.** (1996). A novel class of murine semaphorins with homology to thrombospondin is differentially expressed during early embryogenesis. *Mechanisms of Development* **57**, 33-45.
- Allen, DW, and Greer, JJ.** (1998). Polysialylated NCAM expression during motor axon outgrowth and myogenesis in the fetal rat. *J. Comp. Neurol.* **391**, 275-292.
- Amemiya, CT, Zhong, TP, Silverman, GA, Fishman, MC, and Zon, LI.** (1999). Zebrafish YAC, BAC, and PAC genomic libraries. *Methods Cell Biol.* **60**, 235-58.
- Artigiani, S, Conrotto, P, Fazzari, P, Gilestro, GF, Barberis, D, Giordano, S, Comoglio, PM, and Tamagnone, L.** (2004). Plexin-B3 is a functional receptor form semaphorin 5A. *EMBO Rep.* **7**, 710-714.
- Bair, H and Bonhoeffer, F.** (1992). Axon guidance by gradients of a target-derived component. *Science* **255**, 472-475.
- Bashaw, G. J., Kidd, T., Murray, D., Pawson, T. and Goodman, C. S.** (2000). Repulsive axon guidance: Abelson and Enabled play opposing roles downstream of the roundabout receptor. *Cell* **101**, 703-715.
- Ball, EE, Ho, RK, and Goodman, CS.** (1985). Development of neuromuscular specificity in the grasshopper embryo: guidance of motoneuron growth cones by muscle pioneers. *J Neurosci.* **5**, 1808-1819.
- Beattie, C. B., Raible, D. W., Henion, P. D. and Eisen, J. S.** (1999). Early pressure screens in zebrafish. In *Methods in Cell Biology*, (ed. H. W. Detrich M. Westerfield and L. Zon), pp. 71-83: Academic Press.
- Beattie, C. E.** (2000). Control of motor axon guidance in the zebrafish embryo. *Brain Res. Bull.* **53**, 489-500.
- Beattie, C. E. and Eisen, J. S.** (1997). Notochord alters the permissiveness of myotome for pathfinding by an identified motoneuron in embryonic zebrafish. *Development* **124**, 713-720.

Beattie, C. E., Hatta, K., Halpern, M. E., Liu, H., Eisen, J. S. and Kimmel, C. B. (1997). Temporal separation in the specification of primary and secondary motoneurons in zebrafish. *Dev. Biol.* **187**, 171-82.

Beattie, C. E., Melancon, E. and Eisen, J. S. (2000). Mutations in the *stumpy* gene define intermediate targets for zebrafish motor axons. *Development* **127**, 2653-2662.

Beggs, HE, Soriano, P, and Maness, PF. (1994). NCAM-dependent neurite outgrowth is inhibited in neurons in Fyn-minus mice. *J. Cell. Biol.* **127**, 825-833.

Behar, O, Golden, JA, Mashimo, H, Schoen, FJ, and Fishman, MC. (1996). Semaphorin III is needed for normal patterning and growth of nerves, bones, and heart. *Nature* **383**, 525-528.

Bellosta, P, Costa, M, Lin, DA, and Basilico, C. (1995). The receptor tyrosine kinase ARK mediates cell aggregation by homophilic binding. *Mol. Cell. Biol.* **15**, 614-625.

Bernhardt, RR, Goerlinger, S, Roos, M, and Schachner, N. (1998). Anterior-posterior subdivision of the somite in embryonic zebrafish: implications for motor axon guidance. *Dev. Dyn.* **213**, 334-347.

Bernhardt, RR, and Schachner, N. (2000). Chondroitin sulfates affect the formation of the segmental motor nerves in zebrafish embryos. *Dev. Biol.* **221**, 206-219.

Birely, J, Schneider, VA, Santana, E, Dosch, R, Wagner, DS, Mullins, MC, and Granato, M. (2005). Genetic screens for genes controlling motor nerve-muscle development and interactions. *Developmental Biology* **280**, 162-176.

Bixby, JL, and Jhabvala, P. (1993). Tyrosine phosphorylation in early embryonic growth cones. *J. Neurosci.* **13**, 3421-3432.

Bonhoeffer, F, and Huf, J. (1980). Recognition of cell types by axonal growth cones in vitro. *Nature* **288**, 162-164.

Bonhoeffer, F, and Huf, J. (1982). In vitro experiments on axon guidance demonstrating an anterior-posterior gradient on the tectum. *EMBO J.* **1**, 427-431.

Bonhoeffer, F, and Huf, J. (1985). Position dependent properties of retinal axons and their growth cones. *Nature* **315**, 409-410.

Challa, A.K., Beattie, C.E., and Seeger, M.A. (2001). Identification and characterization of *roundabout* orthologs in zebrafish. *Mech. Dev.* **101**, 249-253.

Colamarino, S, and Tessier-Lavigne, M. (1995). The axonal chemoattractant netrin-1 is also a chemorepellent for trochlear motor axons. *Cell* **81**, 621-629.

Comer, AR, Ahern-Djamali, SM, Juang, JL, Jackson, PD, and Hoffman, FM. (1998). Phosphorylation of Enabled by the Drosophila abelson tyrosine kinase regulates the in vivo function and protein-protein interactions of enabled. *Molecular and Cellular Biology* **18**, 152-160.

Corey, DR, and Abrams, JM. (2001). Morpholino antisense oligonucleotides: tools for investigating vertebrate development. *Genome Biol.* **2**.

Crow, M. T. and Stockdale, F. E. (1986). Myosin expression and specialization among the earliest muscle fibers of the developing avian limb. *Dev. Biol.* **113**, 238-254.

Culotti, JG, and Kolodkin, AL. (1996). Functions of netrins and semaphorins in axon guidance. *Curr. Opin. Neurobiol.* **6**, 81-88.

Desai, CJ, Ginhart, JG, Goldstein, LS, and Zinn, K. (1996). Receptor tyrosine phosphatases are required for motor axon guidance in the Drosophila embryo. *Cell* **84**, 599-609.

Desai, CJ, Krueger, NX, Saito, H, and Zinn, K. (1997). Competition and cooperation among receptor tyrosine phosphatases control motoneuron growth cone guidance in Drosophila. *Development* **124**, 1941-1952.

Devoto, S. H., Melancon, E., Eisen, J. S. and Westerfield, M. (1996). Identification of separate slow and fast muscle precursor cells in vivo, prior to somite formation. *Development* **122**, 3371-80.

du Lac, S, Bastiani, MJ, and Goodman, CS. (1986). Guidance of neuronal growth cones in the grasshopper embryo. II. Recognition of a specific axonal pathway by the aCC neuron. *J. Neurosci.* **6**, 3532-3541.

Eberhart, J., Swartz, M. E., Koblar, S. A., Pasquale, E. B. and Krull, C. E. (2002). EphA4 Constitutes a Population-Specific Guidance Cue for Motor Neurons. *Dev. Biol.* **247**, 89-101.

Eberhart, J, Swartz, M, Koblar, SA, Pasquale, EB, Tanaka, H, and Krull, CE. (2000). Expression of EphA4, ephrin-A2 and ephrin-A5 during axon outgrowth in the hindlimb indicates potential roles in pathfinding. *Dev. Neurosci.* **22**, 237-250.

Edelman, GM. (1993). A golden age for cell adhesion. *Cell Adhes. Commun.* **1**, 1-7

Eikholt, BJ, Mackenzie, SL, Graham, A, Walsh, FS, and Doherty, P. (1999). Evidence for collapsin-1 functioning in the control of neural crest migration in both trunk and hindbrain regions. *Development* **126**, 2181-2189.

Eisen, J. S. (1999). Patterning motoneurons in the vertebrate nervous system. *TINS* **22**, 321-326.

Eisen, J. S., Myers, P. Z. and Westerfield, M. (1986). Pathway selection by growth cones of identified motoneurons in live zebra fish embryos. *Nature* **320**, 269-71.

Eisen, JS, and Pike, SH. (1991). The *spt-1* mutation alters segmental arrangement and axonal development of identified neurons in the spinal cord of the embryonic zebrafish. *Neuron* **6**, 767-776.

Eisen, J. S., Pike, S. H. and Debu, B. (1989). The growth cones of identified motoneurons in embryonic zebrafish select appropriate pathways in the absence of specific cellular interactions. *Neuron* **2**, 1097-1104.

Elizondo, MR, Arduini, BL, Paulson, J, MacDonald, EL, Sabel, JL, Henion, PD, Cornell, RA, and Parichy, DM. (2005). Defective skeletogenesis with kidney stone formation in dwarf zebrafish mutant for *trpm*. *Current Biology* **15**, 667-671.

Felsenfield, A. L., Curry, M. and Kimmel, C. B. (1991). The *fub-1* mutation blocks initial myofibril formation in zebrafish muscle pioneer cells. *Dev. Biol.* **148**, 23-30.

Ferguson, B. (1983). Development of motor innervation of the chick following dorso-ventral limb bud rotations. *J. Neurosci.* **3**, 1760-1772.

Finn, AJ, Feng, G, and Pendergast, AM. (2003). Postsynaptic requirement for Abl kinases in assembly of the neuromuscular junction. *Nat. Neurosci.* , 1-7.

Fiore, R, Rahim, B, Christoffels, VM, Moorman, AF, Puschel, AW. (2005). Inactivation of the *Sema5a* gene results in embryonic lethality and defective remodeling of the cranial vascular system. *Mol Cell Biol.* **6**, 2310-2319.

Gierer, A. (1987). Directional cues for growing axons forming the retinotectal projection. *Development* **122**, 479-489.

Geisler, R, Rauch, GJ, Baier, H, van Bebber, F, Bross, L, Dekens, MP, Finger, K, Fricke, C, Gates, MA, Geiger, H, Geiger-Rudolph, S, Gilmour, D, Glaser, S, Gnugge, L, Habeck, H, Hingst, K, Holley, S, Keenan, J, Kirn, A, Knaut, H, Lashkari, D, Maderspacher, F, Martyn, U, Neuhaus, S, Neumann, C, Nicolson, T, Pelegri, F, Ray, R, Rick, JM, Roehl, H, Roeser, T, Schauer, HE, Schier, AF, Schonberger, U, Schonhaler, HB, Schulte-Merker, S, Seydler, C, Talbot, WS, Weiler, C, Nusslein-Volhard, C, and Haffter, P. (1999). A radiation hybrid map of the zebrafish genome. *Nat. Genetics* **1**, 86-89.

Giniger, E. (2002). How do Rho family GTPases direct axon growth and guidance? A proposal relating signaling pathways to growth cone mechanics. *Differentiation* **70**, 385-396.

Goodman, CS. (1994). The likeness of being: phylogenetically conserved molecular mechanisms of growth cone guidance. *Cell* **78**, 353-356.

Goodman, CS, and Tessier-Lavigne, M. (1997). Molecular mechanisms of axon guidance and target recognition. Cowan WM, Jessel, TM, and Zipursky, SL (Eds.), *Molecular and cellular approaches to neural development*. Oxford University Press, pp. 108-178.

Granato, M, van Eeden, FJ, Schach, U, Trowe, T, Brand, M, Furutani-Seiki, M, Haffter, P, Hammerschmidt, M, Heisenberg, CP, Jiang, YJ, Kane, DA, Kelsh, RN, Mullins, MC, Odenthal, J, and Nusslein-Volhard, C. (1996). Genes controlling and mediating locomotion behavior of the zebrafish embryo and larva. *Development* **123**, 399-413.

Gray, M, Moens, CB, Amacher, SL, Eisen, JS, and Beattie, CE. (2001). Zebrafish deadly seven functions in neurogenesis. *Dev. Biol.* **237**, 306-323.

Guthrie, Sarah. (2001). Axon guidance: Robos make the rules. *Current Biology* **11**, 300-303.

Halloran, MC, Sato-Maeda, M, Warren, JT, Su, F, Lele, Z, Krone, PH, Kuwada, JY, and Shoji, W. (2000). Laser-induced gene expression in specific cells of transgenic zebrafish. *Development* **127**, 1953-1960.

Hatta, K. (1992). Role of the floorplate in axonal patterning in the zebrafish CNS. *Neuron* **9**, 629-642.

He, Z, Wang, KC, Koprivica, V, Ming, G, and Song, HJ. (2002). Knowing how to navigate: mechanisms of semaphorin signaling in the nervous system. *Sci STKE*

Heasman, J. (2002). Morpholino oligos: making sense of antisense? *Dev. Biol.* **243**, 209-214.

Hedgecock, EM, Culotti, JG, and Hall, DH. (1990). The unc-5, unc-6, and unc-40 genes guide circumferential migrations of pioneer axons and mesodermal cells on the epidermis in *C. elegans*. *Neuron* **4**, 61-85.

Helmbacher, F., Schneider-Maunoury, S., Topilko, P., Tiret, L. and Charnay, P. (2000). Targeting of the EphA4 tyrosine kinase receptor affects dorsal/ventral pathfinding of limb motor axons. *Development* **127**, 3313-3324.

Ho, R. K. and Kane, D. A. (1990). Cell-autonomous action of zebrafish spt-1 mutation in specific mesodermal precursors. *Nature* **348**, 728-730.

Hollyday, M. (1995). Chick wing innervation. I. Time course of innervation and early differentiation of the peripheral nerve pattern. *J. Comp. Neurol.* **357**, 242-253.

Ignelzi, M, Miller, DR, Soriano, P, and Maness, PF. (1994). Impaired neurite outgrowth of src-minus cerebellar neurons on the cell adhesion molecule L1. *Neuron* **12**, 873-884.

Ishii, N, Wadsworth, WG, Stern, BD, Culotti, JG, and Hedgecock, EM. (1992). UNC-6, a laminin-related protein, guides cell and pioneer axon migrations in *C. elegans*. *Neuron* **9**, 873-881.

Johnson, S. L., Africa, D., Horne, S. and Postlethwait, J. H. (1995). Half-tetrad analysis in zebrafish: mapping the *ros* mutation and to the centromere of linkage group I. *Genetics* **139**, 1727-1735.

Johnson, S. L., Gates, M. A., Johnson, M., Talbot, W. S., Horne, S., Baik, K., Rude, S., Wong, J. and Postlethwait, J. H. (1996). Centromere-linkage analysis and consolidation fo the zebrafish genetic map. *Genetics* **142**, 1277-1288.

Kantor, DB, Chivatakam, O, Peer, KL, Oster, SF, Inatani, M, Hansen, MJ, Flanagan, JG, Yamaguchi, Y, Stetavan, DW, Giger, RJ, and Kolodkin, AL. (2004). Semaphorin 5A is a bifunctional cue regulated by heparin and chondroitin sulfate proteoglycans. *Neuron* **44**, 961-975.

Keleman, K, Rajagopalan, S, Cleppien, D, Teis D, Paiha, K, Huber, LA, Technau, GM, and Dickson, BJ. (2002). Comm sorts robo to control axon guidance at the Drosophila midline. *Cell* **110**, 415-27.

Keleman, K, Ribeiro C, Dickson, BJ. (2005). Comm function in commissural axon guidance: cell-autonomous sorting of Robo in vivo. *Nat Neurosci* **2**, 156-63.

- Kidd, T, Bland, KS, and Goodman, CS.** (1999). Slit is the midline repellent for the Robo receptor in *Drosophila*. *Cell* **96**, 785-794.
- Kilpatrick, TJ, Brown, A, Lai, C, Gassmann, M, Goulding, M, and Lemke, G.** (1996). Expression of the Tyro4/Mek4/Cek4 gene specifically marks a subset of embryonic motor neurons and their muscle targets. *Mol. Cell. Neurosci.* **7**, 62-74.
- Kimmel, C. B., Ballard, W. W., Kimmel, S. R., Ullmann, B. and Schilling, T. F.** (1995). Stages of embryonic development of the zebrafish. *Dev. Dyn.* **203**, 253-310.
- Kitsukawa, T, Shimizu, M, Sanbo, M, Hirata, T, Taniguchi, M, Bekku, Y, Yagi, T, and Fujisawa, H.** (1997). Neuropilin-semaphorin III/D-mediated chemorepulsive signals play a crucial role in peripheral nerve projection in mice. *Neuron* **19**. 995-1005.
- Kolodkin, AL, Matthes, DJ, O'Conner, TP, Patel, NH, Admon, A, Bentley, D, and Goodman, CS.** (1992). Fasciclin IV: sequence, expression, and function during growth cone guidance in the grasshopper embryo. *Neuron* **9**, 831-845.
- Kolodkin, AL, Matthes, DJ, and Goodman, CS.** (1993). The semaphorin genes encode a family of transmembrane and secreted growth cone guidance molecules. *Cell* **75**, 1389-1399.
- Knapik, EW, Goodman, A, Atkinson, OS, Roberts, CT, Shiozawa, M, Sim, CU, Weksler-Zangen, S, Trolliet, MR, Futrell, C, Innes, BA, Koike, G, McLaughlin, MG, Pierre, L, Simon, JS, Vilallonga, E, Roy, M, Chiang, PW, Fishman, MC, Driever, W, and Jacob, HJ.** (1996). A reference cross DNA panel for zebrafish (*Danio rerio*) anchored with simple sequence length polymorphisms. *Development* **123**, 451-460.
- Knapik, EW, Goodman, A, Ekker, M, Chevrette, M, Delgado, J, Neuhaus, S, Shimoda, N, Driever, W, Fishman, MC, and Jacob, HJ.** (1998). A microsatellite genetic linkage map for zebrafish (*Danio rerio*). *Nat. Genetics* **4**, 301-303.
- Kraut, R, Menon, K, and Zinn, K.** (2001). A gain-of-function screen for genes controlling motor axon guidance and synaptogenesis in *Drosophila*. *Curr. Biol.* **11**, 417-430.
- Kruger, RP, Lee, J, Li, W, Guan, KL.** (2004). Mapping Netin receptor domains of Unc5 regulating its tyrosine phosphorylation. *J. Neuroscience* **24**, 10826-10834.

Kury, P, Gale, N, Connor, R, Pasquale, E, and Guthrie, S. (2000). Eph receptors and ephrin expression in cranial motor neurons and the brachial arches of the chick embryo. *Mol. Cell. Neurosci.* **15**, 123-140.

Kuwada, JY. (1986). Cell recognition by neuronal growth cones in a simple vertebrate embryo. *Science* **233**, 740-746.

Lance-Jones, C, and Landmesser, L. (1980). Motoneurone projection patterns in the chick hind-limb following early partial spinal cord reversals. *J. Physiol.* **302**, 581-602.

Lander, AD. (1987). Molecules that make axons grow. *Mol. Neurobiol.* **1**, 213-245.

Landgraf, M, Bossing, T, Technau, GM, and Bate, M. (1997). The origin, location, and projections of the embryonic abdominal motoneurons of *Drosophila*. *J. Neurosci.* **17**, 9642-9655.

Landmesser, L. (1978). The development of motor projection patterns in the chick hind limb. *J. Physiol.* **284**, 391-414.

Landmesser, L, Dahm, L, Schultz, K, and Rutishauser, U. (1988). Distinct roles for adhesion molecules during innervation of embryonic chick muscle. *Dev. Biol.* **130**, 645-670.

Landmesser, L, Dahm, L, Tang, JC, and Rutishauser, U. (1990). Polysialic acid as a regulator of intramuscular nerve branching during embryonic development. *Neuron* **4**, 655-667.

Landmesser, LT. (1980). The generation of neuromuscular specificity. *Annu. Rev. Neurosci.* **3**, 279-302.

Landmesser, LT. (2001). The acquisition of motoneuron subtype identity and motor circuit formation. *Int. J. Devl. Neuroscience* **19**, 175-182.

Luo, R., An, M., Arduini, B. L., and Henion, P. D. (2001). Specific pan-neural crest expression of zebrafish Crestin throughout embryonic development. *Dev. Dyn.* **220**, 169-174.

McWhorter, ML, Monani, UR, Burghes, AH, and Beattie, CE. (2003). Knockdown of the survival motor neuron (Smn) protein in zebrafish causes defects in motor axon outgrowth and pathfinding. *J. Cell Biol.* **162**, 919-931.

- Melancon, E., Liu, D. W. C., Westerfield, M. and Eisen, J. S.** (1997). Pathfinding by indentified zebrafish motoneurons in the absence of muscle pioneers. *J. Neurosci.* **17**, 7796-7804.
- Mitchell, KJ, Doyle, JL, Serafini, T, Kennedy, TE, Tessier-Lavigne, M, Goodman, CS, and Dickson, BJ.** (1996). Genetic analysis of the Netrin genes in Drosophila: Netrins guide CNS commissural axons and peripheral motor axons. *Neuron* **17**, 203-215.
- Morin-Kensicki, E. M. and Eisen, J. S.** (1997). Sclerotome development and peripheral nervous system segmentation in embryonic zebrafish. *Development*, 159-167.
- Myers, P. Z.** (1985). Spinal motoneurons of the larval zebrafish. *J. Comp. Neurol.* **237**, 555-561.
- Myers, P. Z., Eisen, J. S. and Westerfield, M.** (1986). Development and axonal outgrowth of identified motoneurons in the zebrafish. *J. Neurosci.* **6**, 2278-2289.
- Nakamoto, M, Cheng, HJ, Friedman, GC, McLaughlin, T, Hansen, MJ, Yoon, CH, O'Leary, DDM, and Flanagan, JG.** (1996). Topographically specific effects of ELF-1 on retinal axon guidance in vitro and retinal axon mapping in vivo. *Cell* **86**, 755-766.
- Nakamura, F, Kalb, RG, and Strittmatter, SM.** (2000). Molecular basis of semaphoring-mediated axon guidance. *J Neurobiol.* **44**, 210-229.
- Nasevicius, A, and Ekker, SC.** (2000). Effective targeted gene "knockdown" in zebrafish. *Nat. Genet.* **26**, 216-220.
- Neugebauer, KM, Emmett, CJ, Venstrom, KA, and Reichardt, LF.** (1991). Vitronectin and thrombospondin promote retinal neurite outgrowth: developmental regulation and role of integrins. *Neuron* **6**, 345-358.
- Oakley, RA, and Tosney, KW.** (1993). Contact-mediated mechanisms of motor axon segementation. *J. Neurosci.* **13**, 3773-3792.
- O'Shea, KS, Liu, L, and Dixit, VM.** (1991). Thrombospondin and a 140kd fragment promote adhesion and neurite outgrowth from embryonic central and peripheral neurons and from PC12 cells. *Neuron* **7**, 231-237.
- Osterhout, DJ, Frazier, WA, and Higgins, D.** (1992). Thrombospondin promotes process outgrowth in neurons from the peripheral and central nervous system. *Dev. Biol.* **150**, 256-265.

- Pasterkamp, RJ, and Kolodkin, AL.** (2003). Semaphorin junction: making tracks toward neural connectivity. *Curr. Opin. Neurobiol.* **13**, 79-89.
- Patel, N.H., Kornberg, T.B., and Goodman, C.S.** (1989). Expression of *engrailed* during segmentation in the grasshopper and crayfish. *Development* **107**, 201-212.
- Pike, S. H., Melancon, E. F. and Eisen, J. S.** (1992). Pathfinding by zebrafish motoneurons in the absence of normal pioneer axons. *Development* **114**, 825-831.
- Pike, SH, and Eisen, JS.** (1990). Identified primary motoneurons in embryonic zebrafish select appropriate pathways in the absence of other primary motoneurons. *J. Neurosci.* **10**, 44-49.
- Postlethwait, JH, Johnson, SL, Midson, CN, Talbot, WS, Gates, M, Ballinger, EW, Africa, D, Andrews, R, Carl, T, Eisen, JS, Horne, S, Kimmel, CB, Huthinson, M, Johnson, M, and Rodriguez, A.** (1994). A Genetic Linkage Map for the Zebrafish. *Science* **264**, 699-703.
- Puschel, AW, Adams, RH, and Betz, H.** (1995). Murine semaphorin D/collapsin is a member of a diverse gene family and creates domains inhibitory for axonal extension. *Neuron* **14**, 941-948.
- Raper, JA.** (2000). Semaphorins and their receptors in vertebrates and invertebrates. *Curr. Opin. Neurobiol.* **10**, 88-94.
- Rubinstein, A.L., Lee, D., Luo, R., Henion, P.D., and Halpern, M.E.** (2000). Genes dependent on zebrafish *cyclops* function identified by AFLP differential gene expression screen. *Genesis* **26**, 86-97.
- Rawala, H, Huttunen, HJ, Fages, C, Kaksonen, M, Kinnunen, T, Imai, S, Raulo, E, and Kilpelainen, I.** (2000) *Matrix Biology* **19**, 377-387.
- Rodino-Klapac, LR, and Beattie, CE.** (2004) Zebrafish topped is required for ventral motor axon guidance. *Developmental Biology* **273**: 308–320.
- Roos, M, Schachner, M, and Bernhardt, RR.** (1999). Zebrafish semaphorin Z1b inhibits growing motor axons in vivo. *Mechanisms of Development* **87**, 103-117.
- Schachner, M, Taylor, J, Bartsch, U, and Pesheva, P.** (1994). The perplexing multifunctionality of janusin, a tenascin-related molecule. *Perspect. Devl. Neurobiol.* **2**, 33-41.

Schneider, VA, and Granato, M. (2003). Motor axon migration: a long way to go. *Developmental Biology* **263**, 1-11.

Seeger, M, Tear, G, Ferres-Marco, D, and Goodman, CS. (1993). Mutations affecting growth cone guidance in Drosophila: genes necessary for guidance toward or away from the midline. *Neuron* **10**, 409-426.

Semaphorin Nomenclature Committee. (1999). Unified nomenclature for the semaphorins/collapsins. *Cell* **97**, 551-552.

Shimoda, N, Knapik, EW, Ziniti, J, Sim C, Yamada, E, Kaplan, S, Jackson, D, de Sauvage, F, Jacob, H, Fishman, MC. (1999). Zebrafish genetic map with 2000 microsatellite markers. *Genomics* **58**, 551-552.

Sink, H and Whittington, PM. (1991). Early ablation of target muscles modulates the arborization pattern of an identified embryonic Drosophila motor axon. *Development* **113**, 701-707.

Solnica-Krezel, L., Scheir, A. F. and Driever, W. (1994). Efficient recovery of ENU-induced mutations from the zebrafish germline. *Genetics* **136**, 1401-1420.

Sperry, RW. (1963). Chemoaffinity in the orderly growth of nerve fiber patterns and connections. *Proc. Natl. Acad. Sci.* **50**, 703-710.

Stickney, H. L., Barresi, M. J. and Devoto, S. H. (2000). Somite development in zebrafish. *Dev. Dyn.* **219**, 287-303.

Streisinger, G., Walker, C., Dower, N., Knauber, D. and Singer, F. (1981). Production of clones of homozygous diploid zebra fish (*Brachydanio rerio*). *Nature* **291**, 293-296.

Takeichi, M. (1995). Morphogenetic roles of classic cadherins. *Curr. Opin. Cell Biol.* **7**, 619-627.

Talbot, WS, and Schier, AF. (1999). Positional cloning of mutated zebrafish genes. *Methods Cell Biol.* **60**, 259-286.

Tang, J, Rutishauser, U, and Landmesser, L. (1994). Polysialic acid regulates growth cone behavior during sorting of motor axons at the plexus region. *Neuron* **8**, 1031-1044.

Taniguchi, M, Yuasa, S, Fujisawa, H, Naruse, I, Saga, S, Mishini, M, and Yagi, T. (1997). Disruption of semaphoring III/D gene causes severe abnormality in peripheral nerve projection. *Neuron* **19**, 519-530.

Tannahill, D, Cook, GM, and Keynes, RJ. (1997). Axon guidance and somites. *Cell Tissue Res.* **290**, 275-283.

Taylor, MR, Kikkawa, S, Diez-Juan, A, Ramamurthy, V, Kawakani, K, Carmeliet, P, and Brockhoff, SE. (2005). The Zebrafish *pob* gene encodes a novel protein required for survival of red cone photoreceptor cells. *Genetics* **170**, 263-273.

Tessier-Lavigne, M, Placzek, M, Lumsden, AG, Dodd, J, and Jessell, TM (1988). Chemotropic guidance of developing axons in the mammalian central nervous system. *Nature* **336**, 775-778.

Thanos, S, and Bonhoeffer, F. (1986). Course corrections of deflected retinal axons on the tectum of the chick embryo. *Neurosci. Lett.* **72**, 31-36.

Thanos, S, and Dutting, D. (1987). Outgrowth and directional specificity of fibers from embryonic retinal transplants in the chick optic tectum. *Brain Res.* **429**, 161-179.

Thisse, C., Thisse, B., Schilling, T.F., and Postethwait, J.H. (1993). Structure of the zebrafish *snail1* gene and its expression in wild-type, *spadetail*, and *no tail* mutant embryos. *Development* **119**, 1203-1215.

Thummel, R, Burket, CT, Brewer, JL, Sarras, MP, Li, L, Perry, M, McDermott, JP, Sauer, B, Hyde, DR, and Godwin, AR. (2005). Cre-mediated site-specific recombination in zebrafish embryos. *Dev. Dyn.(ahead of print)*.

Tosney, K. W. (1987). Proximal tissues and patterned neurite outgrowth at the lumbrosacral level of the chick embryo: deletion of the dermamyotome. *Dev. Biol.* **122**, 540-588.

Tosney, KW. (1991). Cells and cell-interactions that guide motor axons in the developing chick embryo. *Bioessays* **13**, 17-23.

Trevarrow, B., Marks, D. L. and Kimmel, C. B. (1990). Organization of hindbrain segments in the zebrafish embryo. *Neuron* **4**, 669-679.

Troeger, C., Zhong, X. Y., Burgemeister, R., Minderer, S., Tercanli, S., Holzgreve, W. and Hahn, S. (1999). Approximately half of the erythroblasts in maternal blood are of fetal origin. *Mol. Hum. Reprod.* **5**, 1162-1165.

Tzarfati-Majar, V, Burstyn-Cohon, T, and Klar, A. (2001). F-spondin is a contact-repellent molecule for embryonic motor neurons. *Proc. Natl. Acad. Sci. USA* **98**, 4722-4727.

Udvardia, AJ, and Linney, E. (2003). Windows into development: historic, current, and future perspectives on transgenic zebrafish. *Dev. Biol.* **256**, 1-17.

Van Vactor, D, Sink, H, Fambrough, D, Tsoo, R, and Goodman, C. (1993). Genes that control neuromuscular specificity in *Drosophila*. *Cell* **73**, 1137-1153.

Varela-Echavarria, A, Tucker, A, Puschel, AW, and Guthrie, S. (1997). Motor axon subpopulations respond differentially to the chemorepellents netrin-1 and semaphorin D. *Neuron* **18**, 193-207.

Vermeren, MM, Cook, GM, Johnson, AR, Keynes, RJ, and Tannahill, D. (2000). Spinal nerve segmentation in the chick embryo: analysis of distinct axon repulsive systems. *Dev. Biol.* **225**, 241-252.

Walter, J, Henke-Fahle, S, and Bonhoeffer, F. (1987). Avoidance of posterior tectal membranes by temporal retinal axons. *Development* **101**, 909-913.

Wang, HU, and Anderson, DJ. (1997). Eph family transmembrane ligands can mediate repulsive guidance of trunk neural crest migration and motor axon outgrowth. *Neuron* **18**, 383-396.

Weinberg, E.S., Allende, M.L., Kelly, C.S., Abdelhanmid, A., Murakami, T., Andermann, P., Doerre, O.G., Grunwald, D.J., and Riggleman, B. (1996). Developmental regulation of zebrafish MyoD in wild-type, *no tail* and *spadetail* embryos. *Development* **122**, 271-280.

Westerfield, M. (1995). *The Zebrafish Book*. Eugene, Oregon: University of Oregon Press.

Westerfield, M, McMurry, JV, and Eisen, JS. (1986). Identified motoneurons and their innervation of axial muscles in the zebrafish. *J. Neurosci.* **6**, 2267-2277.

Wightman, B, Baran, R, and Garriga, G. (1997). Genes that guide growth cones along the *C. elegans* ventral nerve cord. *Development* **124**, 2571-2580.

Willer, GB, Lee, VM, Gregg, RG, and Link, BA. (2005). Analysis of the zebrafish *perplexed* mutation reveals tissue specific roles for de novo pyrimidine synthesis during development. *Genetics* June 3, 2005 *ahead of print*.

Wills, Z., Emerson, M., Rusch, J., Bikoff, J., Baum, B., Perrimon, N. and Van Vactor, D. (2002). A *Drosophila* homolog of cyclase-associated proteins collaborates with the Abl tyrosine kinase to control midline axon pathfinding. *Neuron* **36**, 611-622.

Winberg, ML, Mitchell, KJ, and Goodman, CS. (1998). Genetic analysis of the mechanisms controlling target selection: Complementary and combinatorial functions of netrins, semaphorins, and IgCAMs. *Cell* **93**, 581-591.

Zallen, JA, Kirch, SA, and Bargmann, CJ. (1999). Genes required for axon pathfinding and extension in the *C. elegans* nerve ring. *Development* **126**, 3679-3692.

Zeller, J. and Granato, M. (1999). The zebrafish *diwanka* gene controls an early step of motor growth cone migration. *Development* **126**, 3461-3472.

Zeller, J., Schneider, V., Malayaman, S., Higashijima, S., Okamoto, H., Gui, J., Lin, S., and Granato, M. (2002). Migration of zebrafish spinal motor nerves into the periphery requires multiple myotome-derived cues. *Dev. Biol.* **252**, 241-256.

Zhang, J. and Granato, M. (2000). The zebrafish *unplugged* gene controls motor axon pathway selection. *Development* **127**, 2099-2111.

Zhang, J, Lefebvre, JL, Zhao, S, and Granato, M. (2004). Zebrafish unplugged reveals a role for muscle-specific kinase homologs in axon pathway choice. *Nat. Neurosci.* **7**, 1303-1309.